

**X-RAY CRYSTALLOGRAPHIC  
STUDIES OF BOVINE SERUM  
ALBUMIN AND *HELICOBACTER  
PYLORI* THIOREDOXIN-2**

A Thesis Submitted to the College of Graduate Studies and  
Research in Partial Fulfillment of the Requirements for the  
Degree of Master of Science in the Department of Chemistry

University of Saskatchewan

Saskatoon

Canada

**Heng Chiat Tai**

Department of Chemistry  
University of Saskatchewan  
Copyright ©December 2004  
All Rights Reserved

## **PERMISSION TO USE**

In presenting this thesis in partial fulfillment of the requirements for a postgraduate degree from the University of Saskatchewan, I agree that the libraries of this University may make it freely available for inspection. I further agree that permission for copying of this thesis in any manner, in whole or in part, for scholarly purposes may be granted by the professor or professors who supervised my thesis work, or in their absence, by the Head of the Department or the Dean of the College in which my thesis work was done. It is understood that any copying or publication or use of this thesis or parts thereof for financial gain shall not be allowed without my written permission. It is also understood that due recognition shall be given to me and to the University of Saskatchewan in any scholarly use which may be made of any material in my thesis.

Requests for permission to copy or to make other use of material in this thesis in whole or in part should be addressed to:

Head of the Department of Chemistry

University of Saskatchewan

110 Science Place

Saskatoon, Saskatchewan

S7N 5C9

Canada

## ABSTRACT

The initial motivation for crystallization of Bovine Serum Albumin (BSA) is an interest to understand how thiomolybdates interact with BSA and suppress copper intake from the food sources of cattle. The main objective of my research work is to determine the crystal structure of BSA using X-ray crystallography techniques. Once the tertiary structure of BSA is determined, its structural information can help us to study the interactions between BSA, copper, and thiomolybdates, and to understand the way in which thiomolybdates render copper unavailable in cattle. Many trials for the optimal crystallization conditions of BSA were attempted in order to grow high-quality BSA crystals. However, all crystals only diffract to 8 Å resolution limit. Such resolution is not sufficient to solve the tertiary structure of BSA.

Another objective of my research was to crystallize Thioredoxin-2 (Trx-2) to obtain larger crystals which may lead to high resolution crystallographic data, better than 2.4 Å, for protein structure refinement. This is because Trx-2 diffraction data that had been collected are split at high resolution. The ambiguous data at high resolution might impede the structure refinement and even can cause the three-dimensional structure of Trx-2 to not be refined successfully. A number of attempts were conducted for crystallizing Trx-2 to grow bigger and higher quality of Trx-2 crystals. However, the improvement of crystal dimensions was not significant, the diffraction resolution limits are similar to previous published data, and the split data at high resolution was still observed.

## ACKNOWLEDGEMENTS

First, I would like to thank for my supervisor, Dr. David A. R. Sanders, who spent a lot of time to read my thesis and gave me a lot of useful suggestions and criticisms, and also for being patient with me through all the times. I really appreciate the guidance and assistances that he has provided and very grateful him to accept me as his first student.

The members of my supervisory committee provided with many useful suggestions and comments to me. This includes Dr. J. W. Quail, Dr. R. S. Reid, Dr. M. S. C. Pedras, as well as the former committee chair, Dr. R. E. Verrall.

I want to thank Dr. L. T. J. Delbaere, my supervisor Dr. David A. R. Sanders, and Dr. Y. Luo who taught me the knowledge of protein X-ray crystallography and they provided me a much broader understanding of this subject. Special thanks to Dr. Y. Luo who has given me some useful suggestions about my BSA project, and Ms. Yvonne Leduc who trained me in protein crystallization. Many thanks go to the present and past lab members including Salina, Krishna, Ignace, etc. who provided a friendly working environment in Room 144 at Thorvaldson building.

I would also like to give special thanks to Dr. Edwin Yeow and Dr. Yitao Long who have given me much useful advices and have comforted me when I faced some setbacks in my research work. I also want to thank you my friends in Saskatoon who have given me spiritual support; they are Peter Block and Arlene Block, Milan, Tony Tam, Xia Wang and Luna Nelson.

The financial support of the University of Saskatchewan, The Department of Chemistry, College of Graduate Studies & Research, Agricultural Development Fund (ADF) and Natural Science and Engineering Research Council of Canada (NSERC) is

gratefully acknowledged.

I am very grateful to ShanShan who has given me tremendous spiritual support throughout the year of 2004. Thank you for sharing your opinions with me and I am glad to have a best friend like you. I will remember you forever and will not forget the good time we have in the summer.

Finally, I give my distinguished appreciation to my family especially my mother who prays for me throughout my postgraduate research life as well as my two sisters Karen and Christine who encourage me to be strong and optimistic in life.

# TABLE OF CONTENTS

|   |             |
|---|-------------|
| <b>PERMISSION TO USE</b> .....  | <b>i</b>    |
| <b>ABSTRACT</b> .....   | <b>ii</b>   |
| <b>ACKNOWLEDGEMENTS</b> .....   | <b>iii</b>  |
| <b>TABLE OF CONTENTS</b> .....  | <b>v</b>    |
| <b>LIST OF TABLES</b> .....   | <b>viii</b> |
| <b>LIST OF FIGURES</b> .....  | <b>ix</b>   |
| <b>LIST OF ABBREVIATIONS</b> .....  | <b>xii</b>  |
| <b>1. INTRODUCTION</b> .....  | <b>1</b>    |
| <b>1.1. RESEARCH OBJECTIVE</b> .....  | <b>1</b>    |
| <b>1.2. PROTEIN BACKGROUND</b> .....  | <b>2</b>    |
| <b>1.2.1.</b> History, Structure and Properties of Bovine Serum Albumin ..... | <b>2</b>    |
| <b>1.2.2.</b> Previous Studies on Bovine Serum Albumin .....                  | <b>10</b>   |
| <b>1.2.3.</b> History, Structure and Properties of Thioredoxin-2 .....        | <b>12</b>   |
| <b>1.3. PROTEIN PURIFICATION AND CHARACTERIZATION</b> .....                   | <b>16</b>   |
| <b>1.3.1.</b> Purification Methods and Strategies .....                       | <b>16</b>   |
| <b>1.3.2.</b> SDS-PAGE Gel Electrophoresis and Purity Determination .....     | <b>19</b>   |
| <b>1.3.3.</b> Dialysis .....  | <b>21</b>   |
| <b>1.3.4.</b> Dynamic Light Scattering and Homogeneity Determination .....    | <b>22</b>   |
| <b>1.4. PROTEIN CRYSTALLIZATION</b> .....                                     | <b>25</b>   |
| <b>1.4.1.</b> Principles of Protein Crystallization .....                     | <b>25</b>   |
| <b>1.4.2.</b> Kinetic and Thermodynamic Principles of Crystallization .....   | <b>30</b>   |
| <b>1.4.2.1.</b> Protein Crystal Nucleation .....                              | <b>30</b>   |
| <b>1.4.2.2.</b> Protein Crystal Growth and Cessation .....                    | <b>31</b>   |
| <b>1.4.3.</b> Crystallization Methods .....                                   | <b>33</b>   |
| <b>1.4.4.</b> Importance Considerations in Protein Crystallization .....      | <b>38</b>   |
| <b>1.4.5.</b> Strategies and Approaches in Growing Crystals .....             | <b>42</b>   |
| <b>1.5. PROTEIN CRYOCRYSTALLIZATION</b> .....                                 | <b>47</b>   |
| <b>1.5.1.</b> Cryocrystallography Background .....                            | <b>47</b>   |
| <b>1.5.2.</b> Principle of Cryoprotection .....                               | <b>49</b>   |

|   |           |
|---|-----------|
| 1.5.3. Crystal Handling, Mounting, Cooling, Storage and Transportation .. | 52        |
| <b>1.6. X-RAY DIFFRACTION .....</b>                                       | <b>54</b> |
| 1.6.1. Protein, Crystal and X-ray .....                                   | 54        |
| 1.6.2. Bragg's Law .....  | 55        |
| 1.6.3. Asymmetric Unit, Space Group, Unit Cell and Bravais Lattices.....  | 56        |
| 1.6.4. X-Ray Diffraction Data Collection .....                            | 60        |
| <br>  |           |
| <b>2. MATERIALS AND METHODS .....</b>                                     | <b>61</b> |
| <b>2.1. CHEMICALS .....</b>   | <b>61</b> |
| <b>2.2. EQUIPMENT .....</b>   | <b>65</b> |
| <b>2.3. PROTEIN OVEREXPRESSION .....</b>                                  | <b>66</b> |
| <b>2.4. PROTEIN PURIFICATION .....</b>                                    | <b>67</b> |
| 2.4.1. Purification of Bovine Serum Albumin .....                         | 67        |
| 2.4.1.1. Anion Exchange Chromatography .....                              | 67        |
| 2.4.1.2. Ultrafiltration .....  | 68        |
| 2.4.1.3. Dialysis .....   | 68        |
| 2.4.2. Purification of Thioredoxin-2 .....                                | 69        |
| 2.4.2.1. Cell lysis .....   | 69        |
| 2.4.2.2. Dialysis .....   | 69        |
| 2.4.2.3. Anion Exchange Chromatography .....                              | 70        |
| 2.4.2.4. Ultrafiltration .....  | 70        |
| 2.4.2.5. Cation Exchange Chromatography .....                             | 71        |
| 2.4.2.6. Dialysis after Cation Exchange Chromatography .....              | 71        |
| <b>2.5. PROTEIN CHARACTERIZATION .....</b>                                | <b>71</b> |
| 2.5.1. SDS-PAGE Electrophoresis .....                                     | 71        |
| 2.5.2. Dynamic Light Scattering Measurement .....                         | 72        |
| 2.5.3. Bradford Assay .....   | 73        |
| <b>2.6. PROTEIN CRYSTALLIZATION .....</b>                                 | <b>74</b> |
| 2.6.1. Preparation of Buffer Solutions .....                              | 74        |
| 2.6.2. Crystallization Methods .....                                      | 76        |
| <b>2.7. PROTEIN CRYOCRYSTALLIZATIONS .....</b>                            | <b>77</b> |
| 2.7.1. Flash Cooling of Protein Crystals .....                            | 77        |
| 2.7.2. Protein X-ray Diffraction .....                                    | 79        |

|   |            |
|---|------------|
| <b>3. RESULTS AND DISCUSSION .....</b>                                  | <b>81</b>  |
| <b>3.1. BOVINE SERUM ALBUMIN .....</b>                                  | <b>81</b>  |
| 3.1.1. Introduction .....   | 81         |
| 3.1.2. Purity Determination of Bovine Serum Albumin .....               | 81         |
| 3.1.3. Purification of Bovine Serum Albumin .....                       | 83         |
| 3.1.3.1. Purification of BSA by Anion Exchange<br>Chromatography .....  | 83         |
| 3.1.3.2. SDS-PAGE Analysis after Anion Exchange<br>Chromatography ..... | 83         |
| 3.1.3.3. SDS-PAGE Analysis after Ultrafiltration and Dialysis ....      | 84         |
| 3.1.4. Concentration Determination of Purified Bovine Serum Albumin ... | 85         |
| 3.1.5. Homogeneity Determination of Bovine Serum Albumin .....          | 87         |
| 3.1.6. Crystallization Trials of Bovine Serum Albumin .....             | 90         |
| 3.1.7. Cryocrystallography of Bovine Serum Albumin .....                | 100        |
| <b>3.2. THIOREDOXIN-2 .....</b>   | <b>107</b> |
| 3.2.1. Introduction .....   | 107        |
| 3.2.2. SDS-PAGE Analysis after Overexpression and Cell Lysis .....      | 108        |
| 3.2.3. Purification of Thioredoxin-2 .....                              | 109        |
| 3.2.3.1. Anion Exchange Chromatography Purification .....               | 109        |
| 3.2.3.2. Cation Exchange Chromatography Purification .....              | 110        |
| 3.2.4. Concentration Determination of Purified Thioredoxin-2 .....      | 112        |
| 3.2.5. Homogeneity Determination of Purified Thioredoxin-2 .....        | 114        |
| 3.2.6. Crystallization Trials of Thioredoxin-2 .....                    | 115        |
| 3.2.7. Cryocrystallography of Thioredoxin-2 .....                       | 117        |
| <b>4. CONCLUSIONS AND FUTURE PERSPECTIVES .....</b>                     | <b>122</b> |
| <b>4.1. SUMMARY OF BOVINE SERUM ALBUMIN .....</b>                       | <b>122</b> |
| <b>4.2. SUMMARY OF THIOREDOXIN 2 .....</b>                              | <b>124</b> |
| <b>4.3. CONCLUSIONS .....</b>   | <b>126</b> |
| <b>4.4. FUTURE WORK .....</b>   | <b>127</b> |
| <b>REFERENCES .....</b>   | <b>130</b> |
| <b>APPENDICES .....</b>   | <b>141</b> |

# LIST OF TABLES

| <b>Number</b> | <b>Title</b>  | <b>Page</b> |
|---------------|---|-------------|
| 1.1           | Binding regions of BSA and its binding ligands  | 8           |
| 1.2           | Chromatography and separation parameters used for protein purification  | 18          |
| 1.3           | Range of separation of proteins in SDS-PAGE of different acrylamide concentrations  | 20          |
| 1.4           | Important factors affecting macromolecular crystallization  | 29          |
| 1.5           | List of cryoprotectants used successfully in flash-cooling the macromolecular crystals  | 50          |
| 1.6           | The seven crystal systems   | 59          |
| 2.1           | Preparation of Bradford Assay standard solutions  | 74          |
| 2.2           | The preparation of 50 mM K-PO <sub>4</sub> buffer solution at different pHs at 25°C   | 75          |
| 3.1           | The Bradford Assay absorbance data of the concentrated purified BSA sample solution   | 86          |
| 3.2           | Summary results of various cryo-conditions of BSA crystals that were prepared for X-ray diffraction experiments at the SSSC   | 103         |
| 3.3           | Summary result of the number of molecules in an asymmetric unit (a.s.u.) within a unit cell of a BSA crystal                  | 105         |
| 3.4           | Bradford assay absorbance data of the purified Trx-2 sample solutions   | 113         |
| 3.5           | Summary results of various cryo-conditions of Trx-2 crystals that were prepared for X-ray diffraction experiments at the SSSC | 121         |
| 4.1           | The Comparison between BSA crystallographic data done by Thome and me   | 124         |
| 4.2           | The Comparison between Trx-2 published crystallographic data and my results   | 125         |

# LIST OF FIGURES

| <b>Number</b> | <b>Title</b>   | <b>Page</b> |
|---------------|--|-------------|
| 1.1           | Structure organization of BSA  | 4           |
| 1.2           | Amino acid sequence of BSA   | 6           |
| 1.3           | The tertiary structure of HSA  | 7           |
| 1.4           | The square planar coordination of the metal ions ( $\text{Cu}^{2+}$ and $\text{Ni}^{2+}$ ) interact with BSA, HSA and other serum albumins | 9           |
| 1.5           | The reaction scheme of thioredoxin catalyzed protein disulfide reduction   | 13          |
| 1.6           | The crystal structure of Trx-m (Spinach Chloroplast)   | 15          |
| 1.7           | The size distributions of proteins that explain the protein crystallizability  | 24          |
| 1.8           | The solubility phase diagram for crystallization from solution   | 27          |
| 1.9           | Diagram of the thermodynamic potential of a crystallization system required for forming the critical size of nuclei                        | 31          |
| 1.10          | The hanging-drop vapor diffusion method for protein crystallization  | 35          |
| 1.11          | The sitting-drop vapor diffusion method for protein crystallization  | 36          |
| 1.12          | The microbatch method for protein crystallization  | 37          |
| 1.13          | Bar chart showing the most commonly used crystallization methods   | 38          |
| 1.14          | Pathway for determining the optimal cryoprotectant concentration   | 51          |
| 1.15          | The geometry of diffraction and its relationship to Bragg's Law  | 55          |

|             |   |     |
|-------------|---|-----|
| <b>1.16</b> | There are six unit cells in this crystalline lattice.   | 57  |
| <b>1.17</b> | The unit cell with edges a, b, c and angles $\alpha$ , $\beta$ , and $\gamma$   | 58  |
| <b>3.1</b>  | SDS-PAGE analysis of original BSA samples   | 82  |
| <b>3.2</b>  | Chromatogram of BSA fractions in anion exchange chromatography  | 83  |
| <b>3.3</b>  | SDS-PAGE analysis of BSA samples after anion exchange chromatography  | 84  |
| <b>3.4</b>  | SDS-PAGE analysis of purified BSA samples   | 85  |
| <b>3.5</b>  | The Bradford Assay calibration curve used to determine the concentration of purified BSA sample solution at the wavelength of 595 nm                                  | 86  |
| <b>3.6</b>  | Monomodal histogram of 1 mg/ml purified BSA solution  | 88  |
| <b>3.7</b>  | Monomodal histogram of 1 mg/ml unpurified BSA solution  | 89  |
| <b>3.8</b>  | SDS-PAGE analysis of original and purified BSA samples  | 92  |
| <b>3.9</b>  | The quality of BSA crystals was improved and the quantity of BSA crystals was increased after altering the buffer solution from 50 mM K-PO <sub>4</sub> to 25 mM NaAc | 94  |
| <b>3.10</b> | The difference between the BSA crystals grown in different buffer solutions at 20°C   | 96  |
| <b>3.11</b> | BSA Single Crystal (about 0.35 mm x 0.35 mm x 0.40 mm)  | 98  |
| <b>3.12</b> | BSA single crystal inside the loop located on the goniometer  | 102 |
| <b>3.13</b> | X-Ray Diffraction Pattern of a BSA crystal that cryoprotected by 30% glucose  | 104 |
| <b>3.14</b> | X-ray diffraction pattern of a Trx-2 crystal that had been collected at 2.4 Å resolution  | 107 |

|             |  |     |
|-------------|--|-----|
| <b>3.15</b> | SDS-PAGE analysis of Trx-2 samples after overexpression and purification                               | 108 |
| <b>3.16</b> | Chromatogram of the purification of Trx-2 sample solutions collected in anion exchange chromatography  | 110 |
| <b>3.17</b> | Chromatogram of the purification of Trx-2 sample solutions collected in cation exchange chromatography | 111 |
| <b>3.18</b> | SDS-PAGE analysis of Trx-2 sample solutions after cation exchange chromatography                       | 112 |
| <b>3.19</b> | Bradford assay calibration curve for purified Trx-2 sample solutions                                   | 113 |
| <b>3.20</b> | Monomodal histogram of 1.0 mg/ml of purified Trx-2 solution  | 114 |
| <b>3.21</b> | The optimization of Trx-2 crystals   | 116 |
| <b>3.22</b> | X-ray Diffraction Pattern of a Trx-2 crystal that cryoprotected by 10% PEG 400                         | 118 |
| <b>3.23</b> | X-ray diffraction pattern of a Trx-2 crystal was collected at 3.2 Å resolution at the SSSC             | 119 |

## LIST OF ABBREVIATIONS

|                   |  |
|-------------------|--|
| 3-D               | Three dimensional  |
| Å                 | Angstrom ( $10^{-10}$ m)                                   |
| AEBSF             | [4-(2-Aminoethyl)benzenesulfonylfluoride]                  |
| APS               | Ammonium persulfate  |
| Asn               | Asparagine   |
| Asp               | Aspartic acid  |
| BIS               | Bisacrylamide  |
| BMCD              | Biological macromolecule crystallization database          |
| BSA               | Bovine serum albumin                                       |
| CA                | Citric acid  |
| CCD               | Charge couple device                                       |
| Cu <sup>2+</sup>  | Copper (II)  |
| Cys               | Cysteine   |
| d                 | Interplanar spacing  |
| Da                | Dalton   |
| DIW               | De-ionized water   |
| DLS               | Dynamic light scattering                                   |
| DNase             | Deoxyribonuclease  |
| DTT               | Dithiothreitol   |
| <i>E. coli</i>    | Escherichia coli   |
| EG                | Ethylene glycol  |
| ESA               | Equine serum albumin                                       |
| ESR               | Electron Spin Resonance                                    |
| FAD               | Flavin adenine dinucleotide                                |
| FADH <sub>2</sub> | Flavin adenine dinucleotide (reduced form)                 |
| Gln               | Glutamine  |
| Gly               | Glycine  |
| GSA               | Goat serum albumin   |
| HEPES             | [N- [2-Hydroxyethyl] piperazine-N'- 2-ethanesulfonic acid] |

|                     |  |
|---------------------|--|
| His                 | Histidine  |
| <i>H. pylori</i>    | Helicobacter pylori  |
| HSA                 | Human serum albumin  |
| IPTG                | Isopropyl- $\beta$ -D-thiogalactopyranoside  |
| K                   | Kelvin   |
| K-PO <sub>4</sub>   | The buffer solution mixture of KH <sub>2</sub> PO <sub>4</sub> and K <sub>2</sub> HPO <sub>4</sub> |
| LB                  | Luria-Bertani  |
| MES                 | 2-[N-Morpholino]ethanesulfonic acid  |
| Mo                  | Molybdenum   |
| MPD                 | 2-methyl-2, 4-pentanediol  |
| MSA                 | Mouse serum albumin  |
| MWCO                | Molecule weight cut-off  |
| NaAc                | Sodium acetate   |
| Na-CACO             | Sodium-cacodylate  |
| NaCit               | tri-Sodium citrate   |
| NADP <sup>+</sup>   | Nicotinamide adenine dinucleotide phosphate  |
| NADPH               | Nicotinamide adenine dinucleotide phosphate (reduced form)   |
| Ni <sup>2+</sup>    | Nickel (II)  |
| NMWL                | Nominal molecular weight limit   |
| OD                  | Optical density  |
| OSA                 | Sheep serum albumin  |
| P-S <sub>2</sub>    | Protein with disulfide   |
| P-(SH) <sub>2</sub> | Protein with dithiol   |
| PAGE                | Polyacrylamide gel electrophoresis   |
| PDB                 | Protein data bank  |
| PEG                 | Polyethylene glycol  |
| PEG MME             | Polyethylene glycol monomethyl-ether   |
| Phe                 | Phenylalanine  |
| pI                  | Isoelectric point  |
| Pro                 | Proline  |
| PSA                 | Pig serum albumin  |

|                         |  |
|-------------------------|--|
| rpm                     | Revolution per minutes   |
| RSA                     | Rat serum albumin  |
| RCSB                    | Research collaboratory for structural bioinformatics                   |
| SAS                     | Saturated ammonium sulfate   |
| SDS                     | Sodium dodecyl sulfate   |
| SDS-PAGE                | Sodium dodecyl sulfate–polyacrylamide gel electrophoresis              |
| SSA                     | Salmon serum albumin   |
| SSSC                    | Saskatchewan Structural Science Center                                 |
| TEMED                   | N, N, N', N'-tetramethylethylenediamine                                |
| Thr                     | Threonine  |
| TM                      | Thiomolybdate  |
| Trx                     | Thioredoxin  |
| TrxR                    | Thioredoxin reductase  |
| TrxR-S <sub>2</sub>     | Thioredoxin reductase (oxidized form)                                  |
| TrxR-(SH) <sub>2</sub>  | Thioredoxin reductase (reduced form)                                   |
| Trx-S <sub>2</sub>      | Thioredoxin (oxidized form)  |
| Trx-(SH) <sub>2</sub>   | Thioredoxin (reduced form)   |
| Tris                    | Tris(hydroxymethyl)aminomethane  |
| UV/Visible              | Ultraviolet/Visible  |
| WHO                     | World Health Organization  |
| XSA                     | Frog serum albumin   |
| Zn <sup>2+</sup>        | Zinc (II)  |
| %PolyD                  | %Polydispersity  |
| $\lambda$               | Wavelength   |
| $\theta$                | Angle of reflection  |
| a, b, c                 | Axial lengths of a unit cell along x, y and z coordinates respectively |
| $\alpha, \beta, \gamma$ | Interaxial angles between b & c, c & a, and a & b respectively         |

# CHAPTER 1: INTRODUCTION

## 1.1. RESEARCH OBJECTIVE

Copper deficiency is known as a common issue in cattle (Ward *et al.*, 1996). It is prevalent in regions that have high molybdenum concentration in pastures. The formation of thiomolybdates (TMs) in the rumen can render the copper unavailable (Suttle, 1991). The interactions of copper, molybdenum (Mo) and sulfur (obtained from inorganic or organic sources) in ruminants has the adverse effect on the rumen of grazing animals by depleting the available copper. My primary research objective is to obtain the 3-D crystal structure of bovine serum albumin (BSA) and then to study the interactions of copper (II) ( $\text{Cu}^{2+}$ ) and thiomolybdates with BSA. A detailed knowledge of the 3-D structure of this protein is imperative to understand its physical properties, and binding modes with copper and thiomolybdates. Once the protein tertiary structure is known, it can act as a template to investigate the interactions that occur between TMs,  $\text{Cu}^{2+}$  and BSA. It is anticipated that the mechanism of how thiomolybdates render copper unavailable in BSA will be well defined, characterized, and understood through the solved structure.

High quality crystals in terms of size (at least up to 0.1 mm in each dimension) and appearance (single and sharp-edged) are required for structural determination of BSA. Excellent crystals that produce high resolution diffraction data, better than 3.0 Å are essential to achieve the solution and refinement of the 3-D structure of BSA. If high resolution BSA crystallographic data can be collected, then a 3-D macromolecular model can be built in order to simulate the potential binding site of  $\text{Cu}^{2+}$ , TM, BSA and their binding characteristic in the bovine ruminant system. Additionally, the crystallization of

BSA–Cu<sup>2+</sup>, BSA–TM and BSA–Cu<sup>2+</sup>–TM complexes can be used to study their individual interactions with each other.

The secondary research objective is to obtain high quality crystals of thioredoxin-2 (Trx-2) from *H. pylori* that can be diffracted to better than 2.4 Å resolution and to refine the structure that has been published recently at 2.4 Å resolution (Filson *et al.*, 2003). However the published diffraction data at high resolution have shown some split spots instead of single spots; this might make the process of protein refinement difficult due to the electron density of some neighboring atoms which are close and hardly resolved.

*H. pylori* has been recognized by the World Health Organization (WHO) as a type I carcinogen in the pathogenesis of gastric cancer (Williams, 1996), due to its significant impact towards duodenal ulcer. Our laboratory is interested in solving the 3-D structure of *H. pylori* thioredoxin in order to study its functions, mechanisms and their various interactions with the host cell. The structural analysis of Trx-2 in complex with other protein substrates will be explored in order to fully understand the role performed by Trx-2 in the redox environment of *H. pylori*.

## **1.2. PROTEIN BACKGROUND**

### **1.2.1. History, Structure and Properties of Bovine Serum Albumin**

Serum albumin has been one of the most extensively studied proteins for many years. It is the most abundant protein in blood plasma with a typical concentration of 50 g/L and functions as a transport protein for numerous endogenous and exogenous substances. It also plays an important role in regulating the colloid osmotic pressure of blood. It provides about 80% of the osmotic pressure and is responsible for the pH

maintenance in blood (Carter and Ho, 1994). Many researchers have studied the structures, functions and properties of serum albumins to understand their interactions with other molecules and ligands. Some of these albumins are human serum albumin (HSA), bovine serum albumin (BSA), equine serum albumin (ESA) and rat serum albumin (RSA). The molecules and ligands that have been studied include fatty acids, metal ions, pigments, and numerous drugs (McLachlan and Walker, 1977).

Joseph F. Foster first suggested that the model of albumin was a flexible linkage of semi-independent domains (Foster, 1960). Serum albumin has been a model protein for many years for physiological studies. Apart from HSA, ESA, RSA, the primary sequence of other serum albumins such as mouse serum albumin (MSA), pig serum albumin (PSA), sheep serum albumin (OSA), frog serum albumin (XSA), salmon serum albumin (SSA) have been determined. BSA (Brown, 1975) and HSA (Behrens *et al.*, 1975) were the earliest primary sequences that were determined. So far, the only tertiary structures determined of serum albumins are ESA (Ho *et al.*, 1993) and HSA (Carter *et al.*, 1989; Carter and He, 1990; He and Carter, 1992). No other 3-D structure of serum albumins have been published as of December 2004 according to RCSB Protein Data Bank (PDB) and Biological Macromolecular Crystallization Database (BMCD) (Carter *et al.*, 1989; He and Carter, 1992). The Protein Data Bank (Berman *et al.*, 2000) is a worldwide repository for the processing and distribution of 3-D biological macromolecular structures. The Biological Macromolecule Crystallization Database contains crystal data and the crystallization conditions, which have been compiled from literature. The macromolecules saved in the database include proteins, nucleic acids and viruses.

The primary sequence of BSA was presented in the same year as HSA (Brown, 1975; Brown, 1976). Brown proposed that BSA was composed of 582 amino acid residues. The sequence has 17 disulfide bonds resulting in nine loops formed by the bridges. BSA contains one single cysteine and eight pairs of disulfide bonds arranged in a way similar to those of HSA (He and Carter, 1992). BSA also contains a high content of Asp, Glu, Ala, Leu and Lys residues which is analogous to HSA and RSA. However, there were four amino acid residues (400–403) in the BSA sequence that were not determined at that time. Eventually, these four residues were identified as Gly–Phe–Gln–Asn (Reed *et al.*, 1980).

According to the amino acid sequence proposed by Brown, the structural features of BSA show that it is composed of three homologous domains. Each has about 190 residues, linked together by peptide chain as represented as Figure 1.1 and 1.2.

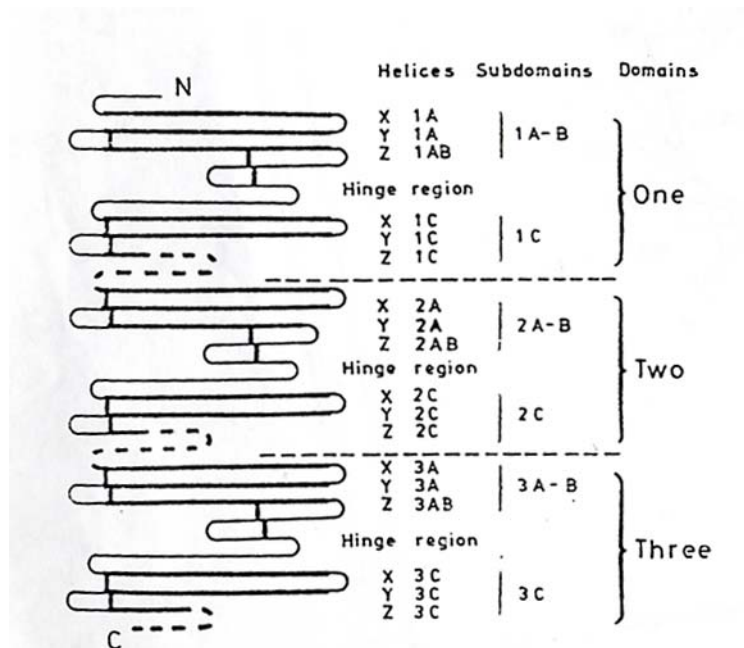


**Figure 1.1:** Structure organization of BSA (Kragh-Hansen, 1981; reproduced with permission of the author).

Each domain can be subdivided into two subdomains, namely A–B and C. The domains mainly contain a long loop and an intradomain hinge region. Every subdomain can be further subdivided into three helices “X”, “Y” and “Z” (Figure 1.1). Brown has compared the three domains (I, II and III) of BSA, which correspond to residues 1–190, 191–382 and 383–582 respectively. If domains I and II are aligned and compared, they show 25% identity, domains II & III and domains I & III show 21% and 18% identity respectively. This illustrates that domains I and II are more alike to each other than either is to domain III. This somewhat greater similarity between domains I and II implies that tandem duplication of a single domain gave rise to the ancestral gene of domains II and III. After passage of time, domains II and III diverged significantly. A single tandem half gene duplication from these domains was then added to domain I, thus giving the triple domain structure of present-day albumin (Brown, 1976).

Circular dichroism measurements suggest that BSA secondary structure content for  $\alpha$ -helix,  $\beta$ -sheet, turn and random coil are 48.7%, 0%, 10.9% and 30.7% respectively (Oberg and Uversky, 2001). In the secondary structure of BSA, it has been suggested that the  $\alpha$ -helices are uniformly placed in the subdomains and in the connections between the domains. Most of the residues in the long loops (except at the end) and the sections linking the domains possibly form  $\alpha$ -helices, whereas the intra-domain hinge regions are mainly non-helical structure. The three long helices in the subdomain are considered as principle elements of the structure. These run parallel with each other, and a trough is formed owing to the middle helix (Y) being slightly lower in position. The helices are mainly linked together by disulfide bridges (Kragh-Hansen, 1981).

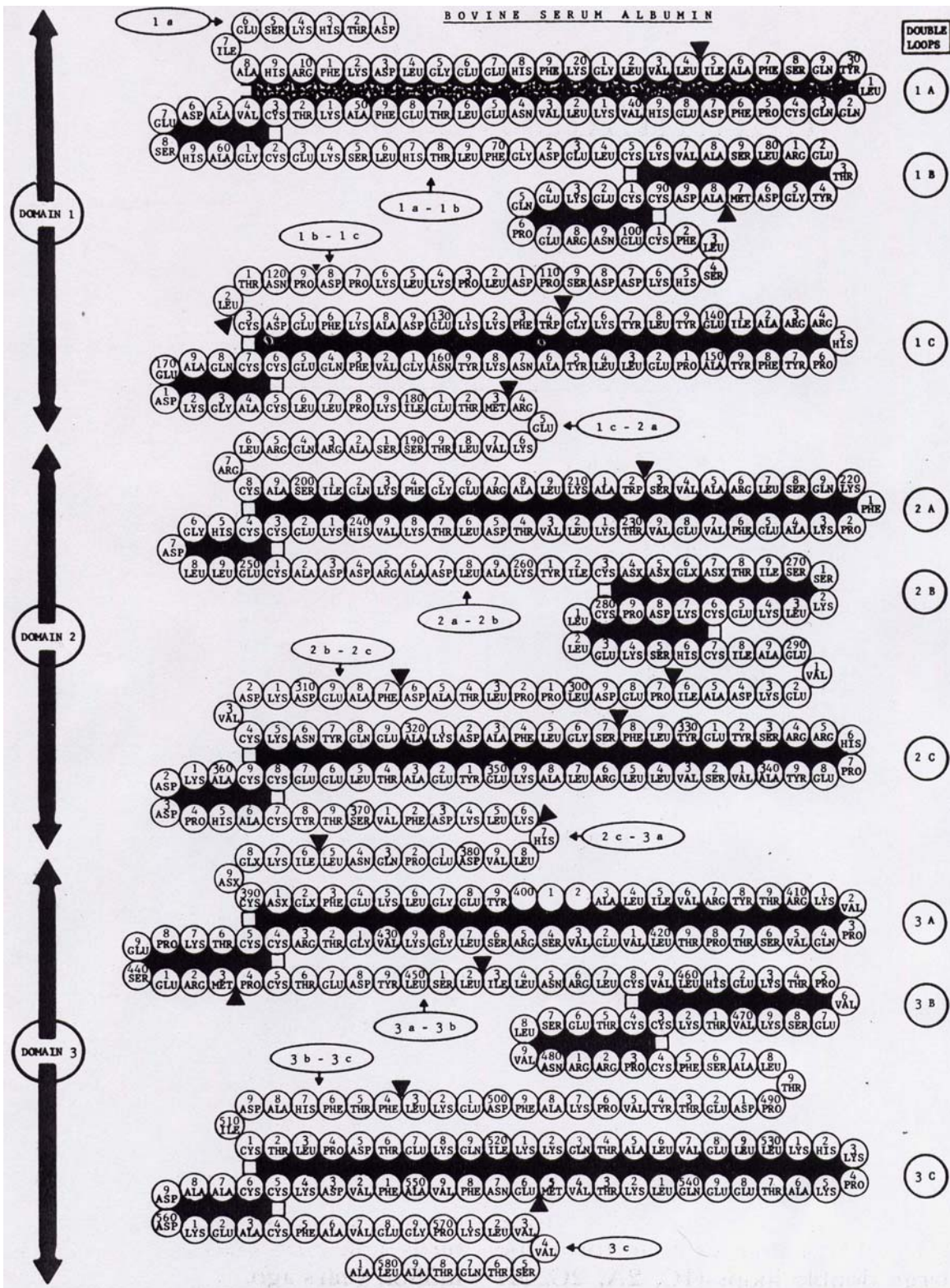
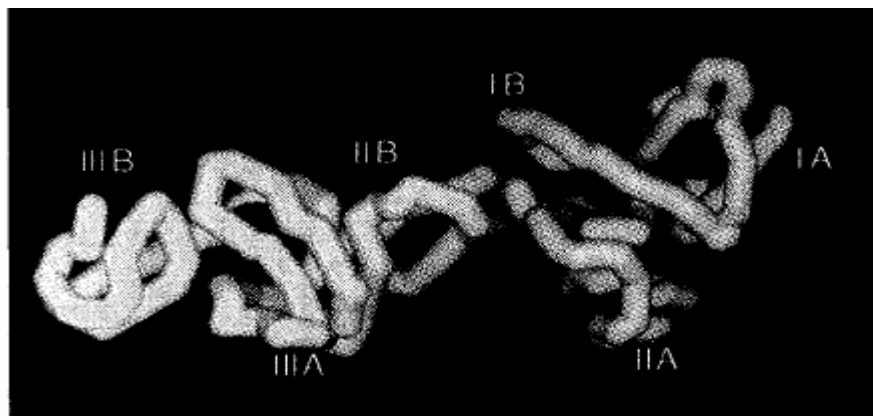


Figure 1.2: Amino acid sequence of BSA (Brown, 1976; reproduced with permission of the publisher).

Almost all the hydrophobic residues are found inside the trough and between the helices, while the polar residues can be mostly observed on the outer wall of the structure. The two subdomains adhere with their grooves toward each other forming a domain, and three such domains eventually form a serum albumin molecule (Kragh-Hansen, 1981).

In comparison with BSA, the tertiary structure of HSA demonstrates overall helical content and high cysteine content with 17 disulfide bonds of the molecule. It has three structurally homologous domains. Each domain is made up of two subdomains referred as A and B that correspond to Brown's model as A-B and C (such as 2A-B & 2C domains of BSA are corresponded to IIA & IIB domains of HSA). Subdomain IA, IB, and IIA pack tightly to form an enlarge head for the molecule whereas the extended tail is constituted by subdomain IIB, IIIA, and IIIB (Carter *et al.*, 1989). BSA and HSA share about 80% primary sequence identity with each other (Peters, 1985). This result implies that BSA and HSA are homologous proteins which might have very similar biological functions.



**Figure 1.3:** The tertiary structure of HSA. It has three domains and each domain consists of two subdomains which refer as (IA, IB), (IIA, IIB) & (IIIA, IIIB) respectively (Carter *et al.*, 1989; reproduced with permission of the publisher).

The most interesting property of serum albumins is the high affinity with various kinds of ligands or negatively charged molecules which are located in different binding regions in serum albumins. Kragh-Hansen has proposed a number of binding regions on the albumin molecule as shown in Table 1.1. The most outstanding feature of the albumin-ligand interactions is the presence of a few high affinity binding sites and a number of low affinity binding sites that interact with various kinds of ligands such as fatty acids, metals, etc (Kragh-Hansen, 1981).

Compared to the proposed BSA-ligand binding studies, the primary binding regions of HSA have been demonstrated to be mostly located in subdomain IIA and IIIA of the molecule. Many ligands, for example tryptophan, fatty acids and bilirubin are found to interact preferentially in those regions at IIIA and IIA sites respectively (He and Carter, 1992). These results are in accordance with Kragh-Hansen proposal.

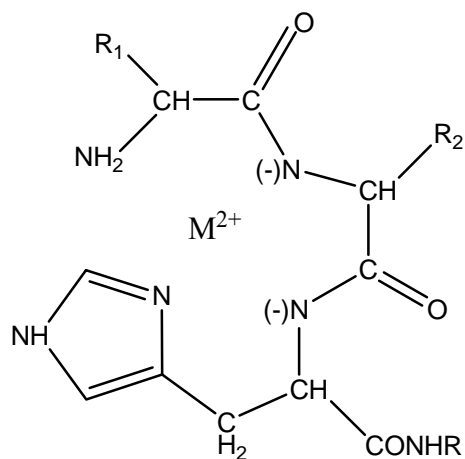
| Binding Region | Domain         | High Affinity Binding Site          |
|----------------|----------------|-------------------------------------|
| 1              | III            | Fatty Acids                         |
| 2              | II or III      | Tryptophan, Octanoate               |
| 3              | II             | Bilirubin                           |
| 4              | N-terminal end | $\text{Cu}^{2+}$ , $\text{Zn}^{2+}$ |
| 5              | II             | Haemin                              |

**Table 1.1:** Binding regions of BSA and its binding ligands.

Spectral and titrimetric studies have showed that the binding of copper (II) ions with bovine serum albumin is on a unique and well-defined binding site at its N-terminus. The binding site is composed of the first three amino acids Asp-Thr-His- (D-T-H-) from the amino terminal end of BSA molecule. It corresponds to the binding region 4 as mentioned in Table 1.1 (Peters and Blumenstock, 1967). A second  $\text{Cu}^{2+}$ -binding site has

been suggested by isothermal titration calorimetry (ITC) data that shows that additional  $\text{Cu}^{2+}$  ions likely bind to a free Cysteine site (a free thiol) in the BSA molecule (Zhang *et al.*, 2000; Zhang and Wilcox, 2002). NMR, ESR, visible spectroscopy and X-ray crystallography have demonstrated that metals (e.g.  $\text{Cu}^{2+}$  and  $\text{Ni}^{2+}$ ) are coordinated in the N-terminus of BSA, HSA and other serum albumins that have an N-terminus X–X–His sequence in a square planar configuration as indicated in Figure 1.4 (Harford and Sarkar, 1997).

Albumins that lack histidine at position 3 in N-terminus sequence have a much lower affinity for  $\text{Cu}^{2+}$  binding (Peters, 1984). HSA, BSA and RSA all have the histidine in the same position 3 and they bind with  $\text{Cu}^{2+}$  specifically. Dog serum albumin which has a tyrosine in position 3, lacks the specific  $\text{Cu}^{2+}$ –serum albumin binding site (Harford and Sarkar, 1997). This result demonstrates that the third residue histidine in N-terminus of serum albumins seems to play an important and specific role in copper binding.



M = Cu, Ni

**Figure 1.4:** The square planar coordination of the metal ions ( $\text{Cu}^{2+}$  and  $\text{Ni}^{2+}$ ) interact with BSA, HSA and other serum albumins (Zhang and Wilcox, 2002).

The formation of thiomolybdates in the ruminant environment has been recognized as an antagonist toward copper binding, and a major cause of the copper deficiency that occurs in cattle (Clark and Laurie, 1980). The thiomolybdate ions including tri-thiomolybdate and tetra-thiomolybdate are involved in the copper antagonism behavior. These TMs interact with copper in ruminants to cause copper deficiency. A ternary complex between  $\text{Cu}^{2+}$ , BSA and TMs has been suggested that the binding between TM and  $\text{Cu}^{2+}$ -albumin, or between  $\text{Cu}^{2+}$  and TM-albumin will be initiated rather than  $\text{Cu}^{2+}$ -TM, because a  $\text{Cu}^{2+}$ -TM complex forms an insoluble product (Quagraine and Reid, 2001). This provides a chemical basis to study the interactions between BSA,  $\text{Cu}^{2+}$  and thiomolybdates.

### **1.2.2. Previous Studies on Bovine Serum Albumin**

X-ray crystallographic studies on BSA have been attempted previously by another research group in Department of Chemistry at the University of Saskatchewan (Thome, 2001). In the Thome studies, the initial crystallization attempt did not produce any crystals. So, he purified the protein that was purchased from the supplier using size exclusion chromatography to collect the purest fractions. The purity of BSA was verified by SDS-PAGE and the concentration of BSA was determined by Bradford Assay (Thome, 2001).

The protein concentration used for BSA crystallization trials was mainly 10 mg/ml. The hanging drop diffusion method was applied to grow BSA crystals at room temperature and 14°C. However BSA crystals only appeared at room temperature. The crystallization conditions of BSA were 50 – 65% Saturated Ammonium Sulfate with

50 mM potassium phosphate buffer (pH 5.6 – 6.6). The BSA crystals took over 2 months to form and their sizes were no larger than 0.4 mm in the largest dimension. Addition of the salts such as NaCl, KCl or MgCl<sub>2</sub> in the crystallization trials reduced the growth time of BSA crystals, large crystals typically formed in 3 – 4 weeks. BSA crystals were also found in the presence of NiCl<sub>2</sub> or CoCl<sub>2</sub> as an additive in the crystallization trials (Thome, 2001).

Two BSA crystals were sent to University of Calgary for conducting X-ray diffraction experiment at room temperature. Both crystals were diffracted with a maximum resolution of about 8 Å. The space group of BSA crystals is a primitive hexagonal, P6, with cell dimensions of a = 148.24 Å, b = 148.24 Å and c = 356.70 Å;  $\alpha = 90^\circ$ ,  $\beta = 90^\circ$ ,  $\gamma = 120^\circ$ . Another two BSA crystals were prepared for X-ray diffraction studies on the in-house diffraction system at the Department of Biochemistry, University of Saskatchewan. The results showed that no diffraction patterns were recorded. For crystals sent to both places, they were crystallized under similar conditions (10 mg/ml BSA, 56 – 57% SAS with 50 mM potassium phosphate buffer at pH 5.6 or 5.8). The only difference was the BSA crystals that were diffracted on the in-house facility were crystallized in the presence of salts, NiCl<sub>2</sub> or CoCl<sub>2</sub> (Thome, 2001).

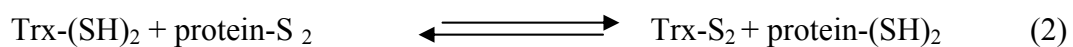
Five BSA crystals which were grown in the presence of different salts (NaCl, KCl, MgCl<sub>2</sub>, NiCl<sub>2</sub> or CoCl<sub>2</sub>) were frozen by the cryo-oil, Paratone-N in order to conduct X-ray diffraction experiments at low temperature on the in-house diffraction system at the Department of Biochemistry, University of Saskatchewan. The results showed that none of the BSA crystals were diffracted and ice rings were observed. Therefore, Paratone-N was not considered as an appropriate cryo-oil to flash cool BSA crystals (Thome, 2001).

In summary, BSA crystals that crystallized under SAS/K-PO<sub>4</sub> condition were diffracted to 8 Å at room temperature, but at low temperature no diffraction patterns were collected due to inappropriate cryoprotectant was chosen. So, at such resolution, the only information could be collected was the crystal symmetry and its unit cell dimensions. As a result the three-dimensional structure of BSA still remains unknown.

### 1.2.3. History, Structure and Properties of Thioredoxin-2

Thioredoxin (Trx) is a ubiquitous and multifunctional small protein, having an active site of conserved amino sequence: –Cys–Gly–Pro–Cys– (–CGPC–). It behaves as an electron transporter containing a disulfide bridge (–S–S–) in its oxidized form (Trx-S<sub>2</sub>) and a dithiol in its reduced form (Trx-(SH)<sub>2</sub>); both forms are catalytically redox-active (Holmgren, 1985). There are a variety of roles played by different thioredoxins. For instances, Trx in plant is known to regulate photosynthetic enzymes in the chloroplast by light via ferredoxin (Bunchanan, 1991). Nevertheless, apart from a few exceptions, most thioredoxins have the highly conserved sequence –CGPC– located in their dithiol/disulfide active site (Arner and Holmgren, 2000). The redox reaction that is catalyzed by thioredoxin reductase is shown below (Holmgren, 1981; Holmgren and Bjornstedt, 1995):

#### Thioredoxin Reductase



The oxidized form of Trx is reduced by NADPH and thioredoxin reductase (TrxR) to form Trx-(SH)<sub>2</sub> and through the reversible oxidation of the Trx-(SH)<sub>2</sub> active site dithiol, to a disulfide again (Trx-S<sub>2</sub>). The thioredoxin, NADPH and thioredoxin reductase together form a system called “The Thioredoxin System”.

The main function of thioredoxin is to reduce the disulfide bonds of target proteins to change the conformation and activity of these proteins. The active form of thioredoxin is Trx-(SH)<sub>2</sub>, the two cysteines at the active site are in the thiol form. The Trx-(SH)<sub>2</sub> behaves as a reducing agent to reduce disulfide bonds in the target proteins. After the reduction of the target proteins, the two cysteines form a disulfide bond between them. The oxidized form (Trx-S<sub>2</sub>) can be reduced by the enzyme TrxR accompanied with NADPH. The mechanism of protein disulfide reduction catalyzed by the thioredoxin system is schemed as below (Arner and Holmgren, 2000; Holmgren, 1981; Holmgren, 1989; Minarik, 1997):

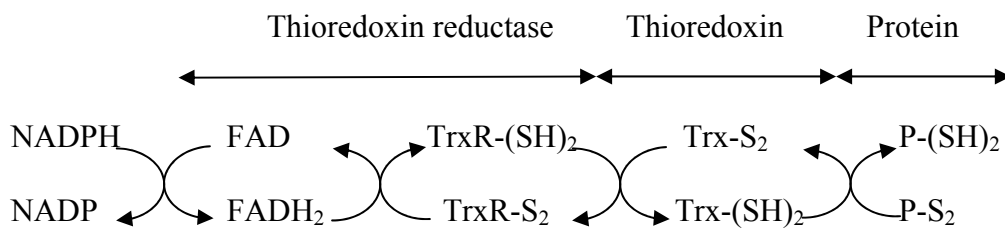


**Figure 1.5:** The reaction scheme of thioredoxin catalyzed protein disulfide reduction.

Thioredoxin can be described as a hydrogen donor or disulfide reductase. It can also function as a regulatory protein to regulate the thiol-disulfide status of the proteins. Thioredoxin is involved in many biological activities such as an antioxidant (Yoshida *et al.*, 2003), cofactor (Masutani *et al.*, 2004) and growth factor (Oblong *et al.*, 1994). It can

activate and regulate the DNA binding transcription factor NF- $\kappa$ B, and bind with various proteins (Powis and Montfort, 2001).

Thioredoxins have been isolated from different prokaryotic and eukaryotic species including mammals, plants, bacteria and yeasts. According to Protein Data Bank, the crystal structures of several thioredoxins from *Anabaena*, *Bacillus acidocaldarius*, *Chlamydomonas reinhardtii*, *E. coli*, human, Spinach chloroplast and *Trypanosoma brucei brucei* have been solved by X- ray crystallography. All of them have similar conformation, disulfide geometry, and share the common conserved active site –CGPC–. Thioredoxins that share the highest sequence similarity with *H. pylori* Trx 2 are Spinach chloroplast (28%), and *E. coli* (29%). One of them can be used as a search model for solving the unknown thioredoxin structure by molecular replacement phasing method.

In order to understand the common features of thioredoxin, Trx-m from Spinach chloroplast (Capitani *et al.*, 2000) can be used as an example. The crystal structure of Trx-m has a conserved active-site sequence –Cys–Gly–Pro–Cys– (–CGPC–) and shows the highly similar tertiary structure among thioredoxins. It shows that Trx is a protein composed of a  $\beta$ -sheet containing 5 parallel and antiparallel strands that forms the core of the molecule, and, flanked by four  $\alpha$ -helices displayed on the external surface (Figure 1.6).

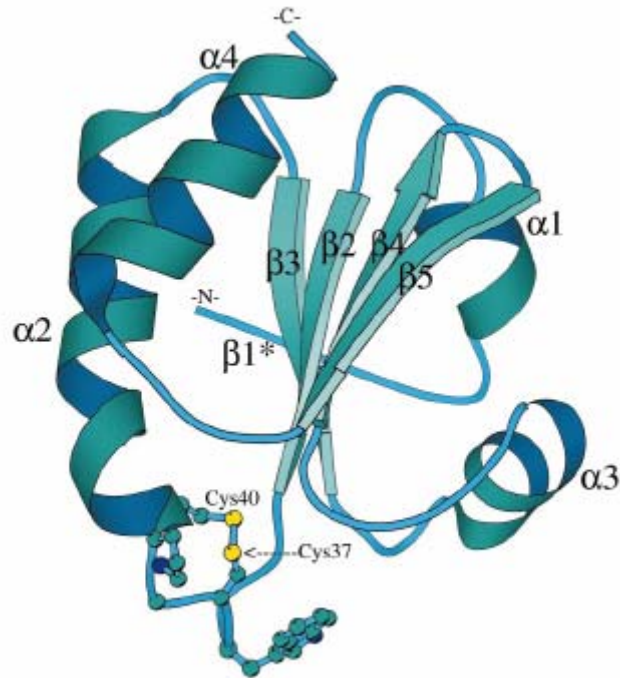


**Figure 1.6:** The crystal structure of Trx-m (Spinach Chloroplast) shows the molecule composed of a five-stranded  $\beta$ -sheet and surrounded by four  $\alpha$ -helices, and, active-site sequence –CGPC–. This structure is highly similar to most thioredoxins (Capitani *et al.*, 2000; reproduced with permission of the publisher).

The thioredoxin I am currently working on is from the gram-negative bacterium *Helicobacter pylori* (*H. pylori*) found in the stomach. *H. pylori* is a spiral shaped bacterium identified as the cause of persistent gastric inflammation in human stomach (Israel and Peek, 2001; Lamarque and Peek, 2003) and damages duodenal tissue resulting in peptic ulcer diseases such as duodenitis and duodenal ulcer and gastric malignancy (Walker and Crabtree, 1998). *H. pylori* has a direct relationship with the activating of the oxidative stress pathway to stimulate the formation of reactive oxygen species such as superoxide radicals that are associated with the inflammatory response. Eventually, the

production of oxygen species results in oxidative damage to gastric mucosa and a predisposition to gastric cancer (Shirin *et al.*, 2001).

*H. pylori* (strain 26695) has a circular genome of 1,667,867 base pairs and 1590 predicted coding sequence. Among all these sequence, there are two encoding genes that are identified as thioredoxins which are Trx A or ***Trx-1*** (HP0824) and Trx or ***Trx-2*** (HP1458) (Tomb *et al.*, 1997). The molecular weight of Trx-2 has been estimated about 11.7 kDa with 104 amino acids (Baker *et al.*, 2003). The two thioredoxins only show 33% primary sequence identity with each other by using sequence alignment software “Blast 2” to compare them (Tatusova and Madden, 1999). This result is comparatively low although they are the only two genes to encode the thioredoxin in *H. pylori* bacterium. Trx 1 has conserved motif –CGPC– but Trx 2 has unusual motif –CPDC–. This suggests that they may have different roles in the cell (Filson *et al.*, 2003).

### **1.3. Protein Purification and Characterization**

#### **1.3.1. Purification Methods and Strategies**

Microorganisms such as *Escherichia coli* (*E. coli*) can be used to produce various kinds of proteins in a biological laboratory. This protocol is popular because it shows good efficiency and high reproducibility (Higgins and Hames, 1999). Once a protein has been overexpressed, cell disruption is employed to release the proteins from the organism’s cytoplasm. Purification steps are then required to purify the proteins. The purified proteins can be characterized and analyzed to ensure that their purity and homogeneity are suitable for crystallization experiments.

Cell disruption is a strategy for isolating and extracting proteins from microorganism cells. In order to liberate the proteins from the cells in a soluble form, the intracellular compartments have to be broken in an appropriate buffer where proteins will be stable. The principle of this method is to not destroy or denature the proteins in terms of their structure, activities and functions. A number of methods have been established and applied including sonication, glass bead vortexing, enzyme digestion, osmotic shock or detergent lysis. Sonication is one of the most common cell disruption methods applicable to many microorganism sources including *E. coli*. In this method, a sonicator with an appropriate frequency is employed. This works by generating vibrations that cause mechanical shearing of the cell wall so that proteins will be released from the cell (Bollag *et al.*, 1996).

Precipitation of proteins by salts, organic solvents, and high molecular weight polymers or by altering the temperature or pH of the solution is an effective way for early protein purification. Precipitation by addition of a neutral salt is the most widespread way to fractionate proteins by the salting-out effect. The salting-out effect is due to the high salt concentration. It can be considered as the competition between salt ions and protein molecules for free water molecules. As the salt concentration increases, salt ions increasingly deprive the protein molecules of their needed solvent molecules. This causes the protein molecules to associate with one another until an aggregate or precipitate is formed.

The most common salts used are ammonium sulfate and sodium sulfate due to their high solubility, harmlessness to proteins and low cost. Organic solvents such as ethanol or acetone can be added into protein solutions to decrease the solubility of the

protein by reducing the dielectric constant of the medium. Low concentration PEG 6,000 and PEG 20,000 are the most frequently used organic polymers; the mechanism is similar to that for organic solvents.

Thermally stable proteins such as canavalin can be heated up to high temperatures to achieve purification without denaturation. This heat precipitation treatment is an alternative way to purify proteins because most proteins will be denatured and can be separated by centrifugation. Adjustments to pH can be another way to purify proteins. Proteins have isoelectric points (pI) in certain narrow pH ranges, so that the pH can be optimized to lower the solubility of the protein of interest, because the protein has minimum solubility at its isoelectric point. Precipitation at low temperature e.g. 4°C is generally required to avoid protein denaturation (McPherson, 1998).

The purification of proteins by various chromatography techniques are standard laboratory protocols. Chromatography is an extremely efficient separation technique to separate sample components (proteins) between stationary phase (absorbent) and mobile phase (buffer) by depending on differential column partitions. Chromatography systems can be classified into a few types according to their interaction between the absorbent and the sample components. A summary of various types of chromatography used for protein purification is shown in Table 1.2 (Janson and Ryden, 1998):

|   | Chromatography Type              | Molecular Property Exploited |
|---|----------------------------------|------------------------------|
| 1 | Affinity                         | Biological affinity          |
| 2 | Hydrophobic Interaction          | Polarity                     |
| 3 | Gel Filtration or Size Exclusion | Size and shape               |
| 4 | Immobilized Metal Ion Affinity   | Metal binding                |
| 5 | Ion Exchange                     | Net charge                   |

**Table 1.2:** Chromatography and separation parameters used for protein purification

For example, ion-exchange chromatography has a stationary phase where ionizable function groups are attached to the stationary phase through chemical bonding. These functional groups (fixed ions) located on the stationary phase carry another kind of ion (so-called counterion) where the charge is opposite to the functional groups. When retention occurs, proteins will displace these counterions and bind with the fixed ions through electrostatic interactions. As the salt concentration in the buffer (eluent) increases, the binding affinity between the fixed ions and the proteins will be reduced. In elution, the salts will displace proteins, due to the greater affinity of the fixed ions for the salts than the proteins. The proteins are eluted from the chromatographic column, and separation of the proteins can be achieved (Rossomando, 1990).

### **1.3.2. SDS Gel Electrophoresis and Purity Determination**

Polyacrylamide gel electrophoresis (PAGE) is an essential procedure used in the biological laboratory as an analytical tool to determine the molecule weight and purity of a protein. It provides a platform to analyze multiple samples simultaneously and multiple components in a single sample. The gel used does not chemically interact with biomolecules during electrophoresis.

Protein electrophoresis depends on the differences in shape, charge density and size of the proteins. Proteins are charged at any pH other than their isoelectric point (pI), thus the charged particles will migrate toward the electrode of opposite sign under the influence of an external electric field. Prior to electrophoresis, protein samples are heated in boiling water for 2 – 5 minutes in a sample buffer containing sodium dodecylsulfate (SDS). This hot ionic detergent is used to dissociate and unfold protein molecules and it

can tightly bind with proteins to confer a uniform negative charge on all of the proteins, so that in the electric field, the proteins will migrate toward the anode solely as a function of protein molecular weight (Rosenberg, 1996).

In electrophoretic separation, acrylamide is used as a medium to separate proteins according to their sizes. The movements of electrically charged particles are retarded by interactions with the surrounding gel matrix. The pore sizes formed in the gel are inversely proportional to the concentration of acrylamide, so individual gels can be prepared to allow certain molar masses of proteins to be analyzed. In summary, the higher the percentage of polyacrylamide gel, the smaller the pore sizes, therefore lower molecular weight of protein is more suitable to be characterized (See Table 1.3).

| [Acrylamide] %(w/v) | Range of Separation for Protein (kDa) |
|---------------------|---------------------------------------|
| 5                   | > 1000                                |
| 8                   | 300 – 1000                            |
| 12                  | 50 – 300                              |
| 15                  | 10 – 80                               |
| 20                  | 5 – 30                                |

**Table 1.3** Range of separation of proteins in SDS-PAGE of different acrylamide concentrations (Sheehan, 2000).

The fundamental principle of gel formation is the polymerization of acrylamide via free radical and chemical cross-linking. Polyacrylamide gels are composed of two chemicals, acrylamide monomer and N, N'-methylene bisacrylamide (BIS). The reaction is initiated by ammonium persulfate (APS) and catalyzed by N,N,N',N'-tetramethylethylenediamine (TEMED) to provide free radicals. The acrylamide monomers are polymerized to form long chains and the BIS molecules, where

incorporated, provide cross-links between the chains. This forms a regular matrix with "holes" that serve as pores in the polyacrylamide gel (Harris and Angal, 1989).

Once the protein samples have been separated in the gel matrix, the next step is to locate the position of each sample, therefore, staining is required. Proteins are usually stained with Coomassie Blue. It is a non-polar sulphated triphenylamine dye with detection limit of 200 ng for proteins. When it binds to the protein, a blue color will be displayed and maintained during electrophoresis (Garfin, 1990; Sheehan, 2000).

The electrophoresis method used is the discontinuous system, where different pHs are used to increase the resolution of polyacrylamide gel electrophoresis. In this system, two gels, the stacking gel and resolving gel are used, and their pH are held at ~ 6.9 and 8 – 9 respectively. The stacking gel has a lower gel concentration (~ 3 – 5 %) and neutral pH compared to resolving gel. It is used to introduce the sample and build up the sample at the interface between the staking and resolving gels to prevent diffusion of sample bands. The resolving gel or so-called separating gel has a higher acrylamide concentration and is used to separate sample components. Tris-glycine at pH 8 – 9 is used as a running buffer to mobilize the sample in the gel electrophoresis system.

### **1.3.3. Dialysis**

Dialysis is a separation process of substances driven by the concentration gradient and their varying diffusion rates through a semi-permeable membrane. It has been designed for desalting or buffer changing. Dialysis is widely used in the preparation and purification of macromolecules to remove or exchange low molecule weight impurities, salts, solvent components and contaminants. It provides a means to change the solution

for a protein sample by exchanging small molecules while retaining the macromolecules. It involves the equilibration of two solutions across a semi-permeable membrane with a size limitation. The membrane itself is made of cellulose acetate and is somewhat chemically inert and will not bind with the protein samples (McPhie, 1971).

In dialysis, the protein solution is placed inside a dialysis bag or tube. The protein solution is then dialyzed against several changes of the desired final buffer over a 24 hour period. The dialysis bag and tube are commercially available, and the varieties of the molecule weight cut-off (MWCO) point are ranged from 100 to 300,000 Daltons (Spectrum Laboratory, Inc.). The molecules that are smaller than the specific molecular weights can freely pass through the membrane but larger molecules are prevented from passage. Normally 3,500 and 10,000 Daltons membranes are used for protein dialysis.

#### **1.3.4. Dynamic Light Scattering and Homogeneity Determination**

Dynamic light scattering (DLS) is a non-invasive solution characterization technique that has been employed to study the nucleation and growth of crystals in protein solutions (Juarez-Martinez *et al.*, 2001). This technique has been exploited to investigate crystal formation by screening stock solutions for any aggregation prior to crystallization trial set-up (Protein Solutions, Application Notes).

Dynamic light scattering is used to measure and monitor intensity fluctuations in scattered light as a function of time. This technique is one of the most popular methods used to determine the hydrodynamic radius ( $R_h$ ) of sub-micron sized molecules such as proteins. The hydrodynamic radius is the effective size of the molecule as they are undergoing constant diffusion or so-called Brownian motion in the solution. The

measured intensities caused by the movement of protein particles in the solution are used to determine the diffusion coefficient and then calculate the hydrodynamic radius of the protein molecules. Hence, the polydispersity and molecular weight of the protein sample can be estimated (Protein Solutions, Lakewood, New Jersey).

The %polydispersity is used as an indicator to determine the homogeneity of a protein solution. It can be determined according to hydrodynamic radius (unit: nm) and polydispersity (unit: nm) of the protein particles where

$$\%polydispersity = (C_p / R_h) \times 100\%$$

The polydispersity ( $C_p$ ) is a value used to represent the standard deviation of a molecular weight distribution (or size distribution) of the protein particles (Dynamic software application notes).

Empirical results demonstrate that monodispersed protein samples have higher crystallizability than those which are polydispersed. Homogenous protein samples will initiate crystal nucleation and growth, so that crystals can be formed (Ferre-D'Amare and Burley, 1994; Ferre-D'Amare and Burley, 1997). It has been suggested that purity is not the only factor to be considered in protein crystallization, homogeneity of the protein sample is an important consideration as well (Ducruix and Giege, 1992). When the size distribution of a protein sample obtained from dynamic light scattering is narrow and monomodal, this indicates that crystals possibly could be formed. If the size distribution shown is either bimodal or trimodal or polydispersed (Figure 1.7), it seems that crystals are rarely formed, because aggregates are detected (Zulauf and D'Arcy, 1992).

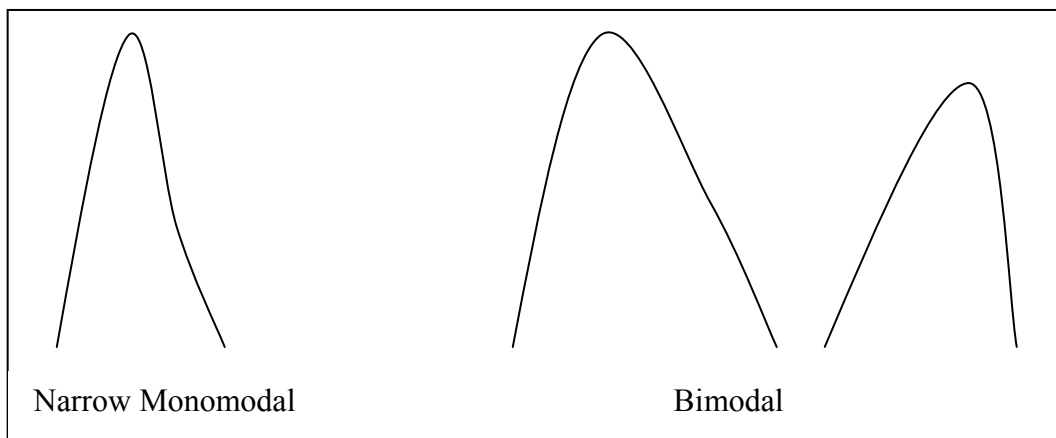


**Figure 1.7:** The size distributions of proteins that explain the protein crystallizability. If the size distribution of a protein is a narrow monomodal, protein crystals might form. If the size distribution of a protein is a broad bimodal, the presence of aggregates is indicated, protein crystals are unlikely to form (Zulauf and D' Arcy, 1992).

The homogeneity of a protein sample solution can be identified through the %polydispersity. The general guideline is that a monodispersed and homogenous sample solution is one that has %polydispersity less than 15% as shown in DLS experiment. If the %polydispersity is more than 30%, the sample solution is considered as polydispersed and not homogenous. If the %polydispersity is 15 – 30%, the sample solution shows the characteristic of moderate polydispersity (Protein Solutions, Instrument User's Guide).

## **1.4. PROTEIN CRYSTALLIZATION**

### **1.4.1. Principle of Protein Crystallization**

Crystallization of macromolecules is the limiting step in protein crystallography. The principles of crystallization of macromolecules are analogous to those of small molecules. Protein molecules themselves are distinctive, composed of approximately 50% solvent though this may vary from 30 – 78% (Matthews, 1985). Proteins are labile, fragile, and sensitive to external environments owing to their high solvent content, and the weak binding energies between protein molecules in the crystal (Littlechild, 1991). The only optimal conditions suitable for their growth are those that cause little or no perturbation of their molecule properties. As a result, crystals must be grown from a medium where temperature is constant and within a broad range of pH 3 – 10 because complete hydration is an essential factor for maintaining the crystal structure integrity.

There are many differences between small molecule crystals and protein crystals. In general, small molecule crystals are grown to large dimensions (1 – 100 cm), they are physically hard, brittle, easy to handle, have strong optical properties and can diffract X-rays intensively. This is because the small molecule crystals exhibit firm lattice interactions and highly ordered lattice arrangements within the crystal. In comparison, protein crystals are generally smaller in size (1 – 1000  $\mu\text{m}$ ), soft and crushed without difficulty, and with weak crystal forces. These kinds of crystals, which will redissolve if dehydration occurs, have weak optical properties and diffract X-rays weakly. They are also temperature sensitive, because protein solubility alters as a function of temperature. In theory, as the temperature rises, the solubility of proteins increases, thus, no crystals are formed or crystals will be redissolved (Bergfors, 1999). When crystals are exposed to

long-standing X-ray radiation, it can cause extensive damage of crystals. This is due to the weak lattice forces within the crystal structure (McPherson, 1982) and the X-rays can produce sufficient free radicals to cause specific chemical changes on the protein molecules such as the breaking of the disulfide bonds (Ravelli and McSweeney, 2000).

The crystallization of proteins from solution is a reversible equilibrium phenomenon. It contains three stages: nucleation, growth and cessation of growth. The formation of crystals is due to the decreasing free energy of the system while the formation of many new chemical bonds simultaneously outweighs the decreasing entropy of the system in order to grow a highly organized internal structure. In other words, the free energy of the system is reduced to its energy minimum and a thermodynamic driving force exists that provides for the ordering process of crystals (McPherson, 1982).

The basic strategy of producing protein crystals is to generate a certain degree of supersaturation in the solution. At the equilibrium point, the amount of protein molecules entering the solution is the same as the amount of protein molecules leaving the solution. This is referred to as the solubility limit of a protein. When the solubility of a protein is below this limit, the solution is undersaturated. If the solubility is equal to the limit, the solution is saturated. Crystals can grow only when the solubility exceeds the limit. Every protein has a unique solubility. Decreasing the solubility of the protein is the most effective way to create supersaturation for crystal growth. Only in a non-equilibrium supersaturated solution, can a crystal grow. Supersaturation can be achieved by different approaches including altering the buffer pH, temperature, protein concentration, dielectric constant of the medium, and precipitant concentration in order to change the protein

solubility to reach the condition that lies just above the supersaturation region (McPherson, 1998).

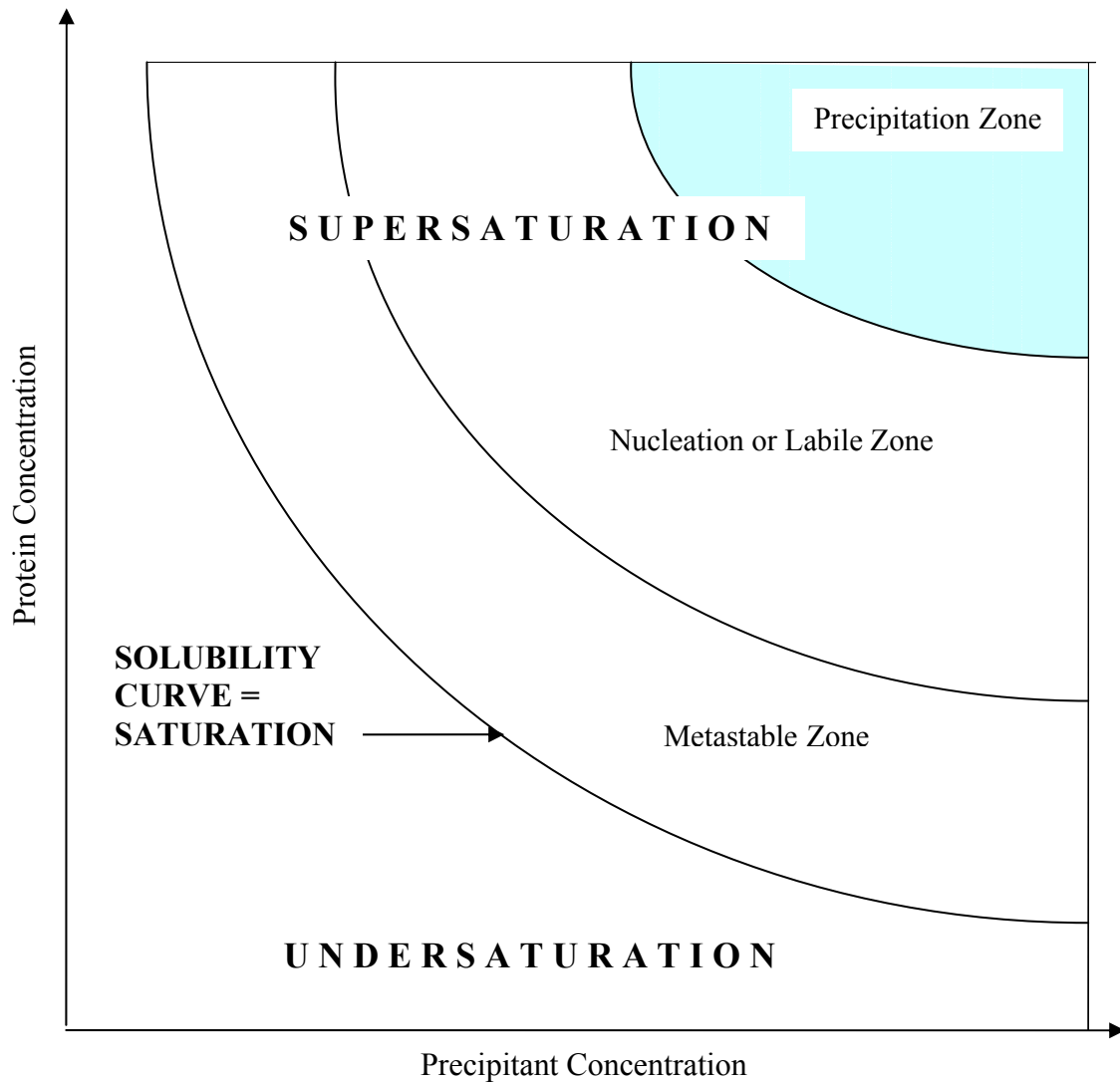


**Figure 1.8:** The solubility phase diagram for crystallization from solution.

A classical explanation of crystal nuclei formation and growth can be visualized by the two-dimensional solubility phase diagram shown in Figure 1.8. The solubility curve divides the concentration space into undersaturation and supersaturation regions. In the undersaturation zone, under the solubility curve, the protein will never crystallize. Above the solubility curve, this region can be subdivided into three zones according to

level of saturation and the kinetics required for reaching equilibrium. In the precipitation zone, excess protein does not remain in solution and exists as an amorphous precipitate. The formation of precipitate implies that no crystals will form. Before a crystal can grow in solution, nucleation has to occur. Nucleation is the beginning of crystal formation. In this process, the nucleus of sufficient size must be formed to initiate aggregation in an ordered manner. In the nucleation zone or labile zone, there is a high probability that critical nuclei will form spontaneously in solution because this corresponds to an increased energy state of the system. In fact, the energy or probability barrier to the formation of the first nucleus allows the creation of a supersaturated solution. If the degree of aggregation is too high, the solution will be oversaturated and a precipitate will be formed. If the degree of aggregation is adequate, stable nuclei can continue to grow to larger size without forming precipitate, and then the crystal can be formed and grown. The metastable zone is ideal for the growth of crystals without nucleation of new crystals. In this zone nuclei will not form, but if nuclei are present or seed crystals are introduced then crystals may grow. When a crystal grows to a certain size, it will stop growing spontaneously (Ducruix and Giege, 1992).

The crystallization of proteins is influenced by a numbers of factors, and each protein is unique. It is not possible to envisage the conditions that can cause the crystallization of a protein. The various parameters that affect crystallization are not independent of each other and their interrelation may be complicated and difficult to distinguish (McPherson, 1998). Finding a rational guideline to crystallize macromolecules successfully is not an easy task. The only way to do this is to identify the important components and refine each of them individually. In general, precipitant type

and concentration, buffer type and pH, temperature, and sample concentration are the most important factors for protein crystallization. They are considered first when performing crystallization experiments. Each parameter is manipulated independently to determine its effect on crystallization. Table 1.4 summarizes the factors which effect the crystallization of macromolecules.

| Physical                                 | Chemical                                   | Biochemical                                   |
|--|--|---|
| Temperature/Temperature fluctuation      | Buffer pH                                  | Purity of macromolecule                       |
| Vibration/Sound/Mechanical Perturbation  | Precipitant Type                           | Substrate/Coenzyme/Ligand/Inhibitor/Effectors |
| Time/Rate of growth                      | Precipitant Concentration                  | Inherent Symmetric of the Macromolecule       |
| Equilibrium Rate                         | Macromolecule Concentration                | Biochemical Modification                      |
| Dielectric Constant of Medium            | Ionic Strength                             | Genetic/Post-transitional Modification        |
| Viscosity of Medium                      | Additive/Specific Ions                     | Isoelectric Point                             |
| Pressure                                 | Metal Ions                                 | Macromolecule Stability                       |
| Gravity                                  | Detergent/Surfactant                       | Aggregation state of Macromolecule            |
| Homogeneity of Macromolecule             | Degree of Supersaturation                  | Storage time of Macromolecule                 |
| Electric/Magnetic Fields                 | Reducing/Oxidizing environment             | Source of Macromolecule                       |
| Volume of crystallization sample drop    | Present of amorphous substances/impurities | Proteolysis/Hydrolysis                        |
| Methodology/ Approach of crystallization | Cross-linker                               | Microbes contamination                        |

**Table 1.4:** Important factors affecting macromolecular crystallization (McPherson 1990; McPherson 1998).

## 1.4.2. Kinetic and Thermodynamic Principles of Crystallization

### 1.4.2.1. Protein Crystal Nucleation

Protein crystallization is comprised of three stages: nucleation, crystal growth and cessation. Nucleation is a fundamental step in the crystallization process. It takes place when the aggregate reaches a critical size at a decisive supersaturation level. The nucleation rate of crystallization can determine the number of crystals that may grow. In principle, the nucleation of protein crystallization occurs at moderate supersaturation levels in the solution. This level corresponds to the region lying within the labile zone according to the phase diagram (Figure 1.8). Protein crystal nucleation requires a higher degree of supersaturation than the growth of existing crystals. Nucleation occurs only in the labile region whereas crystals can grow in both the labile and metastable region. At high supersaturation levels, uncontrollable rapid nucleation occurs. Consequently, numerous microcrystals will grow. Crystal showers will also be found at higher supersaturation levels when no appropriate aggregate is formed. At low supersaturation levels as indicated in Figure 1.8, which is close to and above the solubility curve boundary, no nucleation will be initiated (Luft and Detitta, 1999; Przybylska, 1989).

The understanding of the manner of crystal nucleation is indispensable to comprehend the effect of various parameters on nucleation for crystal formation. Parameter investigations for ribosomal subunit crystals have illustrated that protein purity, precipitant type, buffer pH and temperature are classified as essential parameters for controlling crystal growth (Yonath *et al.*, 1982). Other important factors include the dynamics of the initial equilibration. The control of vapour equilibration experiments of hen egg white lysozyme have been conducted to demonstrate that as the equilibrium time

increased, fewer and larger crystals were produced. The experiment displayed that the lower the rate of evaporation, the lower the nucleation rate. The longer the time required to approach critical supersaturation, the bigger the crystals formed. Therefore, a linear relationship between crystal size and equilibrium time can be established (Gernert *et al.*, 1988).

The best environment for the crucial size of nucleus formation is a high degree of supersaturation. The higher the supersaturation level ( $\delta F_c (1)$ ), the greater would be the thermodynamic driving forces to push the system toward equilibrium. This will favor nucleus formation, so the energy required for producing the critical nucleus will be smaller than at a lower supersaturation level ( $\delta F_c (2)$ ) as shown in Figure 1.9 (McPherson, 1998). The number of growing protein crystals mainly relies on the rate of nucleation (Penkova *et al.*, 2002).

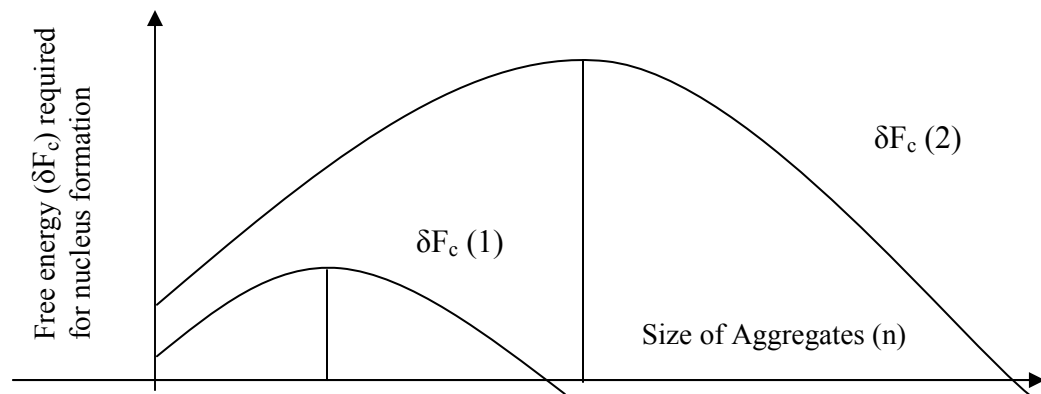


**Figure 1.9:** Diagram of the thermodynamic potential of a crystallization system required for forming the critical size of nuclei.

#### 1.4.2.2. Protein Crystal Growth and Cessation

After the critical size of nuclei has been originated at the higher supersaturation level, the metastable zone is predicted as the optimum zone for crystal growth. It

represents the ideal condition for the growth of diffraction quality crystals. Thermodynamics and kinetics are two major aspects that have to be considered when discussing protein crystal growth because both small and macromolecule crystallizations must adhere to the fundamental laws of thermodynamics. Supersaturation is the thrust to drive crystal nucleation and growth. Thermodynamic theory illustrates that the equilibrium process of crystallization from a supersaturation solution is energetically favorable. The further the system is from equilibrium, the greater the degree of supersaturation and the greater the thermodynamic force would be to push the system toward equilibrium (McPherson, 1998).

If nucleation occurs spontaneously, kinetic theory can be applied to determine the time scale of the process to take place, and the rate of nucleation and growth. The kinetics determines the time required to reach supersaturation and the equilibration of the protein solution with the precipitating solution in the reservoir. Protein droplet size and shape, the vapor pressure, the distance from the droplet to the reservoir are the variables to be considered as major kinetics aspects (Luft and Detitta, 1997; Ries-Kautt and Ducruix, 1997). For instance, the larger the droplet, the longer the time it takes to reach equilibrium with its reservoir. Another example is the larger the distance that separates the droplet and reservoir, the slower the droplet equilibrates with the reservoir (Luft *et al.*, 1996).

The main factor deciding the growth of protein crystals is the rate of transport of protein molecules moving to the existing crystal surface and the probability of protein molecules associating with the crystal lattices. The rate of protein growth ( $k$ ) will be

dependent on either or both process mentioned above, so the rate of growth can be defined as

$$k = Z \times p. \quad (5)$$

The equation (5) is the product of the rate of collision of protein molecules with a crystal per unit concentration and area ( $Z$ ) multiplied by the probability of proteins associating with the crystal per collision ( $p$ ). The quicker the crystal grows, the smaller the crystal formed and higher the number of crystals (Feher and Kam, 1985).

As a result of limited research carried out in this field, the explanation about cessation of crystal growth is insufficient and remains unclear. However, the understanding of this phenomenon is still interesting and a lot of studies can be carried out. A hypothesis is proposed that crystal growth errors such as impurities incorporated into the crystal that affect the crystal surface are most probably the root cause accountable for the cessation of crystal growth (Feher and Kam, 1985).

### **1.4.3. Crystallization Methods**

There are at least seven practical methods used for macromolecule crystallization including vapor diffusion, bulk crystallization, batch, free-interface diffusion, dialysis, temperature-induced, and seeding. Among these methods, vapor diffusion and microbatch (a new developed method from an old technique) are the most popular means being utilized by crystallographers to obtain macromolecule crystals. The method of vapor diffusion is undoubtedly regarded as the most widely employed approach for crystallization. Nucleation occurs when the sample concentration increases as the droplet volume decreases by hydration-driven mechanisms. This is induced by the equilibration

of water vapor between the sample droplet and the reservoir solution. The vapor diffusion technique is an ideal methodology for screening a broad spectrum of crystallization conditions. It can be used to optimize the size of crystals suitable for X-ray diffraction analysis. Vapor diffusion methods include hanging drop, sitting drop, sandwich, and capillary methods. The most common protocols are the hanging drop and sitting drop methods (McPherson, 1998).

The hanging drop vapor diffusion method is an efficient means of screening crystallization parameters. The advantage of this method is that it requires only a small volume of droplet, which can be as low as 2  $\mu\text{L}$  per experiment, so a minimum amount of sample is consumed for screening and optimization of the crystallization conditions (McPherson, 1998). The reason for the popularity of the hanging drop method is the ease of performing the experiment, only a 24 well-plate (such as Linbro or VDX plate), grease and cover slides are needed. The principle of this approach is straightforward, a drop composed of a mixture of macromolecule sample and precipitating solution is placed in vapor equilibration with a reservoir solution of precipitant and buffer. To start the trial, the precipitating solution composed of precipitant, buffer, additive, etc, is dispensed into reservoir. Then equal volumes of the sample and reservoir solution are mixed onto the surface of siliconized glass cover slide (Figure 1.10). The drop has a lower concentration of precipitant than the reservoir solution, so water or volatile chemicals will escape from the drop into the reservoir solution to achieve system equilibrium inside the reservoir. Eventually this causes the sample inside the drop to become more concentrated until the precipitating concentration in the drop is almost equivalent to the reservoir concentration. The major benefits of using the hanging drop method are relative ease of mounting the

crystal for X-ray diffraction experiments by inverting the cover slide with a pair of forceps. This method can be used to place multiple drops in each reservoir as well, thus saving time and material.

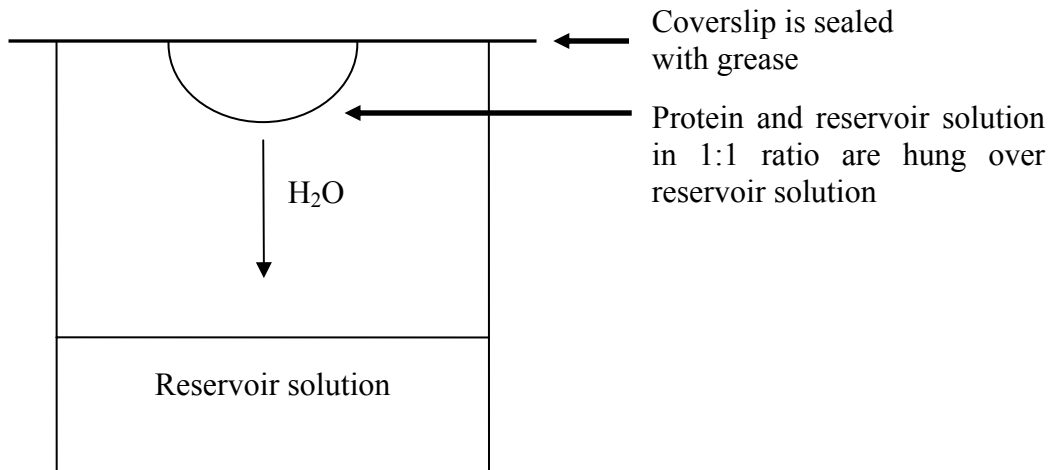


**Figure 1.10:** The hanging-drop vapor diffusion method for protein crystallization (Hampton Research, 2001).

Sitting drop vapor diffusion method is performed using a 96-well depression plate. One  $\mu\text{L}$  of protein solution and 1  $\mu\text{L}$  of reservoir solution are mixed together at the top of a ledge (Figure 1.11). The plate is then sealed with sealing tape and placed inside the incubator for crystal growth. The basic principle of this method is quite similar to the hanging drop method but the differences are that 100  $\mu\text{L}$  of reservoir solution is used instead of 1000  $\mu\text{L}$  and the droplet is not hung but sits on the depression platform. The advantage of sitting drop is that it requires a small amount of material and is ideal for screening a great number of different conditions by using the different screening kits, for example the grid screens and crystal screens supplied by different companies such as Sigma, Hampton Research, and Molecular Dimension.

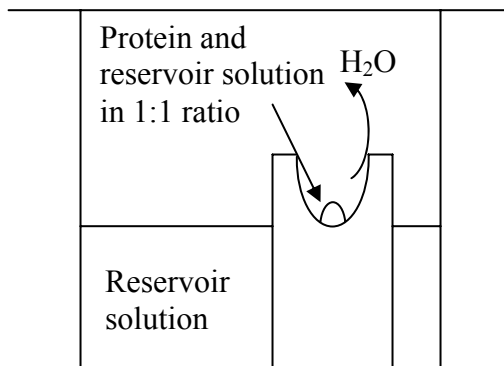


**Figure 1.11:** The sitting-drop vapor diffusion method for protein crystallization (Hampton Research, 2001).

Microbatch method is another approach for rapid protein crystallization using micro-volumes of sample. The objective of this method is to reduce the consumption of sample by generating crystallization trials in tiny amounts. It is a new method developed from the oldest crystallization technique, “The Batch Method”. The batch method has been the conventional crystallization strategy for over 150 years (McPherson, 1991). The most famous example of a protein crystallized by this method is the crystallization of lysozyme (Forsythe *et al.*, 1997). The principle is simple and the procedure involves the direct mixing of the unsaturated protein solutions with precipitating solution. The batch method alters the protein solubility and changes the dielectric properties of the medium to create a supersaturated environment to generate the crystal. This method has been revived by preparing the crystallization samples under oil (Figure 1.12). The typical final sample droplet volume is about 1 – 2  $\mu\text{L}$ . The major advantages of this approach are automatic implementation in an efficient way, high accuracy, low sample consumption, time-saving

screening, and the sample can be protected from evaporation, contamination and physical shock by oil (Chayen and Stewart, 1992).

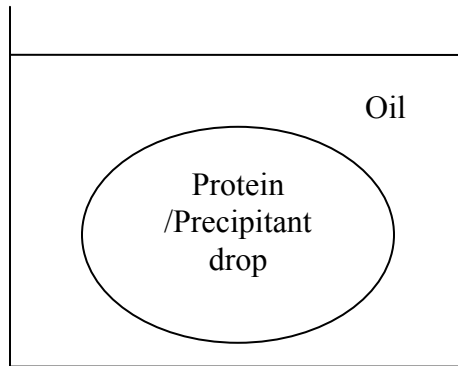


**Figure 1.12:** The microbatch method for protein crystallization (Hampton Research, 2001).

The fundamental distinction between the vapor diffusion and microbatch method is that the former is a dynamic system in which the conditions are changing throughout the whole crystallization process. Thus, there is little control over the experiment once the trial has been set up. The latter process is non-dynamic, the final concentration of the sample has been determined precisely at the beginning of the experiment. The crystallization condition can be maintained with minimum fluctuation for the normal crystallization period of about 1 – 3 weeks (Chayen, 1998).

Other crystallization methods that have been employed include containerless crystallization (Chayen, 1996), crystallization in silica gels (Cudney *et al.*, 1994) and crystallization under microgravity (Littke and John, 1984). According to the BMCD database, vapor diffusion (62.7%), batch method (~12%) and seeding (5.47%) are the most highly employed methods of crystallization (Figure 1.13).

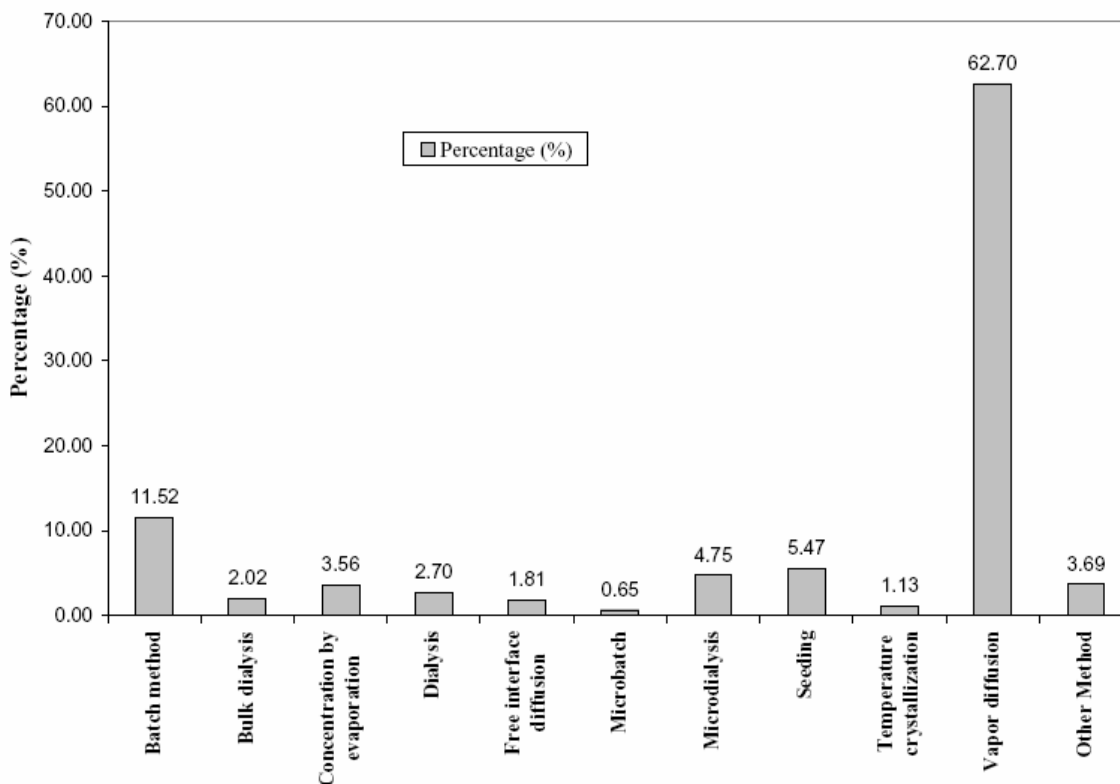


**Figure 1.13:** Bar chart showing the most commonly used crystallization methods.

#### 1.4.4. Important Considerations in Protein Crystallization

Crystallization of proteins has involved a multiple parameters route to influence the nucleation, growth and cessation. There are some important aspects of protein crystallization that must be considered prior to performing protein crystallization (Blundell and Johnson, 1976; Ducruix and Giege, 1992; McPherson, 1990). Along with the physical and chemical issues, biochemical aspects of the protein have also to be examined carefully as these also effect the crystallization of proteins.

In biochemical aspects, the purity is the first issue always considered. Impure protein crystals may contribute to the low resolution X-ray diffraction data, and then the protein structure will not be determined successfully. Purity in this case is defined as the

lack of any contaminant or impurity such as foreign proteins, dust particles, denatured proteins, microbes, and aggregates (McPherson, 1996). In general, the purity of proteins must be at least 90% before the beginning of the crystallization trials (Ducruix and Giege, 1992). Homogeneity of the protein is another major concern for crystallization. If aggregates in protein solutions are detected using dynamic light scattering, then the protein will be less likely to crystallize (Zulauf and D' Arcy, 1992). Another factor that cannot be neglected is the protein itself. For proteins that do not crystallize easily, it may be because they possess surface properties that do not promote the formation of crystal contacts. Sometimes although a protein can be crystallized, the diffraction resolution of the sample is not good enough for resolving the structure, so protein truncation, mutation, limited proteolysis and complex formation can be alternatives to get better quality diffraction crystals (Dale *et al.*, 2003).

In physical aspects, temperature and time are considered the major factors that influence the growth of protein crystals. Others like sound, vibration etc may have some disruptive effects which are not clearly understood (McPherson, 1982).

The effect of temperature on protein solubility has been recognized as one of the major contributors to protein solubility. Experiments have showed that protein solubility is temperature dependent (Christopher *et al.*, 1998). The most widely used temperatures for protein crystallization are 4 °C and 20 °C. A temperature-induced method has been reported as an alternative approach to crystallize macromolecules (Kitano *et al.*, 1998). In this method, a protein crystallization plate was initially set up at 20 °C. Once there were no crystals formed at 20 °C after 3 months, the plate was incubated at 40 °C for 30 minutes. After that, the plate was cooled to 20 °C and incubated at 20 °C; crystals were

formed in 2 days. Another less valuable influence of the temperature effect is that crystals grown at two different temperatures may have differences in their morphology. As a crystallization technique, temperature control is easy and precise. This factor should be taken into account when crystallization is initialized. In general, it may be worthwhile to carry out all crystallization trials at two different temperatures if material quantities are sufficient.

Time is another factor that affects crystallization, mainly attributed to the rate of growth of individual protein crystals. Some crystals may take a few days to a few weeks to grow while others may take a longer time to form the same size of crystal. As a rule of thumb, if the growth rate of crystals is minimized, large and defect free crystals will be grown. Manipulation of the growth kinetics of crystals is another approach that can be attempted even if it is not easy to achieve. The rate of growth is dependent on the level of supersaturation of the protein solution. For instance, the appearance of only microcrystals implies that the rate of equilibration is too fast. This suggests that the level of supersaturation is too high, therefore reduction in the level of supersaturation is desired (Heidnner, 1978; McPherson, 1998).

In chemical aspects, precipitant type and concentration, pH, and buffer are the most crucial factors that dominate the process of crystallization among others factors such as the effect of adding additives, detergents or reducing agents (McPherson, 1990).

Precipitating agents can be classified into four categories which are salts, organic solvents, long-chain polymers and non volatile organic alcohols/low molecular weight polymers. The representatives for the first class of precipitant are ammonium sulfate, potassium sodium tartrate, and sodium chloride. Ethanol and methanol are the typical

representatives of the second class of precipitating agents. Long-chain polymers consist of polyethylene glycol (PEG) 1,000, 3350, 4,000, 6,000, and 8,000. PEG 400 or PEG 600 and MPD are representatives of the last category. Ammonium sulfate is the most popular precipitant, but polyethylene glycol from molecular weight 400 – 20,000 has become increasingly popular as a crystallizing agent (McPherson, 1976; McPherson, 1990). The advantage of using PEG as a precipitant is that it shares some characteristics with salts that compete for water, and exhibits a similar volume exclusion property to organic solvents that reduce the dielectric constant of the medium. For salt precipitants, there is a study which found that sodium malonate is an excellent precipitant alternative to all others salts that have been employed for protein crystallization. It has the advantage of high success rate and can serve as a useful cryoprotectant. The choice of precipitants is a trial and error procedure (McPherson, 2001).

After precipitants, the pH and the crystallization buffer are the most important variables in protein crystal growth. As a general guideline in the protein crystallization, large single good crystals always show up within a narrow range of pH for a protein crystallized either by salt or organic solvent (Zeppezauer, 1971). The isoelectric point (pI) of a protein is the pH where the total net charges on a protein are equal to zero. At this point, protein solubility will be at a minimum therefore crystallization trials can be initiated in the range around this point (McPherson, 1982). If the pI is unknown, a pH range between 4.0 and 9.0 will normally give crystals. Therefore, this pH range should be tried at the beginning of crystallization experiments. Adequate control and monitoring of pH during crystallization is an essential step in the preparation of suitable buffers. The optimization of microcrystals in terms of their size and quality for X-ray diffraction

experiments can be conducted by fine pH adjustment. The buffer can be adjusted up to 0.05 pH unit, and different types of buffer can be employed in parallel (McPherson, 1995).

Once initial crystals are obtained, the crystals can be optimized to improve crystal size or to extend the resolution limits. Additives including sugars, alcohols, cations, polyamines, detergents or surfactants, and dioxane are considered as useful chemical compounds that contribute positively toward protein crystallization (Sauter *et al.*, 1999). For instance, detergents can play an important role in altering a polycrystalline state, promoting crystal clusters into single crystals, enhancing the diffraction ability and improving reproducibility of the growth of a crystal (Guan *et al.*, 2001).  $\beta$ -Octyl-Glucoside has been examined for a number of proteins, RNA and protein-nucleic acid complexes. Experimental results demonstrated that it has positive effects toward crystal growth (McPherson *et al.*, 1986a; McPherson *et al.*, 1986b). Others examples include adding polyols such as glycerol to increase structure stability (Sauter *et al.*, 1999; Sousa, 1995), or adding a reducing agent such as DTT, cysteine,  $\beta$ -mercaptoethanol or glutathione to maintain sulfhydryl groups in a reduced state for preserving the activity and structural integrity of a protein (McPherson, 1998).

#### **1.4.5. Strategies and Approaches to Growing Crystals**

The advances in recombinant DNA technology make pure protein expression feasible. Thus, the crystallization of proteins becomes in demand. With the advent of commercially available sparse matrix screens, it has become trivial to set up crystallization trials covering a huge range of conditions.

There are several screening and optimization strategies that have been reported including randomized approaches such as sparse matrix (Jancarik and Kim, 1991), analytical approaches such as incomplete factorial (Carter and Carter, 1979), biological macromolecule database archives (Gilliland, 1988; Gilliland *et al.*, 1994; Gilliland *et al.*, 1996), automated grid searches (Weber, 1990) and rational approaches such as screening of protein isoelectric point (pI). Other approaches including reverse screening (Stura *et al.*, 1994) and rapid screening (McPherson, 1992). All of these approaches are used to screen the initial crystallization conditions of the protein and can be used for optimization to produce large crystals.

The sparse-matrix approach is the most popular and has been commercialized by Hampton Research (Crystal Screen 1 & 2), Emerald Biostructures (Wizard Screen 1 & 2) and Molecular Dimension (Personal Structure Screen 1 & 2). The screens contain numerous conditions with different types of precipitating agents, precipitant concentrations, buffers, pHs and salts. All three commercially available screening kits demonstrate similar outcomes with high yields of crystals in preliminary crystallization experiments (Wooh *et al.*, 2003). Once initial crystallization conditions have been found, the next step is to optimize the crystallization conditions to give better crystals in terms of size and shape. Attempts should be made to obtain single crystals with a minimum dimension of at least 0.1 mm in each facet. The advantage of the sparse-matrix strategy is that less protein is consumed and fewer trials will be conducted compared to a systematic approach. The optimization strategies that are used include adding additives (Sauter *et al.*, 1999), detergents (Guan *et al.*, 2001; McPherson *et al.*, 1986a), non-ionic surfactants (Mustafa *et al.*, 1998), and control of diffusion rate (Chayen, 1997).

It is quite often that microcrystals, twinned or multi-crystals are difficult to optimize to a single crystal. In these cases, one of the approaches that can be tried to obtain single crystals is seeding. Seeding can be used in combination with other optimization strategies to gain single large crystals. Indeed, seeding is a great tool to separate the process of crystal nucleation from the process of crystal growth. The first problem to tackle for seeding is to obtain a few crystals to serve as seeds. Otherwise seeding cannot be carried out. If seeds are present, then seeding protocols can be applied. There are three major types of seeding commonly used by crystallographers: macroseeding, microseeding, and cross-seeding (Bergfors, 2003).

Seeding is a useful technique used for growing crystals by producing a seed-stock solution if spontaneous homogenous nucleation does not occur in the crystallization of macromolecules. It is generally believed that the nuclei will be initialized at the higher level of supersaturation labile zone (Stura and Wilson, 1991). Therefore, using seeding techniques, good quality crystal seeds are selected and introduced into the metastable zone from the labile zone. After seeding, the seeded crystals will continue to grow. The crystal growth conditions can then be optimized independently without the need to induce nucleation by the proteins themselves (Luft and Detitta, 1999).

Macroseeding involves mature single crystals that can be handled easily and washed in a stabilizing solution or its mother liquor a few times, then transferred into another pre-equilibrated protein-precipitant drop (Stura and Wilson, 1992). The condition of the drop should be a condition expected to give crystal growth, which lies in the metastable zone of the phase diagram of protein-precipitant concentration.

Microseeding involves the transfer of submicroscopic seeds. The seeds themselves are quite small and hard to distinguish independently. Streak seeding is a kind of microseeding technique where an animal whisker is utilized to pick up seeds by touching an existing crystal. Next, seeds are transferred to the new pre-equilibrated protein solution drop by depositing them as a straight line and moving the probe across the drop, eventually crystals will grow up along the streak line. The shortcoming of this approach is the experimenter can't control the number of seed crystals transferred. Another protocol for microseeding is the serial dilution method, where a few small crystals are selected and washed, and then the crystals are crushed so that a seed stock solution is prepared. Normally, the seed stock solution is serially diluted to  $10^{-3} - 10^{-7}$  to avoid too many nuclei inside the solution. Each diluted seed solution is used to examine the best seed concentration for growing large single crystals by streak seeding method or addition of a small aliquot of seed solution (Stura and Wilson, 1990; Stura and Wilson, 1991).

Cross-seeding is another seeding technique, where a homologous protein of the target protein is chosen as seed crystals to commence growth in the crystallization experiment (Bergfors, 2003). Other less popular seeding techniques include feeding and microcrystal selection. Feeding involves more protein being added into the protein drop and the advantage of this technique is more protein available for growing the nuclei (Bergfors, 2003). The microcrystal selection technique involves removing tiny and excess crystals from the drop solution without disturbing the few good crystals. This method is quite convenient and does not require manipulation of the good crystals, which is

beneficial because during crystal manipulation, the crystals may be damaged (Han and Lin, 1996).

Other less common practices used to make crystals grow larger including dilution method and decoupling nucleation method. The dilution method was developed to enhance the size of crystals using vapor diffusion protocols. This method requires that both protein and mother liquor in the crystallization drop are diluted to certain ratio (for example a dilution factor from 1 – 6), while the mother liquor in the well solution remains unchanged. The principle of this dilution method is same as the traditional vapor diffusion method, but since the concentrations of protein and mother liquor in the drop are diluted to n-fold, the crystallization requires a longer time to complete. This ultra-small volume experiment showed that once the dilution factor is determined to an appropriate ratio by a trial and error process, the number of crystals formed will be significantly reduced. Fewer nucleation sites will be expected, thus the size and number of the crystals can be optimized in this protocol (Dunlop and Hazes, 2003).

Decoupling nucleation and growth in the vapor diffusion method involves setting up the crystallization condition where crystals normally grow in a certain incubation period. Afterward, the coverslip with the drop is transferred over wells where the precipitant concentration is much lower and normally no crystals will be formed. Consequently, fewer and larger crystals will appear. The mechanism allows protein nucleation to be induced before any transferring to the lower degree of supersaturation in the droplet (metastable condition). The principle is to allow the protein to nucleate in labile conditions and grow continuously in metastable conditions (Saridakis and Chayen, 2000).

## **1.5. PROTEIN CRYOCRYSTALLOGRAPHY**

### **1.5.1. Cryocrystallography Background**

Cryocrystallography or so-called low temperature X-ray diffraction methods have been reported since 1990 for macromolecule X-ray diffraction experiments. For small molecules, this technique has long been applied as well. Since 1990, the proportion of X-ray diffraction experiments in macromolecular crystallography performed at cryogenic (near 100K) temperature has increased exponentially (Garman and Schneider, 1997). This approach has become an essential technique for crystallographic structure determination of biological macromolecules. Cryogenic techniques are now routinely applied in many laboratories for X-ray data collection on in-house facilities as well as on synchrotron sources (Garman, 2003).

The most important advantage of applying this technique to macromolecular crystallography is the great reduction in X-ray induced radiation damage on crystals at low temperature. At room temperature, macromolecular crystals are susceptible to crystal damage that is caused by interaction between the molecules in the crystal and the X-ray beam. The energy of the X-ray beam will produce reactive radicals and provide energy to diffuse through the crystal to break the bonds between atoms in the crystal structure (Garman, 1999). Cryo-cooling data collection for macromolecule became popular because the diffusion rate of free radicals at low temperature is much lower than that at room temperature, thus radiation damage can be minimized (Garman, 2003). The cryotechnique prevents the formation of ice within the macromolecular sample by adding a cryoprotectant, so that the lattice order of the crystals can be preserved. Thus, X-ray data collection can be exploited to remarkable effect for biological macromolecule

structure determination. For data collection at low temperature, a significant improvement of data resolution can be gained and the duration of data collection can be extended due to the crystal lifetime being lengthened. Therefore, one or more complete data sets can be taken from a single crystal (Garman and Schneider, 1997). Using the cryogenic techniques to cool crystals can also prevent phase change, space group or lattice transformation of most macromolecular crystals during X-ray data collection (Hope, 1988).

The cryocrystallography technique should be applied when this will improve the quality of X-ray data under such circumstances (Watenpaugh, 1991):

- 1) Crystal packing is more stable at cryogenic temperature than at room temperature;
- 2) The macromolecule is unstable at room temperature;
- 3) The reaction rate of protein-substrate complexes is greatly reduced at low temperature;
- 4) Crystals are diffracted at high resolution.

The primary target of cryogenic data collection is to cool the crystal without damage to the crystal lattice. The crystal is removed from the drop and should be soaked into the “cryosolution” for between one second and few minutes or even a few days. It may be necessary to introduce the cryosolution slowly, either by dialysis or serial transfer, to avoid damaging the crystal. Otherwise direct transferring may be applied. The crystal should be allowed to equilibrate with the solution completely prior to crystal mounting and flash cooling (Rodgers, 1994).

For cryogenic data collection, the crystal is held by the surface tension of the cryosolution (thin film) across a thin fiber-made loop attached to micro tube with a metal mounting pin. For short or long term storage, crystals are plunged into cryogen (liquid nitrogen, liquid propane or liquid ethane) and transferred to a Dewar for storing and transporting of crystals for future data collection at any synchrotron facility. For instant cryogenic data collection, the crystal with mounting pin is placed directly on a magnetic base in the goniometer head under gaseous nitrogen at 100 K. One benefit of using the thin fiber loop method to mount the crystal is that the mosaic spread of the crystal can be greatly reduced. This is due to the lower and more uniform background of the thin film. The mosaic spread of crystal is defined as the divergence of a scattered X-ray beam that is caused by the irregularity of orientation of small blocks of unit cells in the crystal. The X-ray absorption effect can also be minimized due to the uniform surface tension in the thin film. This free-standing method for mounting crystals is employed to avoid the crystal coming into contact with any mechanical support which can enhance the mosaic spread of the crystal (Teng, 1990).

### **1.5.2. Principle of Cryoprotectant**

During cryocrystallography, the crystal is cooled to cryogenic temperatures. In an effort to minimize crystal damage during cryogenic cooling, cryoprotective reagents or cryoprotectants are added into the solution to prevent the formation of crystalline ice in the internal and external solution as well as at the interface between crystal and solution. Once the cryoprotectant is added into the mother liquor, the cryosolution is formed.

A general method for maintaining the integrity of protein crystals has been

demonstrated by substituting the crystal mother liquor with salt-free aqueous/organic liquid mixture of high organic concentration and low freezing point. Organic solvents such as MPD, methanol, ethanol, isopropanol, ethylene glycol and glycerol are chosen (Petsko, 1975).

Glycerol is one of the most common cryoprotectants used in protein cryocrystallography. It has been reported that glycerol can be employed as a very useful cryoprotectant to provide cryoprotection for 50 typical protein crystallization solutions (Garman and Mitchell, 1996). Ethylene Glycol, MPD and PEG are also widely used. Other uncommon cryoprotectants such as sucrose have been reported as a satisfactory cryoprotectant (Sharma *et al.*, 1994). The cryoprotectants which have been successfully used by crystallographers are illustrated in Table 1.5 (Rodgers, 1994). The concentration of the cryoprotectants may be higher or lower than the ones indicated in Table 1.5, because after a number of years, more cryo-conditions have been explored.

| <i>Cryoprotectant</i>       | <i>Concentration (%)</i> |
|-----------------------------|--------------------------|
| (2R,3R)-(-)-Butane-2,3-diol | 8 (v/v)                  |
| Erythritol                  | 11 (w/v)                 |
| Ethylene Glycol             | 11-30 (v/v)              |
| Glucose                     | 25 (w/v)                 |
| Glycerol                    | 13-30 (v/v)              |
| MPD                         | 20-30 (v/v)              |
| PEG 400/600                 | 25-35 (v/v)              |
| Sucrose                     | 14 (w/v)                 |
| Xylitol                     | 22 (w/v)                 |

**Table 1.5:** List of cryoprotectants used successfully in flash-cooling the macromolecular crystals.

The simplest approach to choosing good cryoprotectant conditions is to include cryoprotectants in the established mother liquor as a matter of trial and error. The most effective way to find out their optimal concentrations is to perform an initial examination by adding a small amount of cryoprotectant as mentioned in Table 1.5 into mother liquor. A scheme based on this strategy is shown in Figure 1.14.

The main challenge of cooling the crystal to cryogenic temperatures is to avoid the formation of crystalline ice within the sample. So, the cryoprotectant added to the crystal simply slows the crystal nucleation so that a rigid glass is formed prior to ice formation within the crystal lattice.

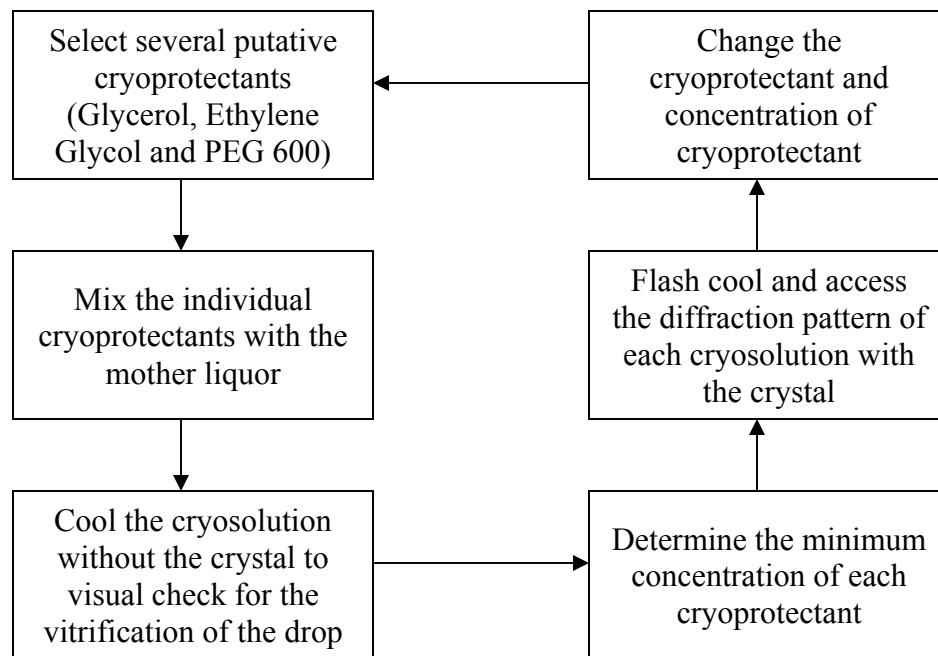


**Figure 1.14:** Pathway for determining the optimal cryoprotectant concentration.

Another approach is to use an immiscible oil such as Paratone-N in combination with cryoprotectants to replace the external liquid around the crystal, or using dry

paraffin oil to cover the crystal (Kwong and Liu, 1999). When crystals are damaged by a high concentration of cryoprotectant, the former procedure can be used because this procedure substantially lowers the concentration of cryoprotectant used. It can also increase the diffraction quality of the crystals. The latter method is simple and does not require that the crystal soaks in solution which can disturb the packing lattice by diffusing into the crystal. So, it has been suggested that this method can be tried as a first choice before trying other cryoprotectants.

Crystals that are induced by high salt concentrations such as ammonium sulfate are frequently faced with the problem of finding a suitable cryoprotectant because of the limited solubility of many salts in aqueous/organic mixtures. The consequence of adding the cryoprotectant into a salt-rich mother liquor is that salt precipitates can be formed that can harm the crystals. To avoid this problem, the method best employed is to use other salts in high solubility such as malonate or tartrate to replace ammonium sulfate in the mother liquor (McPherson, 2001; Rodgers, 1997).

### **1.5.3. Crystal Handling, Mounting, Cooling, Storage and Transportation**

Crystal mounting for cryocrystallography can be carried out using capillary tubes, fine glass capillary tubes, thin glass spatulas, and thin loop films. However, the free-standing loop mounting technique has become the prevalent procedure for crystal mounting at cryogenic temperatures (Rodgers, 1997).

Originally the loops were made from copper or tungsten wire with 1 – 2 mm diameters and 25 – 75  $\mu\text{m}$  thickness, but now, they are made from fine nylon fibers with 0.05 – 1.0 mm diameters and 10 & 20  $\mu\text{m}$  thickness. These types of cryo-loops show

minimal background diffraction due to the optically clear environment and the loops are thin enough to be convenient for fast freezing. The major advantages of using this approach to lift up, transfer, flash cool the crystal are the production of lower X-ray scatter and lower X-ray absorption. Uniform results can be obtained compared to the conventional mounting techniques such as capillary mounting (Teng, 1990).

The loop itself serves as a platform to support the crystal in place and to keep it away from foreign material which has detrimental effects to the crystal. It is a good idea to select a loop size which is just wide enough to keep the crystal from dropping off. For instant data collection, the crystal is picked up and flash-cooled immediately. The cold stream is first deflected from the nitrogen gas nozzle, the crystal is placed on the goniometer, and then the obstruction of the flow is removed immediately.

If the crystal needs a faster rate of cooling, or will be sent away to synchrotron facilities for data analysis, the crystal can be rapidly plunged beneath the surface of liquid nitrogen for a few seconds to a few minutes. Next, the crystal is moved to a diffractometer for experiment or transferred to a storage tank for storage and transportation (Parkin and Hope, 1998).

The other advantage of cryocrystallography is the potential for storing and transporting crystals as soon as they have been flash-cooled. Well-diffracted crystals can be kept and sent to a synchrotron after screening at an in-house facility. Another factor to be considered is that crystals can grow to a limiting size and subsequently degrade. So, crystals can be flash cooled at their finest conditions until data collection is performed. Crystals must be kept at cryogenic temperatures, so a liquid nitrogen Dewar which is portable and provides protection from mechanical shock is highly recommended. In

principle, once the crystals have been successfully cooled to cryogenic temperatures, they can be kept for an indefinite time (Parkin and Hope, 1998).

## **1.6. X-RAYS DIFFRACTION**

### **1.6.1. Proteins, Crystals and X-rays**

X-rays are generated when electrons collide with the atoms of a metal target, e.g. copper. The electrons are liberated from a heated filament and accelerated by high voltage towards the metal target (Stout and Jensen, 1989).

X-rays are a form of electromagnetic radiation, where wavelength is about 0.1 – 10 nm (1 – 100 Å) on the electromagnetic spectrum (Petrucci *et al.*, 2002). The major reason that X-rays have been chosen to study the 3-D structures of proteins in crystallography because the range of wavelengths of X-rays we choose (0.5 Å – 1.6 Å) is on the same order of magnitude as the bond length of the atoms within protein molecules. The bond length between atoms within a protein is about 0.15 nm or 1.5 Å, thus these wavelengths can be utilized to visualize the geometry and structure of protein molecules through X-ray diffraction (Blow, 2002).

Individual atoms in a molecule can diffract X-rays; however, they are weak scatterers of X-rays. Therefore, X-rays may pass through a single molecule without any diffraction, so diffraction might be too weak to be detected by any instrument. However, one can solve the problem by analyzing a crystal diffraction pattern rather than a molecule. This is because a crystal is composed of a number of repeating patterns (unit cells) in a regular and ordered manner. Each molecule within the crystal therefore diffracts equally, and thus strong diffracted X-ray beams can be measured (Rhode, 2000).

## 1.6.2. Bragg's Law

W. L Braggs managed to visualize the scattering X-rays from a crystal by considering that the diffracted beams were reflected by planes passing through points of a crystal lattice. The diffracted X-rays are scattered by the crystal at a certain angle of reflection ( $\theta$ ). This reflection is analogous to that from a mirror, for which the angle of incident X-ray beam is equal to the angle of diffracted X-ray beam. The incident and the diffracted X-rays are in the same plane and the X-rays of wavelength ( $\lambda$ ) are normal to a set of diffracting planes (Figure 1.15). The constructive interference between X-rays scattered from successive planes in the crystal will only take place if the path difference ( $2d$ ) between the X-rays is equivalent to an integral number of wavelength ( $\lambda$ ). That is the Bragg's law equation (Glusker and Trueblood, 1985):

$$n\lambda = 2d \sin \theta$$

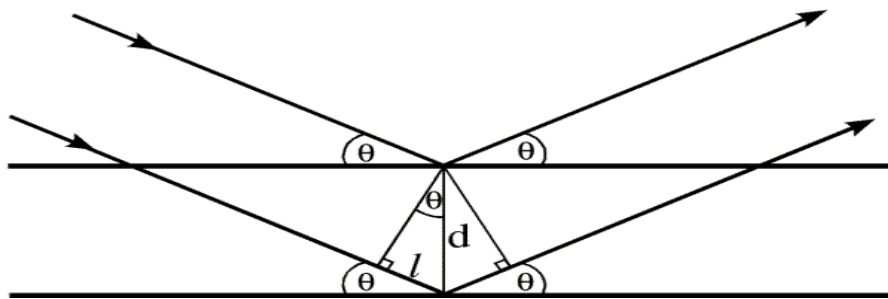


**Figure 1.15:** The geometry of diffraction and its relationship to Bragg's Law (Glusker and Trueblood, 1985).

In Bragg's law, if the wavelength and the diffraction angle of a reflection are known, the perpendicular distance between the lattice planes in the crystal (interplanar spacing,  $d$ ) can be easily calculated. As the angle increases,  $d$  must become smaller for

the path length to remain equal to one wavelength. The equation can be rearranged as:

$$d = n\lambda / (2 \sin\theta)$$

The minimum interplanar spacing ( $d_m$ ), where  $d_m = \lambda/2 (\sin\theta_{\max})$ , is also interpreted as the resolution of an electron density map. Since the maximum possible value of  $\sin\theta$  is 1, so the smaller the  $d_m$  value, the higher the resolution will be of the X-ray diffraction pattern. For instance, if the radiation used for X-ray generation has a wavelength of 1.54 Å, then the maximum resolution that can be observed with this radiation would be 0.77 Å (Blundell and Johnson, 1976; Glusker *et al.*, 1994). Most proteins seldom diffract better than 1.5 Å (Glusker *et al.*, 1994). If a protein is diffracted to a high resolution level (above 2 Å), most fine macromolecular structures can be solved and refined by crystallography.

### **1.6.3. Asymmetric Unit, Space Group, Unit Cell and Bravais Lattices**

Crystals can be characterized by three elements to precisely define the arrangement, coordination, and periodicity of the fundamental unit of which they are composed. These 3 elements are symmetry properties, repetitive features and distribution of the atoms in the repeating unit.

Protein molecules are inherently asymmetric. The asymmetric unit is the smallest component in the crystal. The asymmetric unit may consist of one molecule, part of a molecule or several molecules not related by symmetry. If only one molecule occupies a unit cell, then the cell itself is chiral and has no symmetry elements at all. This object is termed as the asymmetric unit because no part of it is systematically related to any other by crystallographic properties. That means it has no symmetry elements such as rotation

axis or mirror plane (Figure 1.16). In most cases, the unit cell contains more than one identical molecule or oligomeric complexes (dimer, trimer, tetramer, etc.) in an arrangement that produces symmetry elements. So, the largest aggregate of molecule(s) in a cell that possesses no symmetry element but can be juxtaposed on other identical entities by symmetry operation is called the asymmetric unit (Rhode, 2000).

A set of symmetry operations includes rotation, reflection, inversion, rotatory-inversion, screw axes, glide plane, and translation. These operations can be applied to an asymmetric unit. Combination of all these elements in all possible ways generates a total of 230 unique, three-dimensional space groups of symmetry operation. These 230 space groups are described in *International Tables for X-ray Crystallography Vol. A*. (Hahn, 2002).

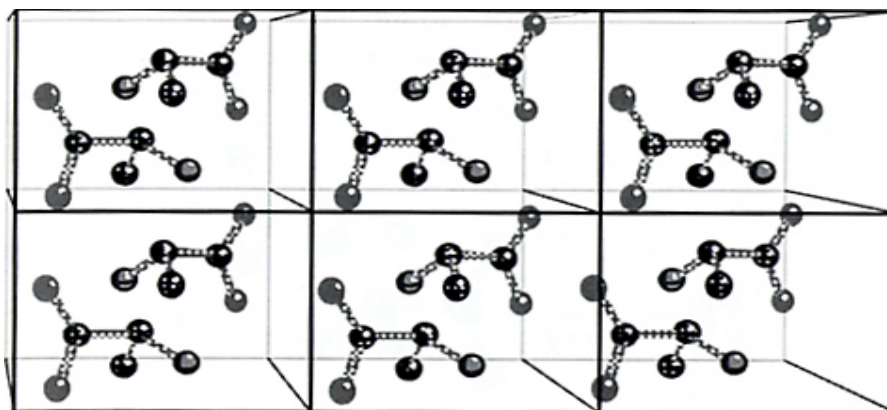


**Figure 1.16:** There are six unit cells in this crystalline lattice. In each unit cell contains two molecules, the asymmetric unit is a dimer (Rhode, 2000; reproduced with permission of the author).

The unit cell is the basic building block of the crystal and is repeated infinitely in three dimensions. The directions of constructive interference depend only on the size and shape of the unit cell. The dimensions of a unit cell are designated by six parameters: the

length of 3 unique edges ( $a$ ,  $b$ ,  $c$ ) which run along  $x$ ,  $y$  and  $z$  coordinates respectively, and 3 unique angles ( $\alpha$ ,  $\beta$ ,  $\gamma$ ) as indicated in Figure 1.17.

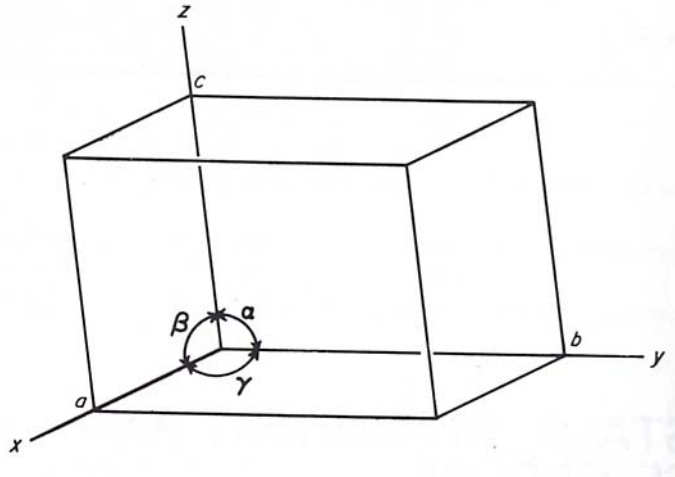


**Figure 1.17:** The unit cell with edges,  $a$ ,  $b$ ,  $c$  and angles,  $\alpha$ ,  $\beta$  and  $\gamma$  (Stout and Jensen, 1989).

In virtually all cases, a crystallographer is concerned only with the content of the individual unit cell and the coordinate of the atoms within the unit cell. There are 14 allowable unit cell types classified as *Bravais lattice* to distinguish their characteristic. The Bravais lattices themselves can be divided into five types of lattice, which are primitive (**P**), centered (**C**), body-centered (**I**), face-centered (**F**) and rhombohedral (**R**) (McPherson, 2003; Stout and Jensen, 1989).

Any crystal can be regarded as being established by consecutively translational repetition of the unit cell and its content along  $a$ ,  $b$ ,  $c$  by distance  $|a|$ ,  $|b|$ ,  $|c|$  respectively, until a continuous three-dimensional array of repeated unit cells in a regular manner has been created (Glusker *et al.*, 1994; Glusker and Trueblood, 1985; Rhode, 2000).

The simple symmetry operations and elements needed to describe unit cell symmetry are translation, rotation and reflection. The symmetry of a unit cell is described in 230 space groups (like  $P2_12_12_1$ ). The space group is a group of symmetry operations consistent with an infinitely extended, regularly repeating pattern. Protein is an asymmetric object since all amino acids except glycine have chirality. However, the D-form of amino acids does not exist in proteins and only the L form does. Thus, there are less symmetry elements (mirror planes, inversion centers and glide planes) involved within the unit cell, and less space groups can be used to designate the protein. This limits the possible space groups to 65 out of the 230 mathematically possible ones (McRae, 1999).

There are seven crystal systems used to classify the symmetry of the crystal, this corresponds to the seven fundamental shapes for unit cells, consistent with the 14 Bravais lattices as displayed in Table 1.6 (Glusker *et al.*, 1994; Stout and Jensen, 1989).

|           | <b>Crystal System</b> | <b>Bravais Lattices</b> | <b>Lattice</b>    | <b>Angle</b>   |
|-----------|-----------------------|-------------------------|-------------------|--|
| <b>1</b>  | Triclinic             | P                       | $a \neq b \neq c$ | $\alpha \neq \beta \neq \gamma$                      |
| <b>2</b>  | Monoclinic            | P, C                    | $a \neq b \neq c$ | $\alpha = \gamma = 90^\circ \neq \beta$              |
| <b>3</b>  | Orthorhombic          | P, C, I, F              | $a \neq b \neq c$ | $\alpha = \beta = \gamma = 90^\circ$                 |
| <b>4</b>  | Tetragonal            | P, I                    | $a = b \neq c$    | $\alpha = \beta = \gamma = 90^\circ$                 |
| <b>5a</b> | Trigonal              | P                       | $a = b \neq c$    | $\alpha = \beta = 90^\circ, \gamma = 120^\circ$      |
| <b>5b</b> | Rhombohedral          | R                       | $a = b = c$       | $\alpha = \beta = \gamma < 120^\circ, \neq 90^\circ$ |
| <b>6</b>  | Hexagonal             | P                       | $a = b \neq c$    | $\alpha = \beta = 90^\circ, \gamma = 120^\circ$      |
| <b>7</b>  | Cubic                 | P, I, F                 | $a = b = c$       | $\alpha = \beta = \gamma = 90^\circ$                 |

**Table 1.6:** The seven crystal systems (Glusker *et al.*, 1994; Stout and Jensen, 1989).

#### 1.6.4. X-ray diffraction Data Collection

For data collection purposes, the most important factor required for evaluating data quality is the completeness of the X-ray data including all the indices and their associated intensities, with their standard uncertainties (Dauter, 1999). Two factors that influence the data completeness are the geometric and informative content. The geometric factor, arising from the symmetry of crystal lattice and the detector setup, is a quantitative factor related to a number of variables including the approach of angular rotating method, the selection of the total rotation range appropriate for the crystal symmetry, crystal-to-detector distance, crystal mosaicity and beam divergence. The informative factor includes the quality of the data, the dynamic range of detector and the R-factor. The longer the exposure time, the greater the intensities and the signal-to-noise ratio, and the better the data quality obtained (Dauter, 1997; Dauter, 1999).

The X-ray data quality for macromolecular crystallography is assessed by a global indicator, the merging R-factor ( $R_{\text{merge}}$ ) or symmetry R-factor ( $R_{\text{sym}}$ ). The merging R-factor is defined by the following equation (Blundell and Johnson, 1976):

$$R_{\text{merge}}(I) = \frac{\sum_{hkl} \sum_i |I_i(hkl) - \langle I(hkl) \rangle|}{\sum_{hkl} \sum_i I_i(hkl)}$$

where  $I_i(hkl)$  is all observed intensities and  $\langle I(hkl) \rangle$  is the average value of all observed intensities.

The  $R_{\text{merge}}$  value will be between 20 – 40% while the signal/noise ( $I/\sigma(I)$ ) falls around 1.0 – 2.0 (Dauter, 1999). The quantity of merging R-factor is almost universally used for evaluating X-ray diffraction data.

## CHAPTER 2: MATERIALS AND METHODS

### 2.1. CHEMICALS

#### Additive:

The volatile reducing agent, DTT (OmniPur<sup>®</sup> Grade), was purchased from VWR International Ltd (Ontario, Canada).

#### Buffers:

| Reagent  | Reagent Grade                       | Supplier                                   |
|--|-------------------------------------|--|
| Citric Acid Anhydrous (C <sub>6</sub> H <sub>8</sub> O <sub>7</sub> )                            | OmniPur <sup>®</sup>                | VWR Canlab (Ontario, Canada)               |
| HEPES (C <sub>8</sub> H <sub>18</sub> N <sub>2</sub> O <sub>4</sub> S)                           | Biotechnology Performance Certified | Sigma-Aldrich Canada Ltd (Ontario, Canada) |
| MES (C <sub>6</sub> H <sub>13</sub> NO <sub>4</sub> S.H <sub>2</sub> O)                          | Biotechnology Performance Certified |  |
| Potassium Phosphate, monobasic(KH <sub>2</sub> PO <sub>4</sub> )                                 | ACS                                 | VWR Canlab (Ontario, Canada)               |
| Potassium Phosphate, dibasic (K <sub>2</sub> HPO <sub>4</sub> )                                  | ACS                                 |  |
| Sodium Acetate Anhydrous (CH <sub>3</sub> COONa)   | AnalaR <sup>®</sup>                 |  |
| Sodium Cacodylate (C <sub>2</sub> H <sub>6</sub> AsO <sub>2</sub> Na)                            | Sigma Ultra                         | Sigma-Aldrich Canada Ltd (Ontario, Canada) |
| Sodium Citrate (Na <sub>3</sub> C <sub>6</sub> H <sub>5</sub> O <sub>7</sub> .2H <sub>2</sub> O) | AnalaR <sup>®</sup>                 | VWR Canlab (Ontario, Canada)               |
| Tris (C <sub>4</sub> H <sub>11</sub> NO <sub>3</sub> )   | Reagent                             | Sigma-Aldrich Canada Ltd (Ontario, Canada) |

#### Precipitants:

PEG 400, PEG 600, PEG 1,000, PEG MME 2,000, PEG 4,000, PEG 6,000 and PEG 8,000 were purchased from Fluka Chemical Cooperation (Wisconsin, USA).

**Cryoprotectants:**

| Reagent   | Reagent Grade | Supplier                                     |
|---|---------------|--|
| Ethylene Glycol (C <sub>2</sub> H <sub>6</sub> O <sub>2</sub> ) | ACS           | Sigma-Aldrich Canada Ltd<br>(Ontario Canada) |
| Glucose (C <sub>6</sub> H <sub>12</sub> O <sub>6</sub> )        | ACS           | VWR Canlab<br>(Ontario, Canada)              |
| Glycerol (C <sub>3</sub> H <sub>8</sub> O <sub>3</sub> )        | ACS           |  |
| MPD (C <sub>6</sub> H <sub>14</sub> O <sub>2</sub> )            | Purum         | Fluka Chemical Coop.<br>(Wisconsin, USA)     |
| PEG 400   | Purum         |  |
| PEG 600   | Purum         |  |
| Sucrose (C <sub>12</sub> H <sub>22</sub> O <sub>11</sub> )      | Ultra Pure    | Fisher Scientific<br>(Ontario, Canada)       |
| Xylitol (C <sub>5</sub> H <sub>12</sub> O <sub>5</sub> )        | -             |  |

**Salts:**

| Reagent   | Reagent Grade        | Supplier                                     |
|---|----------------------|--|
| Copper Sulfate (CuSO <sub>4</sub> )   | ACS                  | Sigma-Aldrich Canada Ltd<br>(Ontario Canada) |
| Potassium Acetate<br>(CH <sub>3</sub> COOK)   |                      | Fisher Scientific<br>(Ontario, Canada)       |
| Ammonium Sulfate<br>(NH <sub>4</sub> ) <sub>2</sub> SO <sub>4</sub>                   |                      | VWR Canlab<br>(Ontario, Canada)              |
| Cadmium Chloride (CdCl <sub>2</sub> )   |                      |  |
| Calcium Chloride (CaCl <sub>2</sub> )   |                      |  |
| Cobalt Chloride (CoCl <sub>2</sub> )  |                      |  |
| Copper Chloride (CuCl <sub>2</sub> )  |                      |  |
| Lithium Chloride (LiCl)   | OmniPur <sup>®</sup> |  |
| Lithium Sulfate (Li <sub>2</sub> SO <sub>4</sub> )                                    | ACS                  |  |
| Magnesium Chloride<br>(MgCl <sub>2</sub> .6H <sub>2</sub> O)                          |                      |  |
| Manganese Chloride<br>(MnCl <sub>2</sub> .4H <sub>2</sub> O)                          |                      |  |
| Nickel Chloride<br>(NiCl <sub>2</sub> .6H <sub>2</sub> O)                             |                      |  |
| Potassium Chloride (KCl)  |                      |  |
| Potassium Sodium Tartrate<br>(KNaC <sub>4</sub> H <sub>4</sub> O <sub>6</sub> )       |                      |  |
| Sodium Chloride (NaCl)  |                      |  |
| Tri-Sodium Citrate<br>(Na <sub>3</sub> C <sub>6</sub> H <sub>5</sub> O <sub>7</sub> ) |                      |  |
| Zinc Acetate<br>((CH <sub>3</sub> COO) <sub>2</sub> Zn.2H <sub>2</sub> O)             | General Reagent      |  |
| Zinc Chloride (ZnCl <sub>2</sub> )  |                      |  |

**Proteins:**

BSA protein was purchased from Sigma-Aldrich Canada Ltd (Ontario, Canada). It was minimum 99% electrophoresis grade and essentially fatty acid free (A0281).

Trx-2 protein was overexpressed and purified from the cloned vectors pPROK1 (Clotech, California, USA) containing the *H. pylori* gene. The construct was provided by Dr. Leslie Poole from Wake Forest University (Baker *et al.*, 2003).

**Protein Overexpression:**

Antibiotics ampicillin-Na salt and chloramphenicol (OmniPur<sup>®</sup> Grade) were purchased from Sigma-Aldrich Canada Ltd (Ontario, Canada) and VWR International Ltd (Ontario, Canada) respectively.

Peptone (Granulated), yeast extract (Granulated, Microbiology Grade), and sodium chloride (ACS Grade) which were used for the purpose of preparing the LB medium were all purchased from VWR International Ltd (Ontario, Canada).

**Protein Purification:**

The DNase I from bovine pancreas (OmniPur<sup>®</sup> grade), DTT (OmniPur<sup>®</sup> Grade), potassium phosphate monobasic (KH<sub>2</sub>PO<sub>4</sub>, ACS Grade) and potassium phosphate dibasic (K<sub>2</sub>HPO<sub>4</sub>, ACS Grade) used for the preparation of potassium phosphate buffer solutions at pH 7.0 (The buffer solution mixture of the monobasic potassium phosphate and dibasic potassium phosphate is referred as potassium phosphate buffer solution or “K-PO<sub>4</sub> buffer solution”.) were purchased from VWR International Ltd (Ontario, Canada). Lysozyme, AEBSF-HCl (HPLC Grade) and Tris-HCl were purchased from Sigma-Aldrich Canada

Ltd (Ontario, Canada) and CalbioChem (San Diego, California, USA) respectively. The packing media, carboxymethyl cellulose CM52, for cation exchange column chromatography was purchased from VWR International Ltd (Ontario, Canada).

Two types of dialysis membrane were used. Spectra/Por<sup>®</sup> 1 (MWCO: 6,000 ~ 8,000 Dalton; Diameter: 20.4 mm, Flat Width: 32 mm and Volume/length: 3.3 ml/cm) was purchased from VWR International Ltd (Ontario, Canada) and Spectra/Por<sup>®</sup> 3.1 (MWCO: 3,500 Dalton; Diameter: 10.0 mm, Flat Width: 16 mm and Volume/length: 0.81 ml/cm) was purchased from Fisher Scientific Ltd (Ontario, Canada).

Two types of Amicon ultracentrifuge membranes were used and purchased from Fisher Scientific Ltd (Ontario, Canada). Regenerated cellulose membranes with NMWL 3,000 either in diameter of 25 mm (Millipore, for 10ml stirred cell) or 63.5 mm (Millipore, for 200 ml stirred cell) were used to concentrate Trx2 protein solutions. Another ultrafiltration membrane with NMWL: 30,000 in 25 mm diameter (Millipore, for 10 ml stirred cell) was used to concentrate BSA protein solutions.

### **Protein Characterization:**

The Bradford reagent, low-molecular weight range Sigma marker, 40% acrylamide/bis-acrylamide, TEMED (C<sub>6</sub>H<sub>16</sub>N<sub>2</sub>) and Tris base (C<sub>4</sub>H<sub>11</sub>NO<sub>3</sub>) were all purchased from Sigma-Aldrich Canada Ltd (Ontario, Canada). Ammonium persulfate (OmniPur<sup>®</sup> Grade), glacial acetic acid (ACS Grade), glycerol (ACS Grade), methanol (HPLC Grade), sodium dodecyl sulfate (C<sub>12</sub>H<sub>25</sub>SO<sub>4</sub>Na, OmniPur<sup>®</sup> Grade) and gel drying film (V7131, 25.4 cm x 28 cm) were purchased from VWR International Ltd (Ontario,

Canada). Glycine ( $C_2H_5NO_2$ , electrophoresis grade) was purchased from Fisher Scientific Ltd (Ontario, Canada).

## **2.2. EQUIPMENT**

The two balances used were a Sartorius BP 221S for delicate sample measurement (weight capacity= 220 g, readability= 0.0001 g), and a Sartorius BP 410 for normal sample measurement (weight capacity: 410 g, readability =0.01 g).

The centrifuges used were Beckman Coulter™ model Micofuge®18 Centrifuge with the maximum speed at 14,000 rpm for small quantity of protein samples up to 1.5 ml and Beckman's model J2-HS Centrifuge with the maximum speed at 8,000 and 18,000 rpm were used for 500 ml & 50 ml sample solutions respectively.

The Dynamic Light Scattering (DLS) instrument used was a DynaPro-99 Model with Dynamic software version 5.26.39 that located in the Saskatchewan Structural Science Center (SSSC) at University of Saskatchewan.

The liquid chromatography instruments used were BioCAD SPRINT and BioCAD 700E perfusion chromatography system with BioCAD software version 3.0. Both systems were coupled to Advantec super fraction collectors model SF-2120. The two columns used were self-packed POROS® 20 Micro HQ anion exchange column (Diameter: 10 mm, Length: 100 mm, and Column Volume: 7.84 ml) and self-packed carboxymethyl cellulose CM 52 cation exchange column (Diameter: 26 mm, Length: 250 mm, and Column Volume: 132.72 ml).

The microscope used was an OLYMPUS model SZ6045 (1.0 – 6.3 X) with 10 X magnification eyepieces and attached with a DP-12 digital camera for image recording.

The pH meter used was a VWR SympHony model SB 21 and calibrated by 3 different standard buffer solutions (pH: 4.01, 7.00 and 10.01) within a range of  $\pm 0.01 - 0.02$  pH units.

Two stirred cells used for ultrafiltration were purchased from Fisher Scientific Ltd (Ontario, Canada). These include a 10 ml stirred cell (model 8010, diameter: 25 mm) and a 200 ml stirred cell (model 8200, diameter: 63.5 mm).

The UV-VISIBLE spectrometer used was a Cary 50 Bio Model with WinUV software package, and coupled with a Hewlett Packard *HP Deskjet 3420* series printer.

The X-ray diffractometer used was a DX8 Proteum Model attached with a 4K CCD detector and connected with Kyro-flex low temperature set-up (Temperature range: 90 – 300K). The software that used for data collection was Proteum version 1.4.1 (Bruker AXS Inc., Madison, Wisconsin, USA). The X-ray instrument is located in the crystallography laboratory at the SSSC of the University of Saskatchewan.

### **2.3. PROTEIN OVEREXPRESSION**

The protein overexpression protocol only applied to the Trx-2 protein; BSA protein was directly obtained from the supplier. The pPROK1 vector (Clontech) containing Trx-2 gene was transformed into *E. coli* BL21 (DE3) pLysS using the heat shock method as described previously (Filson *et al.*, 2003). Glycerol stocks stored at  $-80^{\circ}\text{C}$  were transferred into a sterilized falcon tube containing 5 ml of LB solution with 50  $\mu\text{g/ml}$  of ampicillin and 34  $\mu\text{g/ml}$  of chloramphenicol. The falcon tube was put inside the shaker at  $37^{\circ}\text{C}$  at a speed of 250 rpm overnight in order to grow the cell culture in broth.

About 1 ml of the overnight culture was transferred into a 300 ml volumetric flask that contained 100 ml of sterilized LB medium solution with 50 µg/ml of ampicillin and 34 µg/ml of chloramphenicol. The culture grew under the same condition as the 5 ml LB solution.

Ten milliliters of the overnight grown culture was transferred into a 2800 ml Fernbach flask that contained 1 L LB solution with 50 µg/ml of ampicillin and 34 µg/ml of chloramphenicol. Finally, 4 L of cells were cultivated. When the cultures started to grow in shaker (37°C / 250 rpm), 1 ml of medium solution was taken to act as “Blank” in order to monitor the process and the optical density (OD) value was measured at the wavelength of 595 nm until the OD<sub>595</sub> reached about 0.6 – 0.8. Once the OD range was attained, 0.4 mM IPTG was added to induce the overexpression of the Trx-2 protein. After addition of the IPTG, the cells were grown for a further 3 hours. The cells were then pelleted by centrifugation in 500 ml centrifuged bottles for 15 minutes at a speed of 8,000 rpm at 5°C. After centrifugation, the supernatants were discarded and the cell pellets were collected into a falcon tube and then stored at –80°C until used.

## **2.4. PROTEIN PURIFICATION**

### **2.4.1. Purification of Bovine Serum Albumin**

#### **2.4.1.1. Anion Exchange Chromatography**

Prior to operating the anion exchange chromatography, the column was equilibrated with 50 mM Tris-HCl (pH 8.5) buffer solutions. For purifying BSA, a 5 ml sample of 10 mg/ml BSA solution was prepared. After filtration, the BSA solution was loaded onto HQ 20 anion exchange column. Both 50 mM Tris-HCl (pH 8.5) buffer

solution and 50 mM Tris-HCl/0.5 M NaCl (pH 8.5) buffer solution were used as gradient buffers for sample fractioning. The flow rate was set at 20 ml/min. A total of 16 fractions were collected and the UV absorbance at the wavelength of 280 nm was used for protein sample detection. The fractions that showed an absorbance peak were kept. All sample solutions and buffers were filtered by 0.22 µm sterile Millex<sup>®</sup> GP filters before use.

#### 2.4.1.2. Ultrafiltration

The BSA solutions from the column fractions were reconcentrated in order to recover the proteins. Reconcentration of the diluted BSA solutions was accomplished by using a 10 ml Amicon ultrafiltration stirred cell with ultrafiltration membrane (NMWL: 30,000). The ultrafiltration stirred cell was pressurized under 70 psi of nitrogen gas at 4°C. The BSA solutions were reconcentrated to about 1.5 ml for overnight dialysis.

#### 2.4.1.3. Dialysis

Before the BSA solution was transferred to the dialysis membrane (Spectrum), the membrane was rinsed with DIW for 10 – 20 minutes. The dialysis reservoir was filled with 2 L of 50 mM K-PO<sub>4</sub> (pH 6.0). The dialysis buffer was changed at every hour for 3 changes and then the dialysis was continued overnight. Finally, the BSA solution was reconcentrated to 10 mg/ml as determined by Bradford Assay (Bradford, 1976) for crystallization trials.

## **2.4.2. Purification of Thioredoxin-2**

### **2.4.2.1. Cell Lysis**

The weight of the thawed pellets from the freezer was measured to calculate the total volume of lysing buffer (5mM K-PO<sub>4</sub> buffer solution at pH 7.0 including 1 mM DTT, 2mM AEBSF, 20 µg/ml lysozyme and 20 µg/ml DNase) needed to extract and isolate Trx-2 proteins from the cell. Five milliliters of buffer were used per 10 g of cell pellets. The suspended cell pellets were sonicated on ice for 1 minute. The lysed protein solution was then transferred into a small centrifuge tube (50ml, Nalgene) and centrifuged for 30 minutes using the JA-25.50 rotor at a speed of 14,000 rpm at 5°C. The supernatants were collected, a 30% ammonium sulfate cut was performed to remove further contaminants by adding an appropriate amount of precipitant according to the ammonium sulfate precipitation table (Bollag *et al.*, 1996). For example, 176 g of ammonium sulfate was required for 1000 ml of supernatant. After 30 minutes of stirring at 4°C, the solution was then centrifuged for 30 minutes at a speed of 14,000 rpm at 5°C and the supernatants were collected.

### **2.4.2.2. Dialysis**

Following the 30% ammonium sulfate cut, the supernatant was dialyzed by a 2 L of 5 mM K-PO<sub>4</sub> buffer solutions (pH 7.0) with 2mM DTT overnight with 3 – 4 changes of dialysis buffer.

#### 2.4.2.3. Anion Exchange Chromatography

Prior to the anion exchange chromatography, the column was equilibrated with a 5 mM K-PO<sub>4</sub> buffer solution (pH 7.0). A 5 ml sample was loaded onto a self-packed HQ 20 column. The proteins were not bound with the anion column, so these were eluted from the column very quickly. The fractions containing Trx-2 were collected by fraction collector in a 10 ml volume at the flow rate of 5 ml/min. The fractions that showed an absorbance peak were kept aside for the next step. In the anion exchange chromatography purification protocol, a 5 mM K-PO<sub>4</sub> buffer solution (pH 7.0) and a 5 mM K-PO<sub>4</sub>/1 M NaCl buffer solution (pH 7.0) were used as gradient buffers for sample fractioning. Before proceeding to the next purification procedure, as a result of high volume of fractionated protein solutions, concentration of the protein fractions by ultracentrifugation was essential to reduce the volume of protein solutions and the time consumed for cation exchange chromatography. All samples and buffers were filtered before loading to the perfusion chromatography system (BioCAD 700E).

#### 2.4.2.4. Ultrafiltration

The concentration of the protein solution was required after every chromatographic procedure in order to reconcentrate the protein. Reconcentration of the diluted Trx-2 solutions from the chromatographic fractions was accomplished using a 10 ml or 200 ml Amicon ultrafiltration stirred cell with ultrafiltration membrane (NMWL 3,000). The ultrafiltration cell was pressurized under 70 psi of nitrogen gas inside a 4°C incubator and the Trx 2 solutions were concentrated to 5 – 10 ml for cation exchange chromatography.

#### 2.4.2.5. Cation Exchange Chromatography

Prior to the cation exchange chromatography, the column was equilibrated with a 5 mM K-PO<sub>4</sub> buffer solution (pH 7.0). The pre-concentrated Trx-2 solution was injected into a 5 ml loop, and a 5 mM K-PO<sub>4</sub> buffer solution (pH 7.0) was blended with a 40 mM K-PO<sub>4</sub> buffer solution (pH 7.0) for gradient elution of Trx-2 protein with UV detection at the wavelength of 280 nm. The fractions containing Trx-2 protein were collected for overnight dialysis in order to remove the salts from the gradient buffers or others impurities. Again, the Trx-2 solution was reconcentrated to about 1 – 2 ml for overnight dialysis.

#### 2.4.2.6. Dialysis after Cation Exchange Chromatography

The dialysis reservoir was filled with 500 ml of 30 mM K-PO<sub>4</sub> buffer solution (pH 7.0). The dialysis reservoir was replaced after one hour and repeated three times, and then overnight dialysis was continued. After that, the concentration of purified Trx-2 was determined by Bradford assay as described in Section 2.5.3.

### **2.5. PROTEIN CHARACTERIZATION**

#### **2.5.1. SDS- PAGE Electrophoresis**

SDS-PAGE is a commonly applied technique for protein analysis and characterization using small quantities of proteins of interest. This method is employed to characterize protein purity, because the purity of the protein plays a crucial role in the protein crystallization trials (Ducruix and Giege, 1992).

A 10% gel for BSA and a 15% gel for Trx-2 were prepared according to the standard recipe shown in Appendix 2 (Sambrook and Russell, 2001). The gel was placed into the electrophoresis device that contained Tris-Glycine electrophoresis buffer in the lower buffer chamber. For most of the sample preparations, 20  $\mu$ L of sample solution was mixed with 20  $\mu$ L SDS-gels loading buffer. The samples were boiled for 5 minutes, and then centrifuged for another 5 minutes at a speed of 14,000 rpm. The standard sample used to verify the molecular weight of protein of interest was “Low Molecular Weight Protein” marker (66, 45, 36, 29, 24, 20, 14 & 6.5 KDa). Both samples and standards were loaded into wells of the pre-cast gel. The electrophoresis was run at a constant current, 50 mA, for approximately 30 – 45 minutes until the blue bands almost reached the bottom of the glass plate. The gel was removed from the glass plate and transferred to the staining solution, Coomassie Brilliant Blue. After one hour, the staining solution was replaced with destaining solution 1 (30% Methanol/10% Acetic Acid) for another hour. After that the gel was destained by destaining solution 2 (5% Methanol/7% Acetic Acid) overnight. The next day, the destaining solution was discarded and the drying solution (40% methanol/10% glycerol/7.5% acetic acid) was applied to soak the gel in a few minutes. Then, the gel was dried for a few hours for final inspection of the gel contents in order to determine the purity of the protein samples.

### **2.5.2. Dynamic Light Scattering Measurement**

The dynamic light scattering analysis was performed in the Saskatchewan Structural Science Center (SSSC). The protein sample solution was scanned at least 20 times continuously at 20°C with an acquisition time of 3 seconds per scan. The protein

sample solution was diluted to 1 mg/ml with DIW prior to DLS measurement. The protein sample solution was kept on ice all the time before the experiment. All samples were filtered by MicroFilter (0.02  $\mu\text{m}$  membrane) to remove all dust and particles from the solution. Prior to the sample measurement by DLS, a water blank sample was carried out to ensure the cuvette and syringe used were clean and uncontaminated. Approximately 20  $\mu\text{L}$  of protein sample solution was injected into the cuvette that was then placed into the chamber to collect the %polydispersity to evaluate the homogeneity of the protein.

### **2.5.3. Bradford Assay**

The protein concentration was determined by the Bradford Assay (Bradford, 1976). Six standard solutions were prepared to build a quadratic calibration curve where  $R^2$  should be higher than 0.95. The Bradford reagent, 0.1  $\mu\text{g}/\mu\text{L}$  of BSA stock solution and DIW were mixed accordingly to Table 2.1.

To determine the concentration of purified BSA protein, 0.5  $\mu\text{L}$  of protein sample solution was added to 499.5  $\mu\text{L}$  of DIW and 500  $\mu\text{L}$  of Bradford reagent. Therefore, the BSA sample solution was diluted to 1: 2000. For purified Trx-2 protein, 1  $\mu\text{L}$  of Trx-2 sample solution was added to 499  $\mu\text{L}$  of DIW and 500  $\mu\text{L}$  of Bradford reagent. Therefore, the Trx-2 sample solution was diluted to 1: 1000. Once the sample solutions have been measured by UV/VIS, the concentration must be converted from  $\mu\text{g}/\text{ml}$  into  $\text{mg}/\text{ml}$  (1000  $\mu\text{g}/\text{ml}$ ) to calculate the true concentration of the sample. The sample solutions and standards must be undisturbed at least 10 – 15 minutes before taking any measurement at the wavelength of 595 nm by UV/VIS spectrometer. The

sample has to be blanked in the wavelength of 595 nm prior to every measurement. A standard calibration curve was plotted as the absorption values versus the concentration of the standards. The concentration of purified protein sample can then be determined by fitting the measured absorbance value to the standard calibration curve of the Bradford Assay.

| [Bradford Std.]<br>( $\mu\text{g/ml}$ ) | 0.1 $\mu\text{g}/\mu\text{L}$<br>BSA ( $\mu\text{L}$ ) | DIW ( $\mu\text{L}$ ) | Bradford<br>Reagent ( $\mu\text{L}$ ) | BSA ( $\mu\text{g}$ ) |
|---|--|-----------------------|---------------------------------------|-----------------------|
| 0                                       | 0  | 500                   | 500                                   | 0                     |
| 1                                       | 10   | 490                   | 500                                   | 1                     |
| 2                                       | 20   | 480                   | 500                                   | 2                     |
| 3                                       | 30   | 470                   | 500                                   | 3                     |
| 5                                       | 50   | 450                   | 500                                   | 5                     |
| 10                                      | 100  | 400                   | 500                                   | 10                    |

**Table: 2.1** Preparation of Bradford Assay standard solutions. Each standard solution contains DIW, Bradford reagent and 0.1  $\mu\text{g}/\mu\text{L}$  BSA stock solution. The final volume of the individual standard solutions is 1000  $\mu\text{L}$  (1 ml) each.

## 2.6. PROTEIN CRYSTALLIZATION

### 2.6.1. Preparation of Buffer Solutions

There are a number of buffer solutions that were prepared in the protein crystallization trials. The buffer solutions included citric acid, HEPES, MES, potassium phosphate, sodium acetate, sodium cacodylate, tri-sodium citrate and Tris.

The buffer solution mixture of potassium phosphate monobasic ( $\text{KH}_2\text{PO}_4$ ) and potassium phosphate dibasic ( $\text{K}_2\text{HPO}_4$ ) is referred as potassium phosphate buffer solution or “K- $\text{PO}_4$  buffer solution”. The 1 M individual buffer stock solutions were prepared by

dissolving 136.09 g of  $\text{KH}_2\text{PO}_4$  and 174.18 g of  $\text{K}_2\text{HPO}_4$  powders into DIW to 1 L respectively. Finally, 1 L of 50 mM K- $\text{PO}_4$  buffer solution of the pH of interest can be prepared by mixing the 1 M  $\text{K}_2\text{HPO}_4$  and 1 M  $\text{KH}_2\text{PO}_4$  solutions according to the Table 2.2 (Sambrook and Russell, 2001). This 100 ml mixture was diluted further to 2000 ml by DIW in order to obtain desired pH and concentration of K- $\text{PO}_4$  buffer solution.

| pH  | Volume of 1 M $\text{K}_2\text{HPO}_4$ (ml) | Volume of 1M $\text{KH}_2\text{PO}_4$ (ml) |
|-----|---|--|
| 5.8 | 8.5   | 91.5                                       |
| 6.0 | 13.2  | 86.8                                       |
| 6.2 | 19.2  | 80.8                                       |

**Table 2.2:** The preparation of 50 mM K- $\text{PO}_4$  buffer solution at different pHs at 25°C.

A 1 M stock solution of citric acid buffer was prepared by dissolving 9.606 g of citric acid powder into DIW to 50 ml. This solution is referred to as “citric acid buffer solution” or “CA buffer solution”.

A 1 M stock solution of HEPES buffer was prepared by dissolving 11.915 g of HEPES powder into DIW to 50 ml. This solution is referred to as “HEPES buffer solution”.

A 1 M stock solution of 2-morpholinoethanesulfonic acid (MES) buffer was prepared by dissolving 1.438 g of MES powder into DIW to 50 ml. This solution is referred to as ‘MES buffer solution’.

A 1 M stock solution of sodium acetate buffer was prepared by dissolving 4.104 g of sodium acetate powder into DIW to 50 ml. This solution is referred to as “sodium acetate buffer solution” or “NaAc buffer solution”.

A 1 M stock solution of sodium cacodylate buffer was prepared by dissolving 8.000 g of sodium cacodylate powder into DIW to 50 ml. This solution is referred to as “sodium cacodylate buffer solution” or “Na-CACO buffer solution”.

A 1 M stock solution of tri-sodium citrate buffer was prepared by dissolving 12.905 g of tri-sodium citrate powder into DIW to 50 ml. This solution is referred to as “sodium citrate buffer solution” or “Nacit buffer solution”.

A 1 M stock solution of Tris(hydroxymethyl)aminomethane buffer was prepared by dissolving 6.055 g of Tris powder into DIW to 50 ml. This solution is referred to as ‘Tris buffer solution’.

All the buffer stock solutions that mentioned above were filtered through 0.22  $\mu\text{m}$  sterile Millex®GP filters prior to use. The desired pH values of all the buffers mentioned above were adjusted by adding either concentrated HCl or 10 M NaOH prior to bring solutions to 50 ml.

### **2.6.2. Crystallization Methods**

The methods used for crystallization were the vapor diffusion method, both hanging drop and sitting drop methods, and the microbatch method. Hanging drop vapor diffusion method used a VDX 24-well plate that had a fine bead of vacuum grease applied around the edge of the well. Precipitating solutions (1000  $\mu\text{L}$  each) that were composed of precipitant, buffer solution, additive, and DIW were pipetted into the 24 reservoirs of the crystallization plate individually. Then 1  $\mu\text{L}$  of protein solution was pipetted onto the center of a clean siliconized 22 mm circle glass cover slide and mixed with 1  $\mu\text{L}$  of reservoir solution immediately. The cover slide was inverted using tweezers

without losing the drop and sealed over the reservoir with gentle pressure to ensure a proper seal. The plate was placed inside the 4°C or 20°C incubator for crystal growth.

The sitting drop vapor diffusion method was performed using 96-well CrystalClear Strip plate. The method was similar to the hanging drop method, but only 100  $\mu$ L reservoir solution was needed instead of 1000  $\mu$ L. In this method, 1  $\mu$ L of protein solution and 1  $\mu$ L of reservoir solution were mixed together at the top of the ledge, and finally the plate was sealed with sealing tape and placed inside the 4°C or 20°C incubator for crystals growth.

The microbatch vapor diffusion method directly mixing 0.5  $\mu$ L of protein solution and 0.5  $\mu$ L of precipitating solution in a well and then 9  $\mu$ L of oil (either paraffin oil or Al's oil) was added into same well immediately. At the end, the 72-well "MicroBatch" plate was filled up with the oil to fully cover all the wells. The plate was placed inside the 4°C or 20°C incubator for crystals growth.

## **2.7. PROTEIN CRYOCRYSTALLOGRAPHY**

### **2.7.1. Flashing Cooling of Protein Crystals**

A few potential and commonly used cryoprotectants for crystal freezing are glycerol, ethylene glycol, MPD, PEG 400, PEG 600, glucose, sucrose and xylitol. All of them were tried to screen the cryo-conditions of BSA and Trx-2 crystals. The cryosolution was prepared according to the well solution that produced crystals. The composition of potential cryosolution included cryoprotectant, precipitant, buffer, salt, additive and DIW. The concentrations of the precipitant, buffer, salt or additive (if

needed) in the cryosolution were kept the same as the well solution and only DIW was replaced by selected concentration of the cryoprotectants. For instance, one of the best crystallization conditions of BSA (precipitant/buffer: 55% SAS/25mM NaAc at pH = 5.1) where crystals were consistently grown was chosen for this preliminary screening. Glycerol was the first cryoprotectant chosen for the screening at different concentrations from 15% – 35%. Cryosolutions, about 5  $\mu$ L, which have different concentrations of glycerol (without any crystal) were prepared to immerse into liquid nitrogen for 5 – 10 seconds and then observed as to whether the cryosolution drop was glassy upon freezing. Other cryoprotectants were examined under the same methodology. However, diffraction experiments have to be carried out in order to examine the diffraction pattern of the samples to assure that the chosen cryoprotectants can cryoprotect the protein crystal appropriately and diffract to high resolution for protein structure determination.

The method used for crystal cooling was very similar to that used for testing the cryosolution. Suitable crystals that were sharp-edged and large (a minimum 0.1 mm and 0.05 mm in each dimension for BSA and Trx-2 crystals respectively) were selected for X-ray diffraction experiments. There were two usual ways to cryoprotect crystals. The first method was to put 5  $\mu$ L of cryosolution just beside the drop of crystal ready to be lifted up, with the use of CrystalCap and CryoLoop aided by the CrystalWand (purchased from Hampton Research). A crystal was removed from the drop and transferred into the cryosolution for a given amount of time, after which the crystal was ready for X-ray diffraction. The second method was to mix the same volume of cryosolution directly onto the drop of the crystal (such as 5  $\mu$ l + 5  $\mu$ l), afterward, the crystal was transferred into the full cryosolution as quickly as possible. For BSA crystals that grown in high

concentration of SAS conditions, a thin layer was formed on the drop; therefore, the second method was applied to dilute out the layer, and then the crystal could be transferred into pure cryosolution without any difficulty. Otherwise, if the crystal can be easily looped up, the first method can be applied conveniently. For the second method, instead of cryosolution, mother liquor can be used as well.

### **2.7.2. Protein X-Ray Diffraction**

Frozen BSA and Trx-2 crystals were diffracted on the in-house X-ray diffraction facility at the SSSC. Crystals were cryoprotected by the selected cryosolution. The procedure as described in Section 2.7.1 for cryoprotecting the crystals was followed. The crystal was mounted on the goniometer head using a cryo-loop. The cryo-jet (Kryo-flex, Bruker) as part of the X-ray diffractometer was used to freeze the crystal. The cryo-jet used liquid nitrogen to achieve the temperature desired for cryo-temperature diffraction. The temperature was set to 100 K. The X-rays were generated using copper radiation at the wavelength of 1.5418 Å.

After crystal mounting, the crystal was aligned to the center of the X-ray beam and the detector was placed to an appropriate distance (normally at 7 cm for initial exposure). For X-ray diffraction experiments, the crystals were exposed to X-rays for 60 seconds to collect a still image. If there was a diffraction pattern shown on the image, an initial image was collected to determine the cell dimensions of the crystal. The exposure time of initial image was 300 seconds. The purpose of increasing the exposure time of the initial image from 60 to 300 seconds was to increase the intensities of all diffraction spots. The stronger the intensities of the diffraction spots, the more reliable of the unit cell

dimensions could be determined. After the exposure time, the diffraction resolution limit of crystal was determined and analysis of diffraction pattern was analyzed by PROTEUM software to determine the unit cell dimensions and space group of the crystal.

## **CHAPTER 3: RESULTS AND DISCUSSION**

### **3.1. BOVINE SERUM ALBUMIN**

#### **3.1.1. Introduction**

BSA is a soluble and large globular protein and has a molecular weight of approximately 66,400 Dalton. The primary structure of BSA (Brown, 1975) has been known for a few decades but its crystal structure has not been solved. In order to investigate and understand the antagonistic behavior of thiomolybdates towards copper in the bovine ruminant environment, the tertiary structure of BSA must be determined. Growing high quality crystals is an essential requirement to obtain the structural information of BSA in order to determine the location of binding sites of thiomolybdates. Therefore, pure and homogenous BSA protein is required prior to performing the protein crystallization trials. Once high quality BSA crystals are obtained, finding the appropriate cryo-conditions for flash-cooling the BSA crystals is important to diffract crystals to high resolution using X-ray radiation.

#### **3.1.2. Purity Determination of Bovine Serum Albumin**

The first crystallization trials were done using SAS/K-PO<sub>4</sub> (Thome, 2001) and the BSA was purchased from the supplier without any purification prior to use. However, the reproducibility of growing crystals under SAS/K-PO<sub>4</sub> conditions was low and the growth period of crystals was long (at least 2 – 3 months). So, the impurity of the BSA samples

was suspected as the main reason that impeded the growth of BSA crystals when the BSA concentration was 10 mg/ml.

The supplier claimed that the BSA supplied was a minimum 99% electrophoresis purity grade product. SDS-PAGE analysis was used to determine the purity of BSA. The SDS-PAGE gels were prepared as described in Section 2.5.1. From the SDS-PAGE gel displayed in Fig. 3.1, it was observed that there were quite a number of low-molecular-weight and high-molecular-weight contaminants shown in the original BSA sample (Lane 2). This seemed to show that the BSA bought from commercial source was not ideally pure enough for crystallization trials. Even after performing centrifugation (Lane 3) and the following ultrafiltration (Lane 4) twice respectively, the impurities still existed. Hence, purification of BSA by perfusion chromatography was carried out for the purpose of getting much purer sample to obtain good diffraction quality crystals and obtaining consistent results.

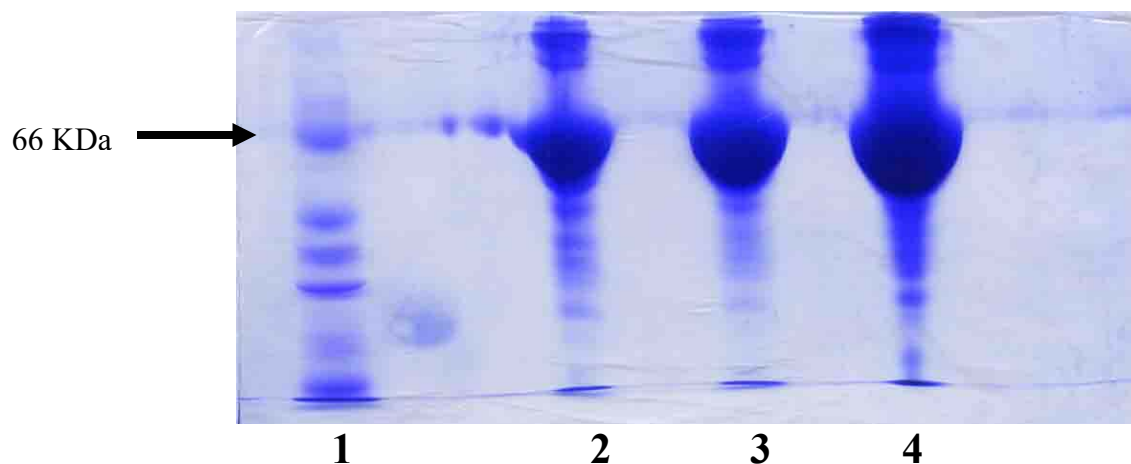


**Figure 3.1:** SDS-PAGE analysis of original BSA samples. The arrow on the left indicates the 66 KDa molecular weight level (**1: Protein marker, 2: BSA sample directly obtained from supplier, 3: BSA sample after 2x centrifugation, 4: BSA sample after 2x centrifugation followed by 2x ultrafiltration. The concentrations of BSA samples were 10 mg/ml).**

### 3.1.3. Purification of Bovine Serum Albumin

#### 3.1.3.1. Purification of BSA by Anion Exchange Chromatography

A filtered BSA sample was injected onto the anion exchange column (see Section 2.4.1.1), and 16 fractions were collected. According to UV absorbance value of 0.7329 at the wavelength of 280 nm as shown in Figure 3.2, fraction numbers #8 and #9 represented the highest purity samples among all the fractions. These 2 fractions were used for further SDS-PAGE analysis to confirm the purity of the BSA samples.

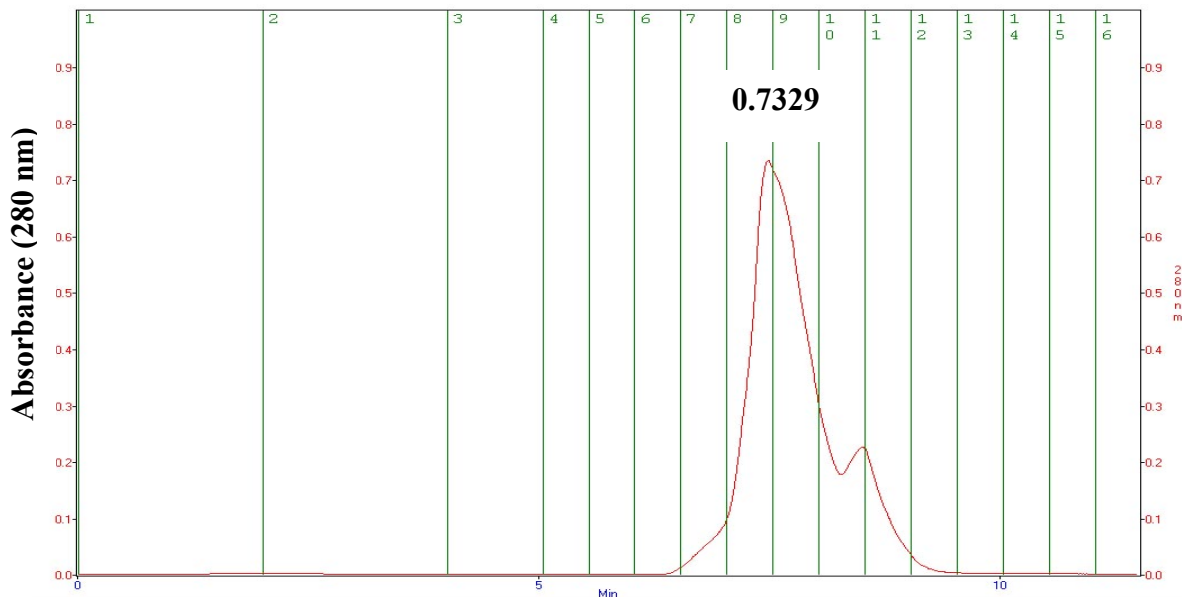


**Figure 3.2:** Chromatogram of BSA fractions in anion exchange chromatography.

#### 3.1.3.2. SDS-PAGE Analysis after Anion Exchange Chromatography

The result of the BSA purification after anion exchange chromatography is shown on Figure 3.3. The SDS-PAGE gels were prepared as described in Section 2.5.1. Lane 2 and lane 3 were the two BSA samples collected from fractions #8 and #9 after anion exchange chromatography. From the SDS-PAGE gel shown in Figure 3.3, there were no high-molecule weight impurities higher than 66 KDa, but there were still some low

molecule weight impurities in the sample, so the purities of BSA samples were considered higher than 95%. It clearly showed the intensive reduction of the overall amount of contamination presented in the BSA samples.

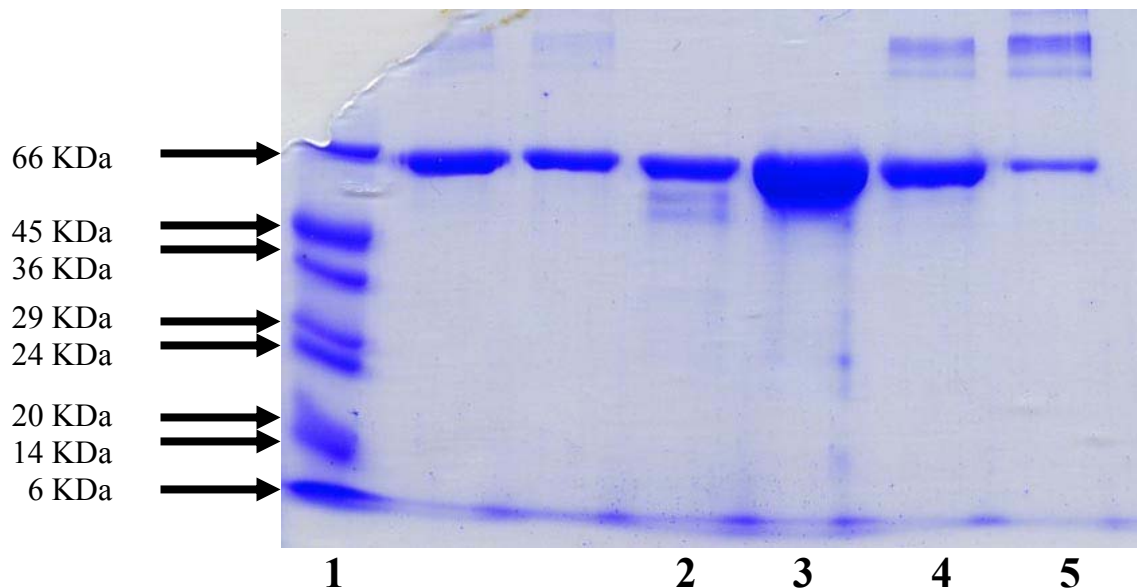


**Figure 3.3:** SDS-PAGE analysis of BSA samples after anion exchange chromatography. The protein marker is shown on the leftmost column as indicated by the arrows. **(1: Protein marker, 2 & 3: BSA sample solutions collected from chromatographic fraction # 8 and # 9, 4 & 5: BSA sample solutions collected from chromatographic fraction # 10 and # 11, the two unlabelled lanes are the BSA samples from other test run).**

### 3.1.3.3. SDS-PAGE Analysis after Ultrafiltration and Dialysis

After anion exchange chromatography, the fractions that contained BSA were reconcentrated by the ultrafiltration method (see Section 2.4.1.2), and dialyzed overnight (see Section 2.4.1.3). After reconcentration of the BSA sample solutions and overnight dialysis, SDS-PAGE analysis was performed to determine protein purity. From the SDS-PAGE gel shown in Figure 3.4, there were still some low-molecule weight impurities

after purification through chromatography, ultrafiltration and dialysis, however, the quality was deemed to be good enough for protein crystallization trials.

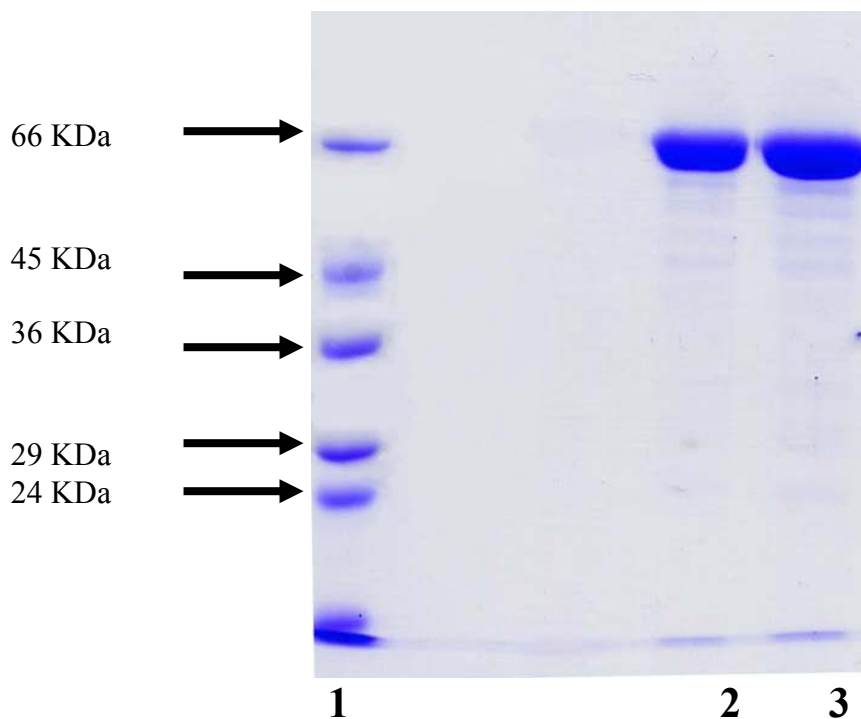


**Figure 3.4:** SDS-PAGE analysis of purified BSA samples. The protein marker is shown on the leftmost column as indicated by the arrows. For running a SDS-PAGE analysis, 20  $\mu\text{L}$  of BSA sample solutions from the individual fractions were mixed with 20  $\mu\text{L}$  of SDS-gel loading buffers respectively (**1: Protein marker, 2: BSA sample after overnight dialysis; 3: BSA sample after ultrafiltration**).

### **3.1.4. Concentration Determination of Purified Bovine Serum Albumin**

After overnight dialysis, the actual concentration of BSA sample solution was measured by Bradford method. Six Bradford standards were prepared according to Table 2.1 (see Section 2.5.3), and used to establish the calibration curve to determine the concentration of BSA sample solution (Figure 3.5). From Table 3.1, the UV absorbance value of the sample was detected as 0.6453 at the wavelength of 595 nm. According to the calibration curve, it corresponded to 11.3 mg/L. After the conversion to the dilution

factor 1: 2000 (see Section 2.5.3), the true BSA concentration was determined as 22.6 mg/ml. In order to prepare a 10 mg/ml BSA sample solution, 442.5  $\mu$ l concentrated BSA sample solution was mixed with 557.5  $\mu$ l buffer, then the solution was combined and centrifuged to ensure complete mixing to get a 1000  $\mu$ l of 10 mg/ml purified BSA solution. This final solution was ready for protein crystallization trials as well as DLS measurement to determine the homogeneity of the protein.

| Sample | Measured Concentration (mg/L) | Absorbance (Abs) | BSA Final Concentration (mg/ml) |
|--------|-------------------------------|------------------|---------------------------------|
| BSA    | 11.3                          | 0.6453           | 22.6                            |

**Table 3.1:** The Bradford Assay absorbance data of the concentrated purified BSA sample solution, the final concentration of the purified BSA is 22.6mg/ml.

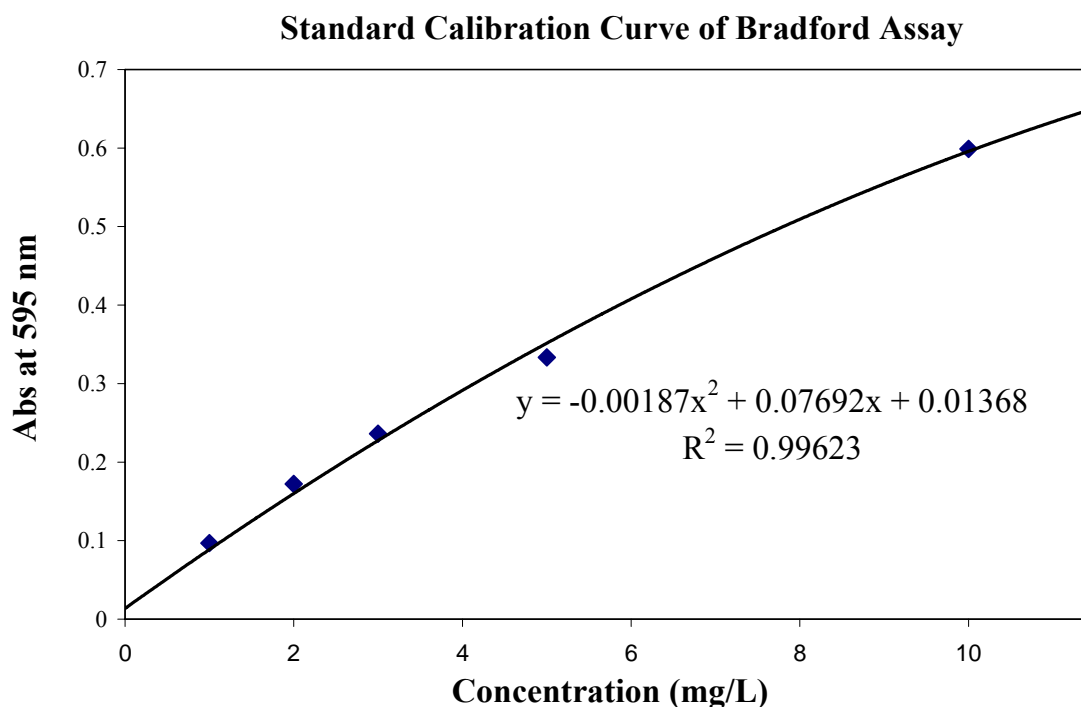


**Figure 3.5:** The Bradford Assay calibration curve used to determine the concentration of purified BSA sample solution at the wavelength of 595 nm.

### **3.1.5. Homogeneity Determination of Bovine Serum Albumin**

The monomodal histograms for purified BSA (Figure 3.6) and unpurified BSA (Figure 3.7) sample solutions from the DLS experiments are shown. Both curves were highly symmetrical and narrowly distributed. The %polydispersity of purified BSA and unpurified BSA solutions were 12.2% and 12.6% respectively for the 1 mg/ml BSA samples. These values were less than 30% upper limit of protein crystallizability as described in the literature (Ferre-D'Amare and Burley, 1997) or 15% upper limit of polydispersity as mentioned in the supplier instrument user's manual. The calculations of %polydispersity were based on the intensity peak distribution. The DLS experimental results of both purified and unpurified BSA sample solutions demonstrated that, in terms of homogeneity, their qualities were equivalent, they were considered as homogenous and monodispersed proteins. The BSA protein samples, whether purified or not, were homogenous and ready for protein crystallization trials as measured by DLS.

From my observations while performing the DLS experiments, the experimental results were occasionally not so consistent. This might be attributed to the micro-volume of the sample solution and the sensitivity of the instrument, even a tiny bubble might have a significant effect on the results. I suggest that %polydispersity determined from DLS experiments can be only regarded as a reference indicator. If the %polydispersity is more than 30%, it is very likely that crystals will not form in crystallization trials. If the %polydispersity is less than 30%, crystals are more likely to grow (Ferre-D'Amare and Burley, 1994; Ferre-D'Amare and Burley, 1997; Zulauf and D' Arcy, 1992).

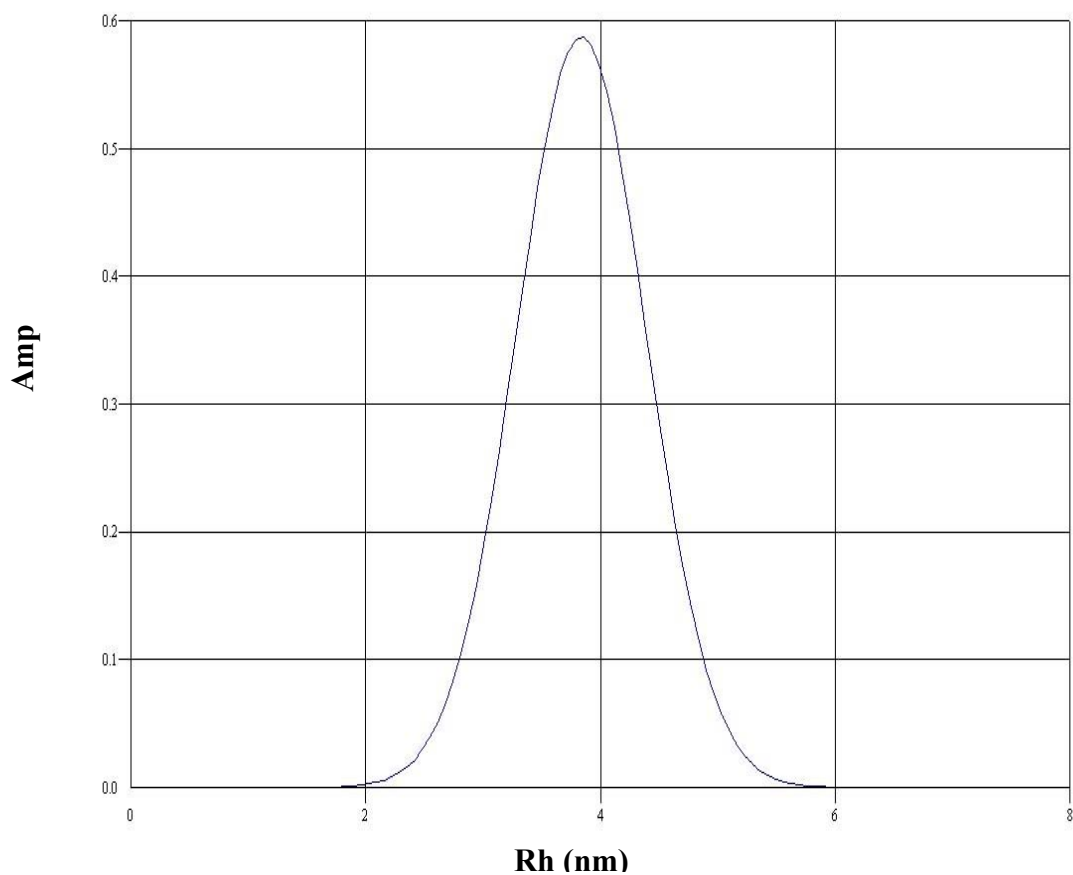


**Figure 3.6:** Monomodal histogram of 1 mg/ml purified BSA solution. The %polydispersity of the 1 mg/ml purified BSA sample solution is 12.2%.

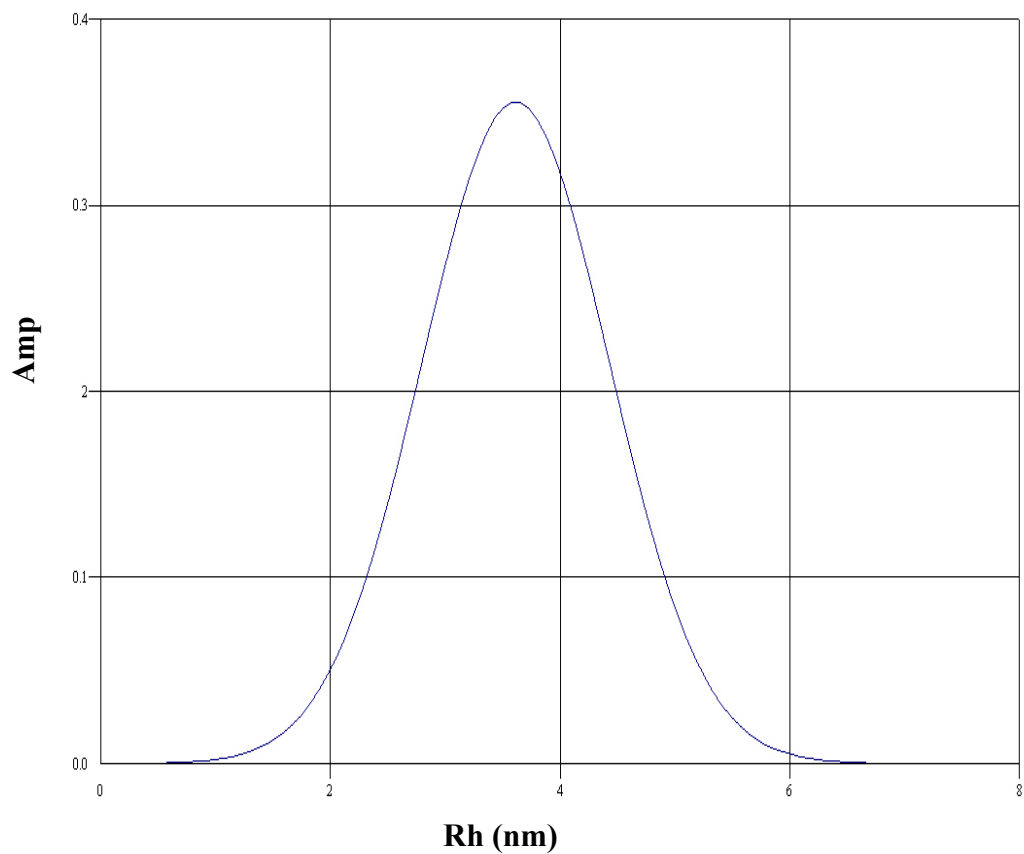


**Figure 3.7:** Monomodal histogram of 1 mg/ml unpurified BSA solution. The %polydispersity of the unpurified 1 mg/ml BSA sample solution is 12.6%.

### 3.1.6. Crystallization Trials of Bovine Serum Albumin

A number of different crystallizing conditions, (see Appendix 1 for the summary of BSA crystallization trials) including different types of precipitants, precipitant concentrations, protein concentration, buffers, pHs, salts, additives, and different crystallization methods (see Section 2.6), have been attempted. The initial trials of BSA crystallization were based on the crystallization conditions done by Thome (Thome, 2001). Crystals were grown in potassium phosphate buffer solutions between pH 5.5 – 6.2 (Asanov *et al.*, 1997a; Asanov *et al.*, 1997b). The precipitant used for BSA crystallization was saturated ammonium sulfate (SAS) at a concentration of about 40 – 60%. The concentration of BSA can be varied from 10 mg/ml to 80 mg/ml, but between the ranges of 50 – 60 mg/ml were highly reproducible. Crystals normally took at least a month to appear and spent another month to grow to bigger sizes before cessation of crystal growth.

The first conditions that I tried and got BSA crystals were under 52.5 – 57.5% SAS/100 mM K-PO<sub>4</sub> at pH 6.0 condition using hanging drop diffusion method in a 2 – 3 month period (Thome, 2001). BSA from the supplier was directly used, without any purification prior to BSA crystallization trials and its concentration was 10 mg/ml. However, the crystallization results could not be reproduced even after adding different kinds of salts (NaCl, MgCl<sub>2</sub>, KCl, CdCl<sub>2</sub>, ZnCl<sub>2</sub>, and NiCl<sub>2</sub>) in an attempt to enhance the crystals growth rate. Only CoCl<sub>2</sub> showed that it can be a useful additive to grow crystals in about 2 months. The crystallization trials were repeated in the similar conditions (SAS/K-PO<sub>4</sub>) with or without salts NaCl, MgCl<sub>2</sub> and KCl at different temperatures (4°C and 15°C), but no crystals formed. Therefore, BSA was purified by anion exchange

chromatography to improve its purity and try to crystallize BSA in a shorter period of time after protein purification. A solution of 10 mg/ml purified BSA was crystallized, under 55 – 60% SAS/50 mM K-PO<sub>4</sub> (pH 5.7 – 6.0)/1 – 20 mM CoCl<sub>2</sub> conditions. These crystals can be produced in about 1 – 2 months.

The crystallization results showed that the crystallization of purified BSA was still not reproducible. As a result of the poor reproducibility of crystals formation under SAS/K-PO<sub>4</sub> conditions, high concentrations (30 – 80 mg/ml) of unpurified BSA were attempted (Dr Luo, personal communication) instead of 10 mg/ml purified BSA in most of the crystallization trials. The purpose is to crystallize protein under the same crystallization conditions (SAS/K-PO<sub>4</sub>) which 10 mg/ml of purified BSA gave crystals. The changing the concentration of BSA from low concentration (10 mg/ml) to high concentration (e.g. 60 mg/ml) demonstrated that under such modified conditions BSA protein can be crystallized without any purification and the quality of crystals did not deteriorate. The growth period of such unpurified BSA crystals was similar to the purified BSA crystals. The most important factor to consider for using high concentration of BSA in the crystallization trials was the higher reproducibility of the BSA crystals grown in the crystallization trials compared to the 10 mg/ml of unpurified BSA and 10 mg/ml of purified BSA. Although the SDS-PAGE gel shown on Figure 3.8 illustrated that the unpurified 50 – 60 mg/ml BSA proteins have some high molecular-weight impurities as well as some low molecular-weight impurities (see the arrows on lane 4, 5), a number of single crystals still can be produced under such conditions. Therefore, the purification of BSA was not required if high concentration of BSA were used in the crystallization experiments. In summary, the most successful trials occurred at 51 – 55%

SAS/50 mM K-PO<sub>4</sub> (pH 5.6 – 5.9)/with or without CoCl<sub>2</sub> using hanging drop diffusion method when protein concentration was about 50 – 60 mg/ml. Consequently, purity is not considered to be playing a crucial role in the BSA crystallization experiments if the BSA concentration is maintained at high concentration (e.g. 50 mg/ml above) in the SAS/K-PO<sub>4</sub> or later the SAS/NaAc crystallization conditions.

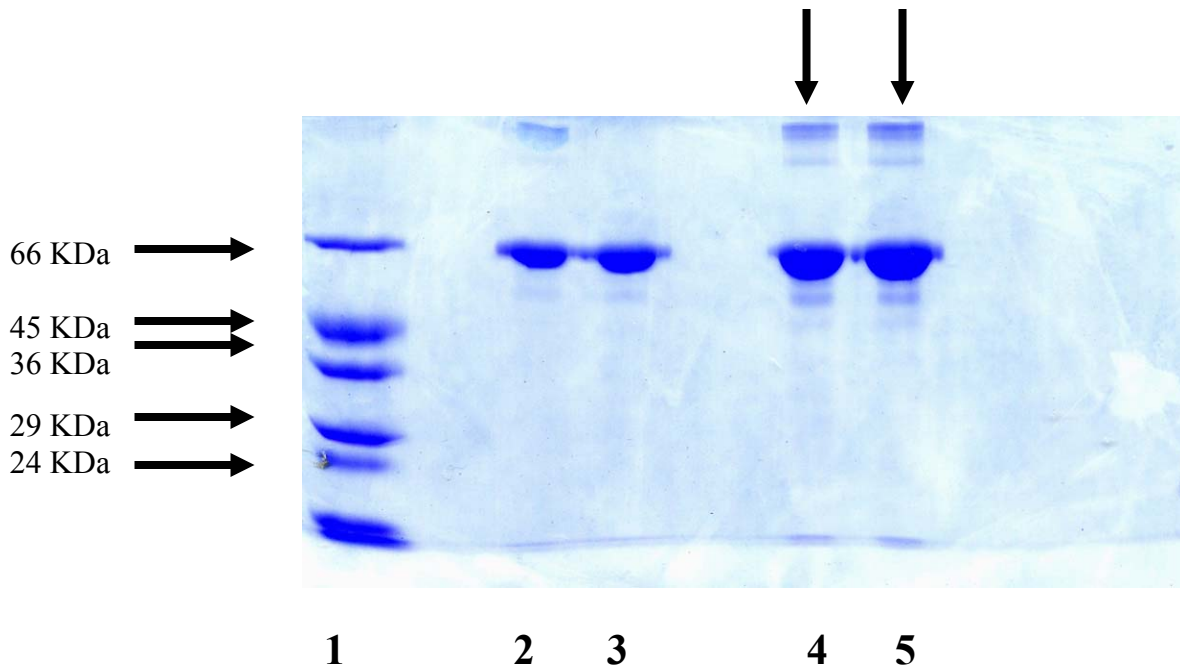


**Figure 3.8:** SDS-PAGE analysis of original and purified BSA samples. The protein marker is shown on the leftmost column as indicated by the arrows. The other two arrows on the top highlight the high-molecular-weight impurities in the BSA samples. For running a SDS-PAGE analysis, 1  $\mu$ L of 10 mg/ml BSA samples were mixed with 19  $\mu$ L DIW and 20  $\mu$ L of SDS-gel loading buffers, and 0.5  $\mu$ L of 50 mg/ml (or 60 mg/ml) BSA samples were mixed with 19.5  $\mu$ L DIW and 20  $\mu$ L of SDS-gel loading buffers respectively (**1: Marker, 2: Unpurified 10 mg/ml BSA, 3: Purified 10mg/ml BSA, 4 & 5: Unpurified 50 & 60 mg/ml BSA**).

The crystals produced under SAS/K-PO<sub>4</sub> conditions in high concentration of BSA were not very stable. For instance, the crystals kept in 20°C incubator were clear and glassy under inspection by microscope. When the crystal plate was put back to incubator after first inspection and taken out again within 10 minutes, it was found that the drops where crystals had grown started to precipitate. The BSA crystals no longer existed and the drops were covered by precipitate instead. The reproducibility of crystal formation under K-PO<sub>4</sub> buffer solution was not satisfactory and fluctuated. Therefore, a highly similar crystallization condition was established except that the growing buffer solution has been changed from K-PO<sub>4</sub> buffer solution to sodium acetate (NaAc) buffer solution (Christopher *et al.*, 1998). The rest of the chemical reagents including the precipitant and additive, and the concentrations of individual components of the crystallization solution remained the same. After altering the K-PO<sub>4</sub> buffer solution to NaAc buffer solution, the quality of crystals was better in terms of appearance and shape, the stability of crystals was enhanced and the quantity of crystals was higher as well (Figure 3.9).

A variety of salts have been evaluated for adding into SAS/K-PO<sub>4</sub> or SAS/NaAc buffer solutions to enhance the crystal-growing rate. The salts can be classified as monovalent ions such as LiCl, NaCl and KCl, and divalent ions such as MgCl<sub>2</sub>, CoCl<sub>2</sub>, NiCl<sub>2</sub>, ZnCl<sub>2</sub> and CdCl<sub>2</sub>. Only CoCl<sub>2</sub> showed a positive influence in getting single crystals. The sizes of crystals grown were between the ranges of 0.1 mm – 0.4 mm, other salts neither enhanced the growth rate of crystals nor produced any crystals that were suitable for X-ray diffraction. Therefore, CoCl<sub>2</sub> was chosen as an additive in the crystallization trials in NaAc buffer solution because the growth rate of crystals grown in such conditions will be slightly faster than those without CoCl<sub>2</sub> in the crystallization trials.

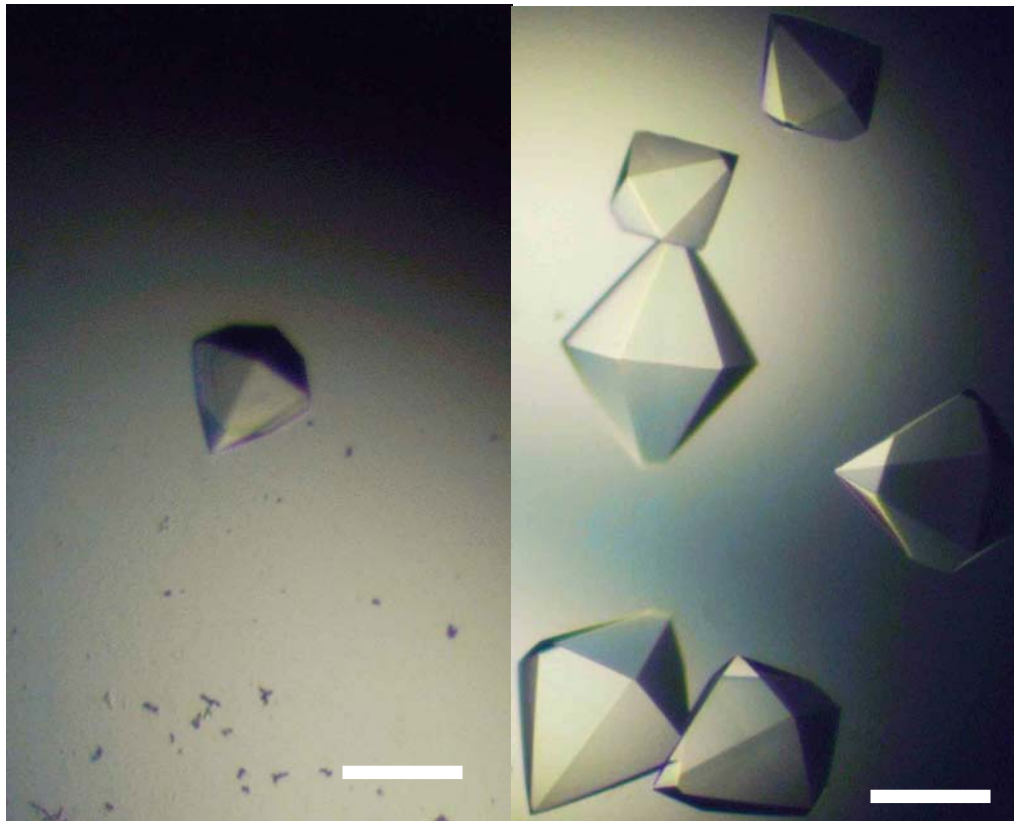


**Figure 3.9:** The quality of BSA crystals was improved and the quantity of BSA crystals was increased after altering the buffer solution from 50 mM K-PO<sub>4</sub> (left) to 25 mM NaAc (right). The scale bar represents a distance of about 0.2 mm.

Other buffer solutions such as sodium cacodylic, MES, citric acid and tri-sodium citrate buffers that have similar pH range (5.0 – 7.0) to K-PO<sub>4</sub> or NaAc buffer solutions have been tried. The crystals appeared after at least a month, they were neither sharp-edged nor stable as the ones grown in NaAc buffer solution, and most of them were formed in precipitate (Figure 3.10). Sodium acetate buffer solution was therefore considered as the best buffer solution among all the buffer solutions that have been attempted.

The Hampton Research's grid screens (MPD, (NH<sub>4</sub>)<sub>2</sub>SO<sub>4</sub>, PEG 6,000 & PEG 6,000/LiCl) and crystal screens (I & II) were also used to perform initial general screening to examine the protein supersaturation conditions. Using the grid screen, it was found that 30% PEG 6,000/1 M LiCl/100 mM MES at pH 6.0 can produce needle-like crystal under hanging drop diffusion method. The concentration of BSA used in the crystallization trials, either purified or unpurified, was 10 mg/ml. The result outcomes were not consistent and reproducible. Some trials for optimizing the crystallization conditions has been attempted, these included using high concentration (e.g. 30 mg/ml) of unpurified BSA, screening of precipitant concentration (5 – 30% PEG 6,000), using different kinds of salts with different concentrations (NaCl, KCl, MgCl<sub>2</sub>, NH<sub>4</sub>(SO<sub>4</sub>)<sub>2</sub>), different precipitants with different concentrations (PEG 400, PEG 600, PEG 1,000, PEG MME 2,000, PEG 4,000 and PEG 8,000), different buffer solutions (Tris, HEPES), and using sitting drop or microbatch methods to repeat some crystallization conditions. After all these trials have been attempted, no single crystal was obtained and most of the crystals grown were needle clusters.

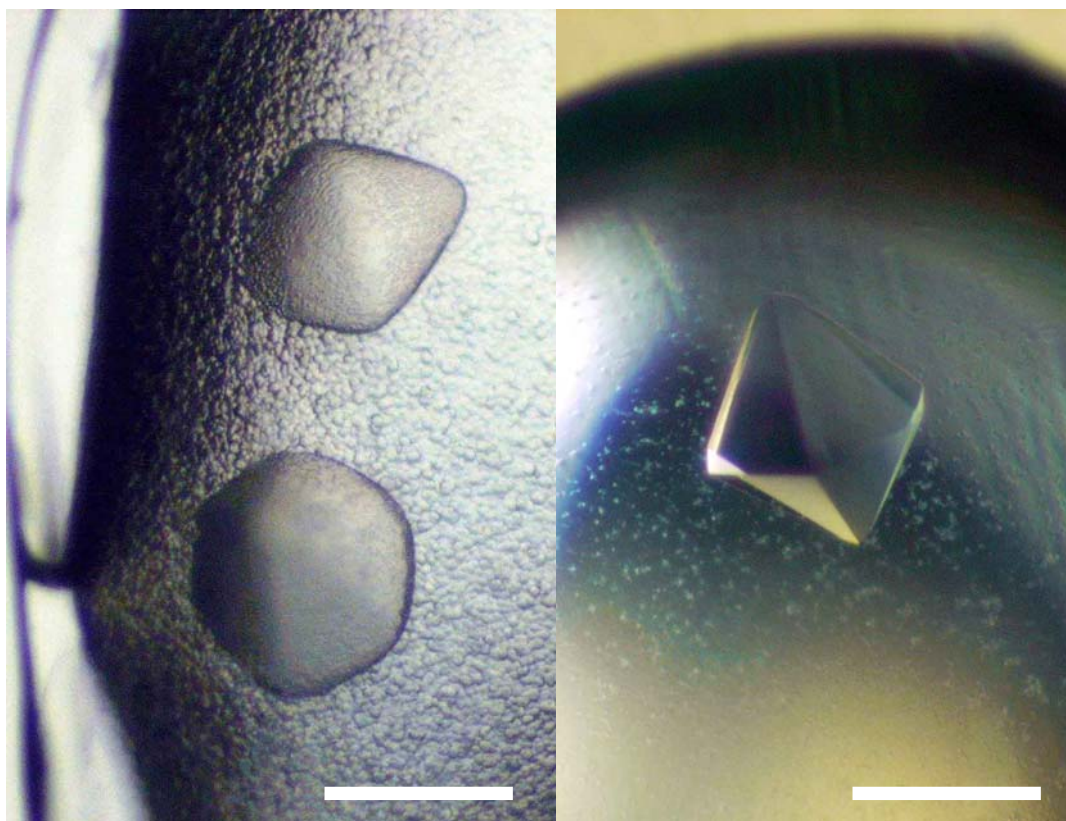


**Figure 3.10:** The difference between the BSA crystals grown in different buffer solutions at 20°C. The crystals on the left were grown in 100 mM sodium cacodylate buffer solution at pH 5.2 (52% SAS). The crystal in the right was grown in 25 mM NaAc buffer solution at pH 5.3 (48% SAS). The scale bar represents a distance of about 0.4 mm.

Another condition that showed crystals was 20% PEG MME 2,000/10 mM NiCl<sub>2</sub>/100 mM Tris at pH 8.5. The concentration of BSA mostly used in the crystallization trials was 10 mg/ml, either purified or unpurified; the rest of concentrations used were unpurified BSA. The optimization trials were done using sitting drop or microbatch method. The broad screening of buffer pH (7.0 – 9.0) and precipitant concentrations (10 – 40%) were carried out, and different BSA concentrations (5.0, 7.5, 10 & 20 mg/ml) have been used as well. The optimization strategies that were applied to both crystallization methods included narrowing the pH range of the buffer solutions and reducing the concentration of the precipitants. These strategies could not successfully optimize the multi-crystals to single crystals. The crystals grown were either too small or no single crystals were formed.

Although the optimization of these two conditions has been tried, the attempts to optimize the multi crystals to single crystals were unsuccessful and the reproducibility of crystal formation was poor as well. Both crystallization conditions gave needle clusters.

The crystals grown in SAS/NaAc are much better than those grown at the SAS/K-PO<sub>4</sub> condition in terms of crystal size, quality, growing time and reproducibility. For X-ray data collection, only the crystals which were sharp-edged, single and grown from clear drops as shown in Figure 3.11 were considered as good crystals and were selected to perform in-house X-ray diffraction experiments for screening the cryo-conditions of the crystals as well as determining the diffraction limits of the crystals themselves.

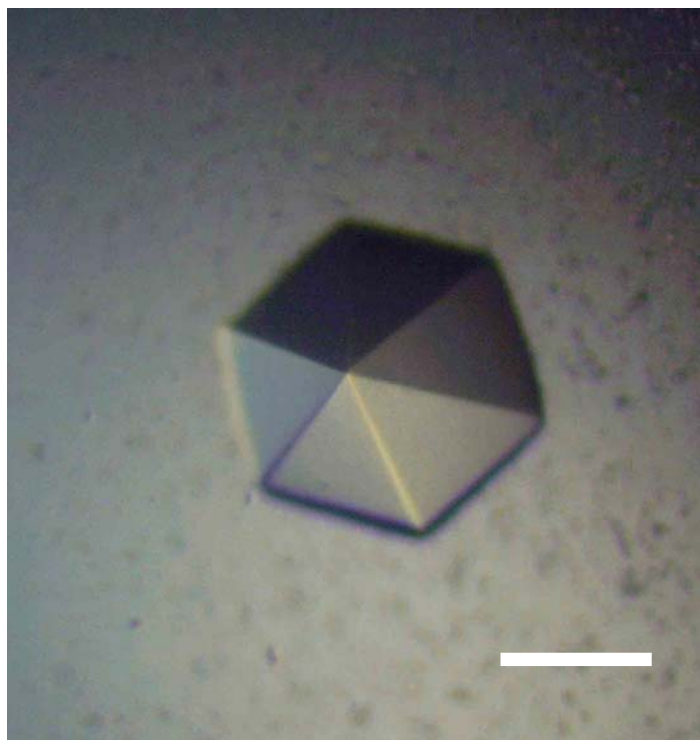


**Figure 3.11:** BSA Single Crystal (about 0.35 mm x 0.35 mm x 0.40 mm). The scale bar represents a distance of 0.2 mm approximately. This single crystal grown in 51% saturated ammonium sulfate with 25 mM sodium acetate buffer solution and 10 mM  $\text{CoCl}_2$ . The 2  $\mu\text{l}$  protein equally mixed with 2  $\mu\text{l}$  precipitating solution in 24-well VDX plate at 20°C using hanging drop diffusion method.

Compared to previous work (Thome, 2001); the crystallization conditions of BSA have been modified in two aspects. First, the K-PO<sub>4</sub> buffer solution has been changed to NaAc buffer solution in order to enhance the crystal reproducibility and crystal quality, in terms of size and appearance. Second, the concentration of BSA has been increased from 10 mg/ml to 50 – 60 mg/ml (or even higher up to 80 mg/ml) that makes the purification of BSA protein unnecessary.

The best crystallizations of BSA crystals which are highly reproducible are summarized in below:

50mg/ml: 48 – 50 % SAS  
25mM Sodium Acetate (pH 5.2 – 5.3)  
10mM CoCl<sub>2</sub> or without any additive  
Hanging or sitting drop  
20°C

60mg/ml: 48 – 52 % SAS  
25mM Sodium Acetate (pH 5.4 – 5.6)  
10mM CoCl<sub>2</sub> or without any additive  
Hanging or sitting drop  
20°C

### 3.1.7. Cryocrystallography of Bovine Serum Albumin

Cryoprotectants such as ethylene glycol, glycerol, glucose, sucrose, MPD, PEG 400, PEG 600, and xylitol have been tried (see Section 2.7.1). Preparing cryosolutions using 25 – 35% glycerol made the frozen drop looked glassy after immersing the drop into liquid nitrogen for few seconds, so 25 – 35% glycerol was preliminary used for cryoprotecting all BSA crystals that were produced under the SAS/K-PO<sub>4</sub> or SAS/NaAc conditions either with or without any additives. MPD, PEG 400 and PEG 600 were demonstrated to be inappropriate cryoprotectants, because once the cryosolutions were immersed in liquid nitrogen, the drop became opaque. This implies that once these cryosolutions were used to mount the crystals, the crystals would not be properly flash-cooled. Other cryoprotectants, 25 – 30% ethylene glycol, 35 – 40% sucrose, 30 – 35% glucose and 30% Xylitol showed promising results in the preliminary cryo-solution examination.

On observation, a higher concentration cryosolution or mother liquor was needed to cryoprotect the crystals grown in SAS precipitating solution. After a 1 – 2 month crystallization period, the concentration of the ammonium sulfate was no longer the same as in the initial condition. This is the likely reason why these kinds of crystals seemed to dissolve once the mother liquor from the same well or the same SAS concentration in the cryosolution were added to the crystal drop. Consequently, a higher concentration of mother liquor or cryosolution might be needed. For instance, 55% SAS/25% glycerol/ 25 mM NaAc cryosolution was used to flash cool the crystals that were grown in 50% SAS/25 mM NaAc solution. Normally, the concentration of SAS required was 5 – 10% higher in the cryosolution than that in the reservoir solution.

After the preliminary examination for testing the suitable cryoprotectants, various cryosolutions were prepared to examine their ability to cryoprotect the BSA crystals. The cryosolutions prepared were the same as the precipitating solutions that produced crystals except DIW were replaced by cryoprotectants and the concentration of SAS would be increased by 5 – 10% in some cases. The minimum sizes of BSA crystals for X-ray diffraction studies were at least 0.10 mm in each dimension. All cryo-conditions tested are summarized in Table 3.2. Diffraction of BSA crystals under a variety of cryo-conditions was carried out at the SSSC (see Section 2.7.2). The results demonstrated that none of the cryo-conditions allows crystals to be diffracted to better than 8 Å resolution. For instance, 55% SAS/30% Xylitol/25 mM NaAc (pH 5.2) cryosolution seems that it can flash cool the crystal quite well based on its glassy appearance as shown in Figure 3.12. However, the crystal did not diffract at all. So, such cryosolution conditions did not guarantee that the crystal would diffract if the judgment was based on the glassy appearance of the crystal solution. Among all cryoprotectants, ethylene glycol and xylitol were the worst, no diffraction pattern was observed. The other cryoprotectants such as sucrose displayed diffractions to limited resolution beyond 10 Å. Other cryoprotectants such as paraffin oil have shown similar results to 35% sucrose with both displaying ice rings in the diffraction pattern, therefore, they were not considered as ideal cryoprotectants. Replacement of the saturated ammonium sulfate by sodium malonate has been tried, but no diffraction was observed.

In X-rays diffraction experiments, the performances of cryosolutions, in terms of resolution, that contain the NaAc buffer solution are better than those contain K-PO<sub>4</sub>

buffer solution. This might be attributed to the nature of buffer itself or because the sizes of the crystals grown in K-PO<sub>4</sub> buffer were smaller than those grown in NaAc buffer.



**Figure 3.12:** BSA single crystal inside the loop located on the goniometer, the cryosolution used was 55% SAS/30% xylitol/25 mM NaAc (pH 5.2).

The best cryo-conditions that BSA crystal can be diffracted to 8 Å are SAS/NaAc/25% glycerol and SAS/NaAc/30% glucose respectively. Comparing these two and the other conditions, it suggests that the most satisfactory cryoprotectants used were 25 – 35% glycerol and 30 – 35 % glucose. There were no ice-rings on both cases but the best diffraction obtained was only to resolution of 8 Å. This resolution is not sufficient for solving a protein tertiary structure.

| Cryoprotectant (Cy) | [Cy] (%) | [BSA] (mg/ml) | [Precipitant] | Buffer/pH  | Additive              | Crystal (mm)          | Resolution (Å) |
|---------------------|----------|---------------|---------------|------------|-----------------------|-----------------------|----------------|
| EG                  | 25       | 50            | 55% SAS       | K-PO4 /5.6 | NA                    | 0.40                  | ND             |
|                     | 30       | 80            | 50%SAS        | K-PO4 /5.6 | NA                    | 0.15                  | ND             |
| Glycerol            | 25       | 60            | 49% SAS       | K-PO4 /5.7 | NA                    | 0.10                  | ~ 10.0         |
|                     | 30       | 60            | 48% SAS       | K-PO4 /5.7 | NA                    | 0.10                  | ND             |
|                     | 35       | 60            | 49% SAS       | K-PO4 /5.8 | NA                    | 0.10                  | ND             |
|                     | 25       | 50            | 47% SAS       | NaAc/5.2   | NA                    | 0.25                  | ~ 9.0          |
|                     | 25       | 50            | 45% SAS       | NaAc/5.4   | NA                    | 0.30                  | ~ 8.0          |
|                     | 25       | 60            | 48% SAS       | NaAc/5.2   | NA                    | 0.25                  | ~ 10.0         |
|                     | 25       | 50            | 48% SAS       | NaAc/5.5   | 10mMCoCl <sub>2</sub> | 0.20                  | ~ 10.0         |
|                     | 25       | 50            | 50% SAS       | NaAc/5.5   | 10mMCoCl <sub>2</sub> | 0.30                  | ~ 9.5          |
|                     | 30       | 60            | 50% SAS       | NaAc/5.4   | NA                    | 0.30                  | ~ 9.0          |
|                     | 35       | 60            | 54% SAS       | NaAc/5.2   | NA                    | 0.20                  | ~ 9.6          |
|                     | 30       | 50            | 55% SAS       | NaAc/5.2   | 3% Xylitol            | 0.10                  | ND             |
|                     | Glucose  | 30            | 60            | 51% SAS    | NaAc/5.2              | 10mMCoCl <sub>2</sub> | 0.10           |
| 30                  |          | 60            | 56% SAS       | NaAc/5.4   | 10mMCoCl <sub>2</sub> | 0.10                  | ~ 8.6          |
| 30                  |          | 30            | 49% SAS       | NaAc/5.4   | NA                    | 0.10                  | ~ 8.0          |
| 35                  |          | 60            | 48% SAS       | NaAc/5.5   | NA                    | 0.10                  | ~ 8.8          |
| 35                  |          | 60            | 51% SAS       | NaAc/5.5   | NA                    | 0.10                  | ~ 10.8         |
| Sucrose             | 35       | 30            | 54% SAS       | NaAc/5.2   | NA                    | 0.15                  | ND             |
|                     | 35       | 60            | 55% SAS       | NaAc/5.1   | NA                    | 0.10                  | ND             |
|                     | 35       | 70            | 57% SAS       | NaAc/5.4   | NA                    | 0.15                  | ND             |
| Xylitol             | 30       | 50            | 55% SAS       | NaAc/5.2   | NA                    | 0.10                  | ND             |

**Table 3.2:** Summary results of various cryo-conditions of BSA crystals that were prepared for X-ray diffraction experiments at the SSSC. The preparation of cryosolution was done according to concentration of cryoprotectant, precipitant, additive, buffer, and buffer pH. The concentrations of all K-PO<sub>4</sub> and NaAc buffer solutions are 50 mM and 25 mM respectively. The concentrations of SAS shown above are the crystallization conditions. ND: No diffraction.

Even though the crystals cannot be diffracted to resolutions better than 3.5 Å, the low resolution data was collected to define the unit cell parameters of a BSA crystal. A BSA crystal grown in 49% SAS/25 mM NaAc at pH 5.4 was cryoprotected by 30% glucose. The cell dimension of the crystal was determined in the SSSC X-ray laboratory, which was  $a = 147.624 \text{ \AA}$ ,  $b = 147.624 \text{ \AA}$ ,  $c = 351.117 \text{ \AA}$ ;  $\alpha = 90^\circ$ ,  $\beta = 90^\circ$ ,  $\gamma = 120^\circ$  and the crystal space group was hexagonal P6 (Figure 3.13).

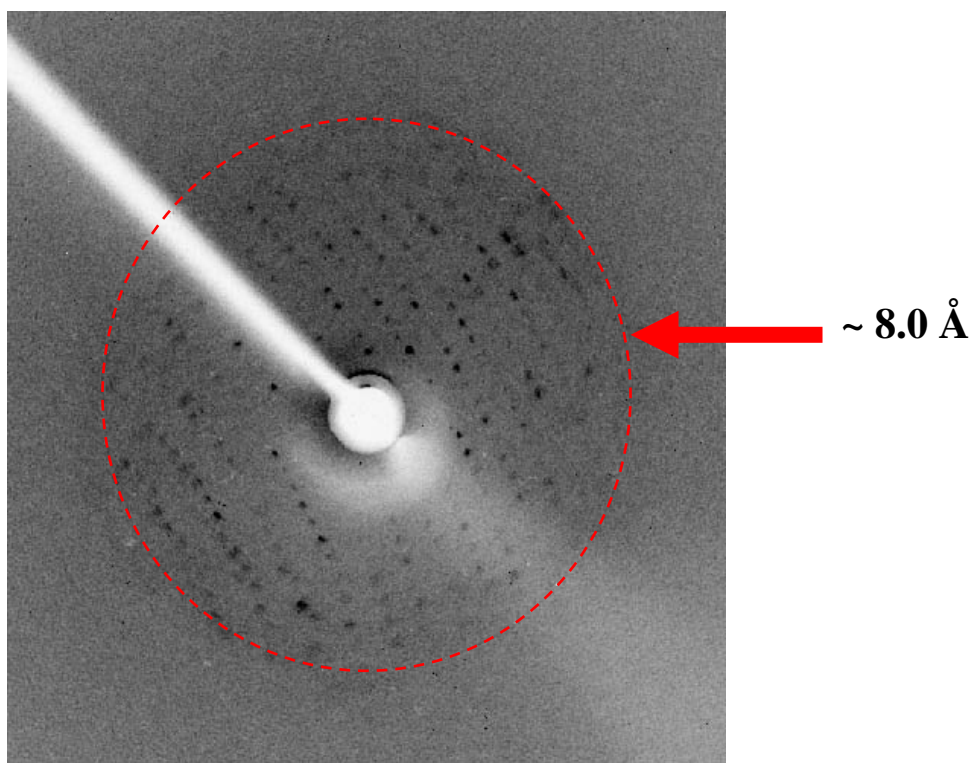


**Figure 3.13:** X-Ray Diffraction Pattern of a BSA crystal that cryoprotected by 30% glucose. The diffraction resolution is 8.0 Å.

According to Matthew's coefficient (Matthews, 1968), the range of solvent content of BSA crystal is shown on Table 3.3. The calculation is based on the assumption of 1 – 9 molecules per asymmetric unit (a.s.u) and the molecular weight of BSA is 66,400 Da. From Table 3.3, it shows that there are a number of possibilities of the solvent

content of BSA crystals. The Matthew's coefficient of protein crystals is usually between 1.7 – 3.5 Å<sup>3</sup>/Da, so most likely there are 6 – 8 molecules exist in one asymmetric unit in a crystal unit cell.

| No. of molecule/ a.s.u. | Matthews coefficient | Solvent content (%) |
|-------------------------|----------------------|---------------------|
| 1                       | 16.6                 | 92.5                |
| 2                       | 8.3                  | 85.1                |
| 3                       | 5.5                  | 77.6                |
| 4                       | 4.2                  | 70.2                |
| 5                       | 3.3                  | 62.7                |
| 6                       | 2.8                  | 55.3                |
| 7                       | 2.4                  | 47.8                |
| 8                       | 2.1                  | 40.4                |
| 9                       | 1.9                  | 32.9                |
| 10                      | 1.7                  | 25.5                |

**Table 3.3:** Summary result of the number of molecules in an asymmetric unit (a.s.u.) within a unit cell of a BSA crystal.

Compared to the diffraction data collected above with the previous work done (Thome, 2001), the space group and cell parameters of the BSA that collected by Thome are: P6, a = 148.24 Å, b = 148.24 Å, c = 356.70 Å and  $\alpha = 90^\circ$ ,  $\beta = 90^\circ$ ,  $\gamma = 120^\circ$ . This indicates that both results done by me and Thome are similar with each other. The cell dimensions of crystals are almost same as each other, and the space groups of both crystals are hexagonal, P6. The major difference is Thome employed room temperature techniques to diffract crystals but I used the cryo-temperature technique to diffract crystals. This implies that BSA crystals diffracted either at room temperature or at cryo-temperature are weakly diffracted to 8 Å.

The results tell us that we have to find another way to obtain well diffracted BSA crystals in order to solve its crystal structure. Otherwise, structural information of BSA protein can not be gained and no clues for finding the binding site of thiomolybdates or copper ions on BSA. The results demonstrate that BSA crystals grown in SAS/K-PO<sub>4</sub> or SAS/NaAc and cryoprotected by glycerol or glucose do not diffract very well. The reason is still unclear, but this might attributed to protein characteristics. This is probably due to three-dimensional flexibility in some flexible regions (such as N-terminus or C-terminus regions) of BSA that causes crystal lattices in these regions disordered. In order to diffract BSA crystals to high resolution, we need to either grow BSA crystals under a totally new condition, or find another cryoprotectant or cryo-condition that can protect the BSA crystals. Limited proteolysis may be worth to trying to remove the suspect flexible region to obtain high-quality crystals if this is a reason that leads to poor diffraction of BSA crystals (Xie *et al.*, 1996).

For looking at new crystallization conditions, a number of crystallization screening kits supplied by different vendors (Emerald Biostructures, Molecular Dimension, etc) can be explored or different crystallization strategies can be applied as well. Seeding might be attempted to transfer some BSA crystal seeds into PEG 6,000/MES/LiCl precipitating conditions, to observe whether BSA crystals could be grown under such circumstances. Replacement of SAS by another precipitant is worthwhile to try for decreasing the crystal growth rate and reducing the difficulty in handling the crystals during cryocrystallography. For finding suitable cryo-conditions to flash cool BSA crystals, a combination of different cryoprotectants might be attempted.

## 3.2. THIOREDOXIN-2

### 3.2.1. Introduction

Trx-2 (HP1458) is one of the Trx homologues from *Helicobacter pylori*, which has a molecular weight of approximately 12 KDa. X-ray diffraction data of Trx-2 has been collected at 2.4 Å (Filson *et al.*, 2003). Hence, the data is expected to provide information to determine the structure of Trx-2. However, the reflections at high resolution are split (Figure 3.14), which means each spot is divided into 2 pieces, so better quality crystals that can diffract to high resolution and without split spots are required. The purification procedure was followed as previously described (Filson *et al.*, 2003) to obtain pure and homogenous proteins. Different crystallization conditions for crystallizing Trx-2 were attempted. Then, cryo-conditions to flash-cool the Trx-2 crystals were examined.

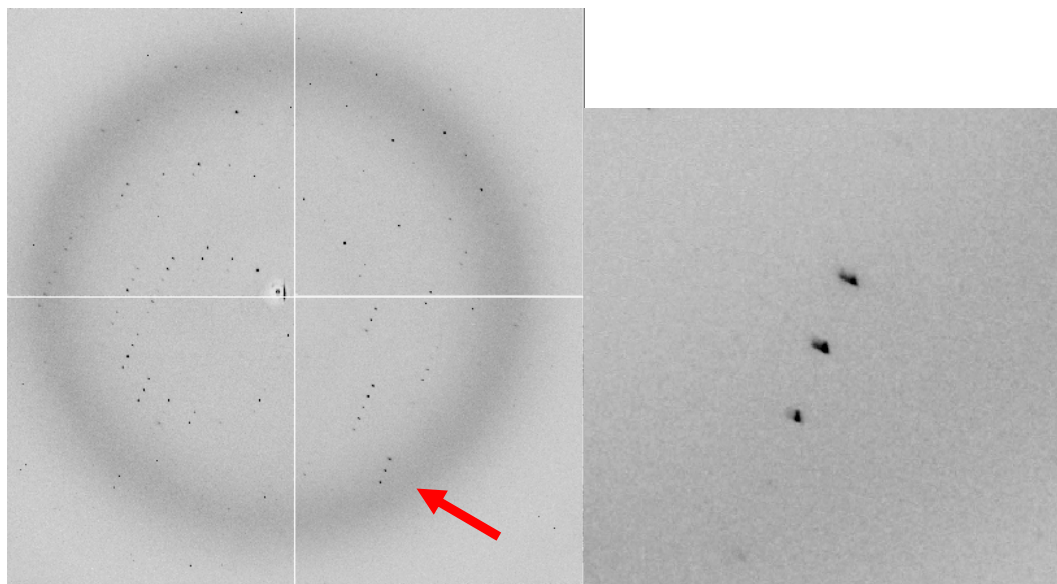


**Figure 3.14:** X-ray diffraction pattern of a Trx-2 crystal that had been collected at 2.4 Å resolution (Filson *et al.*, 2003) is shown on the left. The arrow indicates 3 split spots. The graph on the right is the enlarge portion of these split spots.

### 3.2.2. SDS-PAGE Analysis after Overexpression and Cell Lysis

The SDS-PAGE analysis results were shown in Figure 3.15 to demonstrate the improvement of the purity of Trx-2 proteins. After the protein overexpression (see Section 2.3), the Trx-2 proteins were released from the cell and purified through lysis (Lane 2), centrifugation (Lane 3), ammonium sulfate precipitation (Lane 4), overnight dialysis (Lane 5) and anion exchange chromatography (Lane 6 & 7). The impurities that originated from the cells were removed through the protein purification procedures.

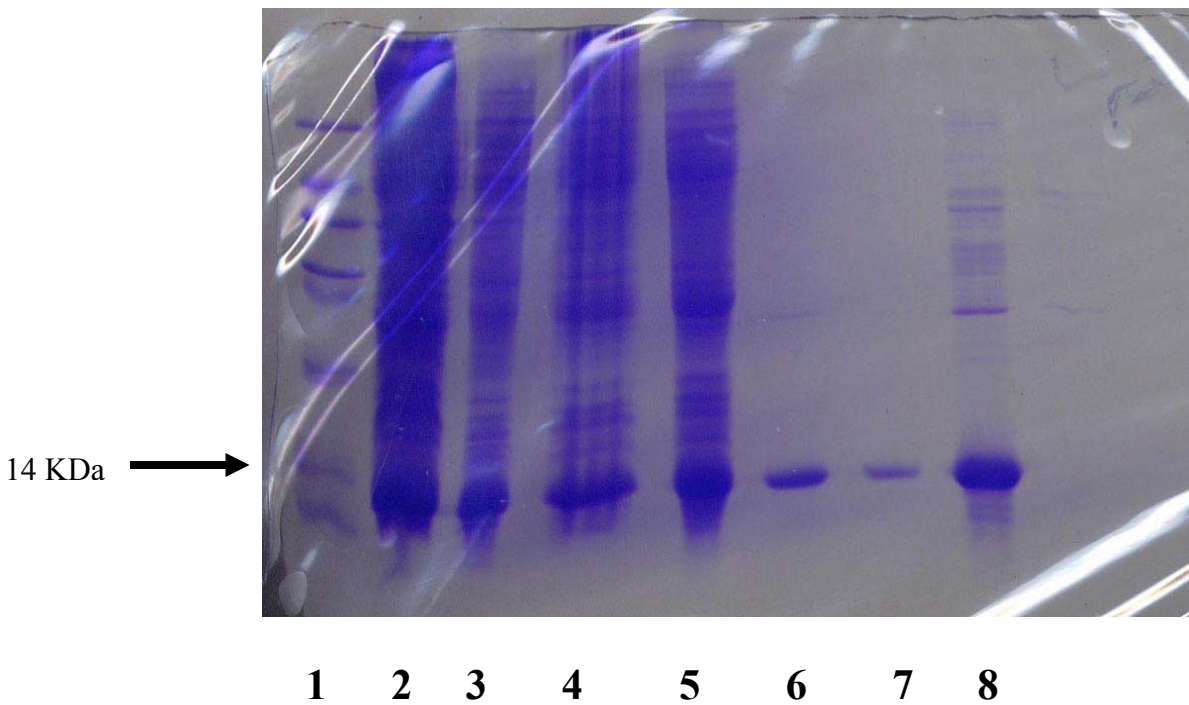


**Figure 3.15:** SDS-PAGE analysis of Trx-2 samples after overexpression and purification. The arrow on the left indicates the 14 KDa molecular weight level (1: Protein marker, 2: After lysis, 3: After centrifugation, 4: After ammonium sulfate precipitation, 5: After dialysis, 6 & 7: Fraction 1 & 2 in anion exchange chromatography, 8: After ultrafiltration).

### **3.2.3. Purification of Thioredoxin-2**

#### **3.2.3.1. Anion Exchange Chromatography Purification**

After lysis and overnight dialysis, anion exchange chromatography was performed. The Trx-2 sample solution was loaded onto the HQ 20 column (see Section 2.4.2.3). Seven fractions were collected and only the first two fractions (fraction number #1 and #2) contained purified Trx-2 and represented as protein samples according to chromatogram (Figure 3.16). The UV absorbance of this peak was detected as 0.6837 at a wavelength of 280 nm. These 2 fractions were used for the further SDS-PAGE analysis for determining the purity of Trx-2 protein. Comparing lane 2 with lane 6 or 7 (Figure 3.15), the purity of Trx-2 was improving. Lane 8 demonstrated that after ultrafiltration (see Section 2.4.2.4) Trx-2 was approximately 90% pure. It also showed that the intensive reduction of the overall amount of contamination presented in the Trx-2 protein samples through the protein purification. So, the purification of Trx-2 proteins by cation exchange chromatography (see Section 2.4.2.5) would be continued in order to obtain high purity Trx-2 protein.

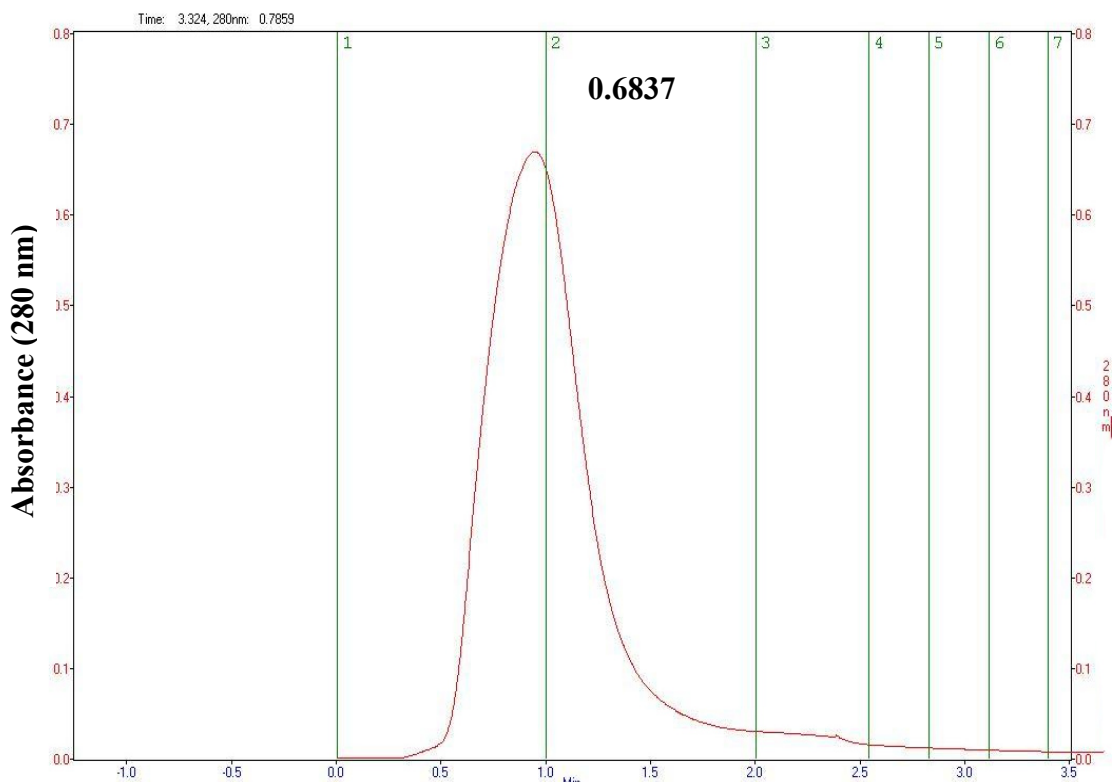


**Figure 3.16:** Chromatogram of the purification of Trx-2 sample solutions collected in anion exchange chromatography.

### 3.2.3.2. Cation Exchange Chromatography Purification

The Trx-2 sample solution was reconcentrated using ultrafiltration after anion exchange chromatography; 5 – 10 ml of reconcentrated sample solution was loaded into the self-packed carboxymethyl cation exchange column. Eventually, 40 fractions were collected, and only the fractions #26 – #30 represented the highest purity of Trx-2 proteins among all fractions collected according to the UV detector where UV absorbance value was given as 0.7494 at the wavelength of 280 nm as shown in Figure 3.17.

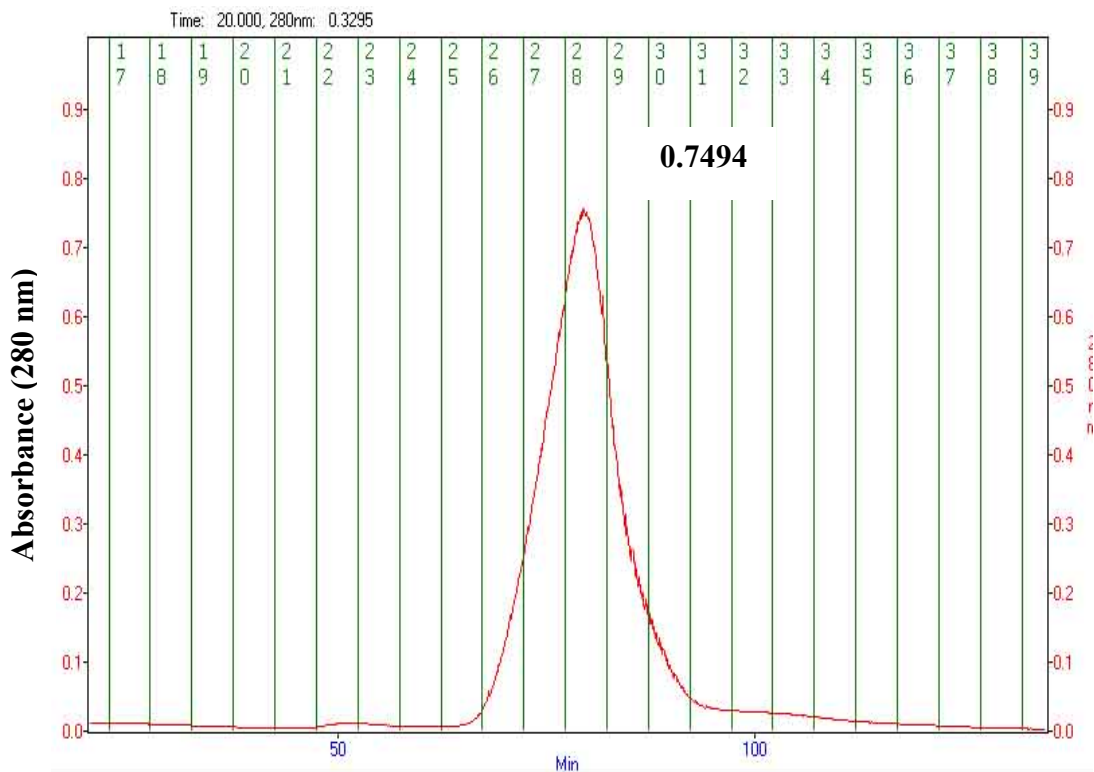


**Figure 3.17:** Chromatogram of the purification of Trx-2 sample solutions collected in cation exchange chromatography.

These 5 fractions were collected individually and used for further SDS-PAGE analysis to confirm their purity. From Figure 3.18, it demonstrated that there were no high-molecular-weight and low-molecular-weight impurities in the sample, so the purity of Trx-2 sample was considered as greater than 99%. The fractions were combined and concentrated to 1 – 2 ml.

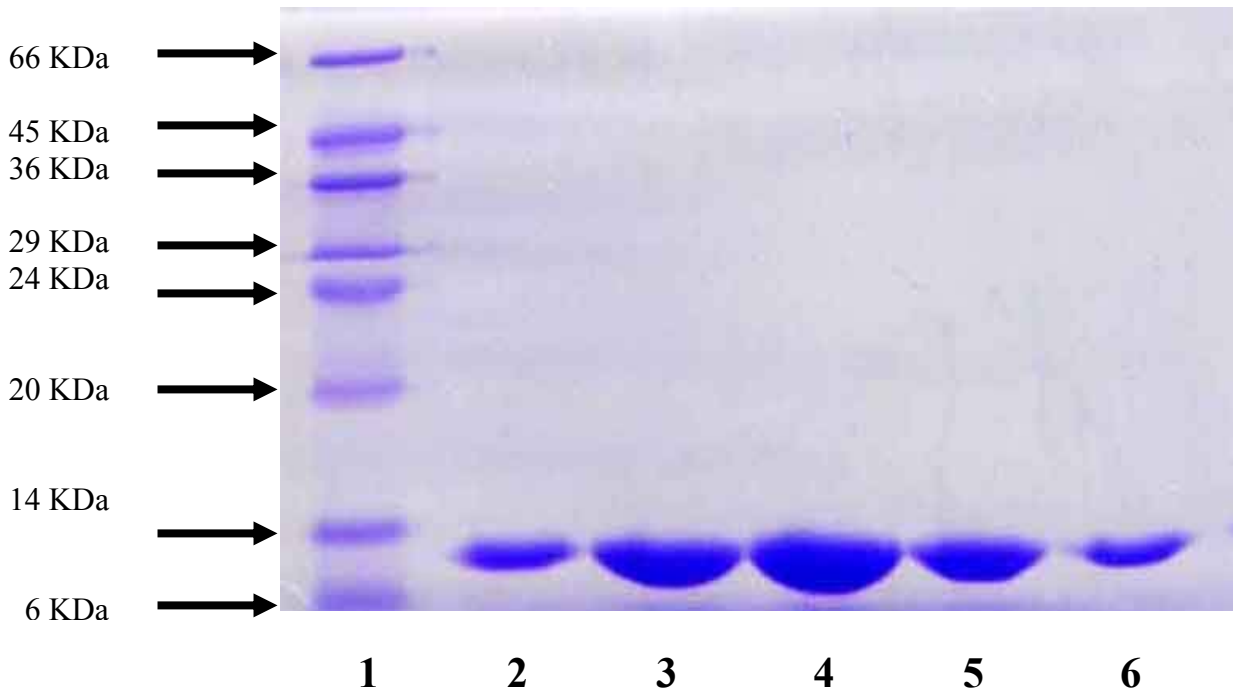


**Figure 3.18:** SDS-PAGE analysis of Trx-2 sample solutions after cation exchange chromatography. The leftmost column represents the “Low Molecular Weight Protein” marker and the arrow on the left indicates the individual molecular weight levels. The other 5 columns represented the Trx-2 samples that collected from fractions #26 – #30. **(1: Protein marker, 2: Purified Trx-2 collected from fraction # 26 after 2<sup>nd</sup> cation column chromatography, 2: Fraction #27, 4: Fraction #28, 5: Fraction #29, 5: Fraction #30).**

### 3.2.4. Concentration Determination of Purified Thioredoxin-2

Six Bradford standards were prepared according to Table 2.1. All standards were used to establish the calibration curve shown in Figure 3.19 to determine the concentration of Trx-2. Two sets of samples that from the same purified Trx-2 samples were prepared to determine the actual concentration of Trx-2 after purification. From Table 3.4, the absorbance values of both samples were detected as 0.4337 and 0.4316 respectively. These values were corresponded to 6.3 mg/L and 6.3 mg/L individually.

The concentration average of the Trx-2 was 6.3 mg/L. After the conversion of the 1000 times dilution factor (see Section 2.5.3), the true Trx-2 concentration was determined as 6.3 mg/ml. The purified Trx-2 samples were then utilized to perform the DLS measurement for determining the homogeneity of Trx-2 protein.

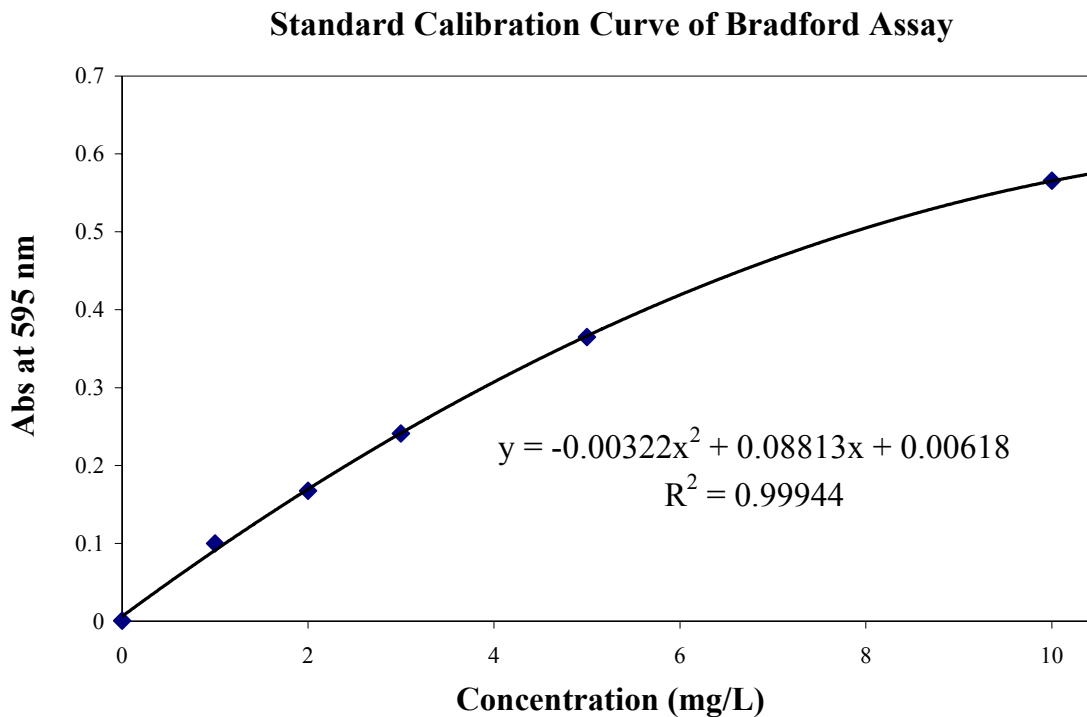


**Figure 3.19:** Bradford assay calibration curve for purified Trx-2 sample solutions.

| Sample         | Concentration (mg/ml) | Absorbance |
|----------------|-----------------------|------------|
| Trx Sample 1   | 6.3                   | 0.4316     |
| Trx Sample 2   | 6.3                   | 0.4337     |
| <b>Average</b> | <b>6.3</b>            |            |

**Table 3.4:** Bradford assay absorbance data of the purified Trx-2 sample solutions to determine the true concentration of purified Trx-2 sample solutions.

### 3.2.5. Homogeneity Determination of Purified Thioredoxin-2

Prior to sample measurement, the Trx-2 sample solutions of 6.3 mg/ml were diluted to 1.0 mg/ml for DLS measurements (see Section 2.5.2). From the monomodal histogram of 1 mg/ml of Trx-2 displayed in Figure 3.20, the curve was highly symmetrical and narrow distributed. The %polydispersity (%PolyD) calculated was based on the distribution of peak intensity. The %PolyD of purified Trx-2 was 12.5% which was less than the upper limit 30% that described in the supplier application note (Protein Solutions, New Jersey, USA) as well as the literature (Ferre-D'Amare and Burley, 1997). Thus, the purified Trx-2 proteins can be considered to be monodispersed. The quality of the purified Trx-2 was satisfactory to perform crystallization trial in terms of purity and homogeneity.

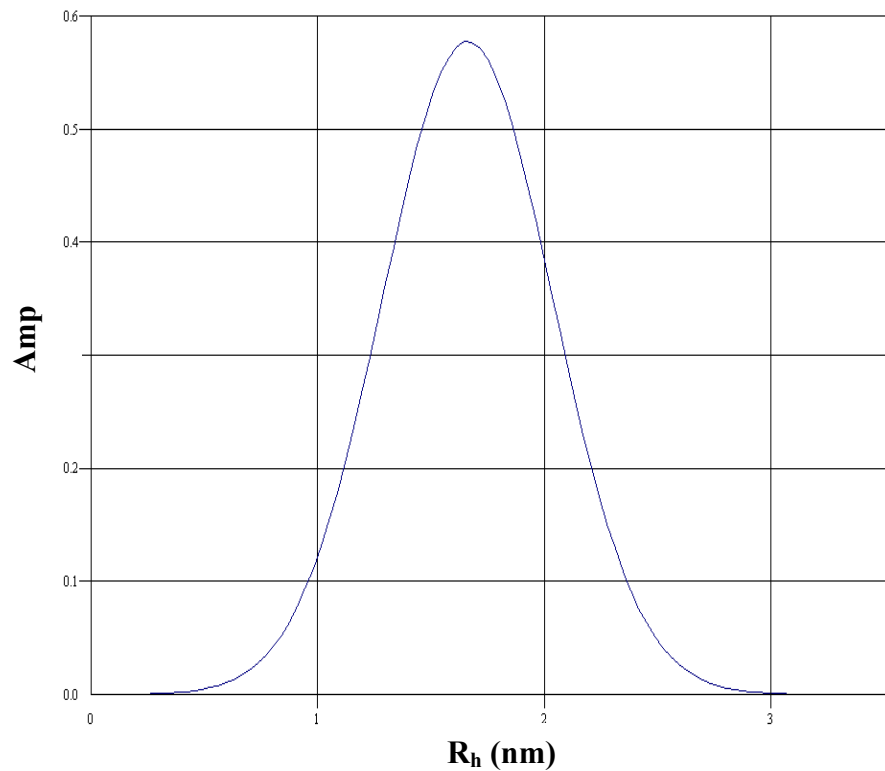


**Figure 3.20:** Monomodal histogram of 1.0 mg/ml of purified Trx-2 solution. The %polydispersity of the purified sample solution is 12.5%.

### 3.2.6. Crystallization Trials of Thioredoxin-2

The Trx-2 protein has been crystallized and the crystallization condition has already been published (Filson *et al.*, 2003). The condition is 30% PEG 6,000/0.1 M  $(\text{NH}_4)_2\text{SO}_4$ /10 mM DTT. However, the crystallization condition was re-optimized in order to obtain much better quality crystals (see Appendix 1 for the summary of Trx-2 crystallization trials). Initially, the crystallization condition: 30% PEG 6,000/100 mM citric acid buffer (pH 4.5)/vapor diffusion method was considered as the most satisfactory condition among all Hampton Research screening kits conditions. The crystals formed within 1 – 2 weeks. There were many crystals in the drops but quality of the crystals was better than the crystals that were grown under all other screening conditions in terms of crystal appearance. The crystallization condition was similar to the published result as well. After that, the additive and detergent screens were employed to optimize the crystallization condition. Acetonitrile, n-butanol, DTT and methylene chloride were found to produce better crystals in terms of shape among all of the reagents used. However, DTT was the best among all of them. The initial trials that have been attempted were based on 24 – 36% PEG 6,000/100 mM citric acid buffer (pH 3.7 – 4.5)/10 mM DTT sitting drop method. The well solution of the sitting drop method contained 90  $\mu\text{l}$  of the precipitating solution that mixed with 10  $\mu\text{l}$  of 100 mM DTT. The drop volume was 2  $\mu\text{l}$  of Trx-2 mixed with 2  $\mu\text{l}$  of well solution. The rod-like long crystal showers appeared as shown in Figure 3.21 after about 3 – 7 days and another 1 – 2 weeks for growing before cessation. Different precipitants (PEG 4,000 and PEG 8,000), precipitant concentrations (14 – 36% PEG), different additives [acetonitrile, n-butanol and methylene chloride], additive concentrations (5 – 50mM) and pHs (3.6 – 4.9) have been

tried to optimize the crystallization condition. Other optimization strategies such as adding paraffin or Al's oil to slow down the evaporation rate, dilution method used to reduce the numbers of the crystals and seeding (either macro- or micro-) have been attempted in order to obtain single crystals. However, the most reproducible and reliable single crystals were grown at 24% – 26% PEG 6,000/10 mM DTT/100mM citric acid buffer at pH 4.0 – 4.2 using either hanging drop or sitting drop diffusion methods as shown in Figure 3.21. Co-crystallization of PEG 6,000/10 mM DTT/100 mM citric acid buffer with 10% glycerol has also been tried. The crystal growth time was almost the same but crystal sizes were slightly smaller.

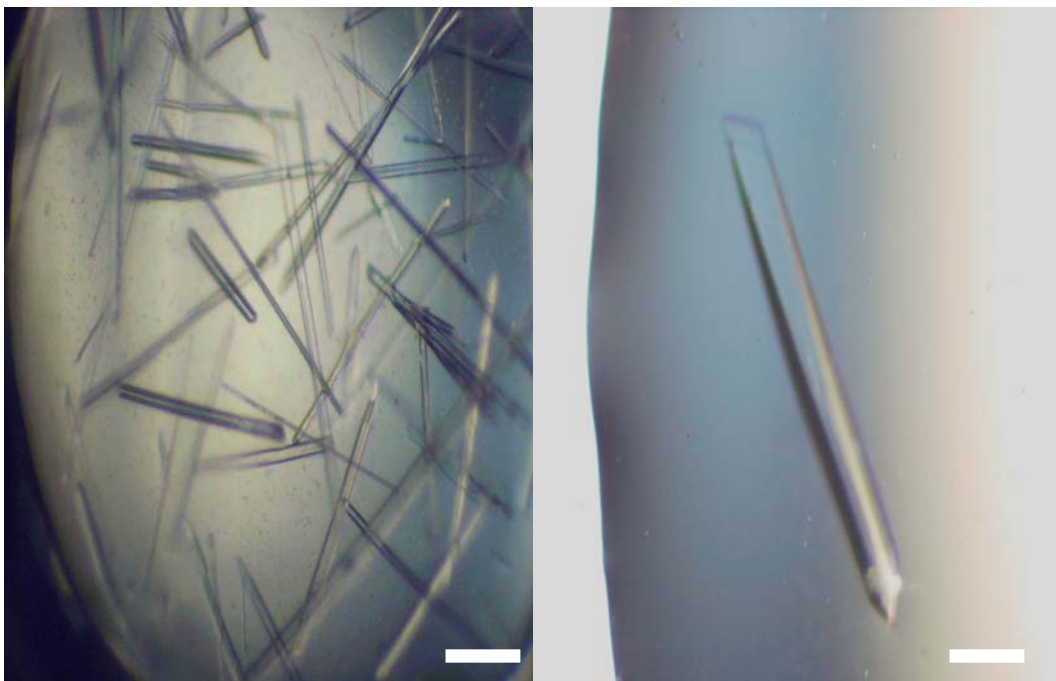


**Figure 3.21:** The optimization of Trx-2 crystals. Initial crystal grown from screening kit is shown on the left, the condition is: 33 % PEG 6000/1000 mM citric acid buffer (pH 4.3). After optimization, Trx-2 multiple crystals were optimized into single crystals as shown on the right, the condition is: 24% PEG 6000/100 mM citric acid buffer (pH 4.2)/10 mM DTT. The scale bar represents a distance of about 0.2 mm. Trx-2 single crystal shown on the right (about 0.12 mm x 0.12 mm x 0.9 mm).

### 3.2.7. Cryocrystallography of Thioredoxin-2

At first, glycerol at different percentages from 10% – 30% was examined for its capability to cryoprotect the Trx-2 crystals by immersing the cryosolution into liquid nitrogen about 5 – 10 seconds (see Section 2.7.1). Glycerol at 10% was found to be suitable to properly freeze the mother liquor, so 10% glycerol was used as cryoprotectant for the Trx-2 crystals that crystallized under the PEG 6,000/citric acid buffer/DTT condition. The concentration of the precipitant, buffer, salt in the well solution remained the same, only the DIW was replaced by 10% glycerol. The sizes of crystals were between 0.05 – 0.15 mm at the minimum dimension. Other cryoprotectants such as ethylene glycol, glucose, PEG 400, PEG 600, MPD, sucrose and xylitol were also tried. Only 15 – 20% glucose and 10 – 15% PEG 400 were considered appropriate, because after immersing the cryosolutions without any crystal into liquid nitrogen, the frozen solution looked glassy.

After the preliminary screening for choosing appropriate cryoprotectants, Trx-2 crystals were used to examine the cryo-conditions using 10% glycerol, 15 – 20% glucose, and 10 – 15% PEG 400. For the screening using the X-ray diffractometer (see Section 2.7.2) of Trx 2 crystals, a crystal was scooped up and soaked in 25 % PEG 6,000/100 mM citric acid buffer (pH 4.2)/10 mM DTT with 10 % PEG 400. As a result, a 3.2 Å diffraction data was preliminary obtained. No ice ring was formed and observed in the diffraction image as shown in Figure 3.22. The cell dimension of Trx-2 crystal was determined in the SSSC laboratory, which was  $a = b = 42.65 \text{ \AA}$ ,  $c = 64.64 \text{ \AA}$ ;  $\alpha = \beta = \gamma = 90^\circ$  and its space group is tetragonal, P4.

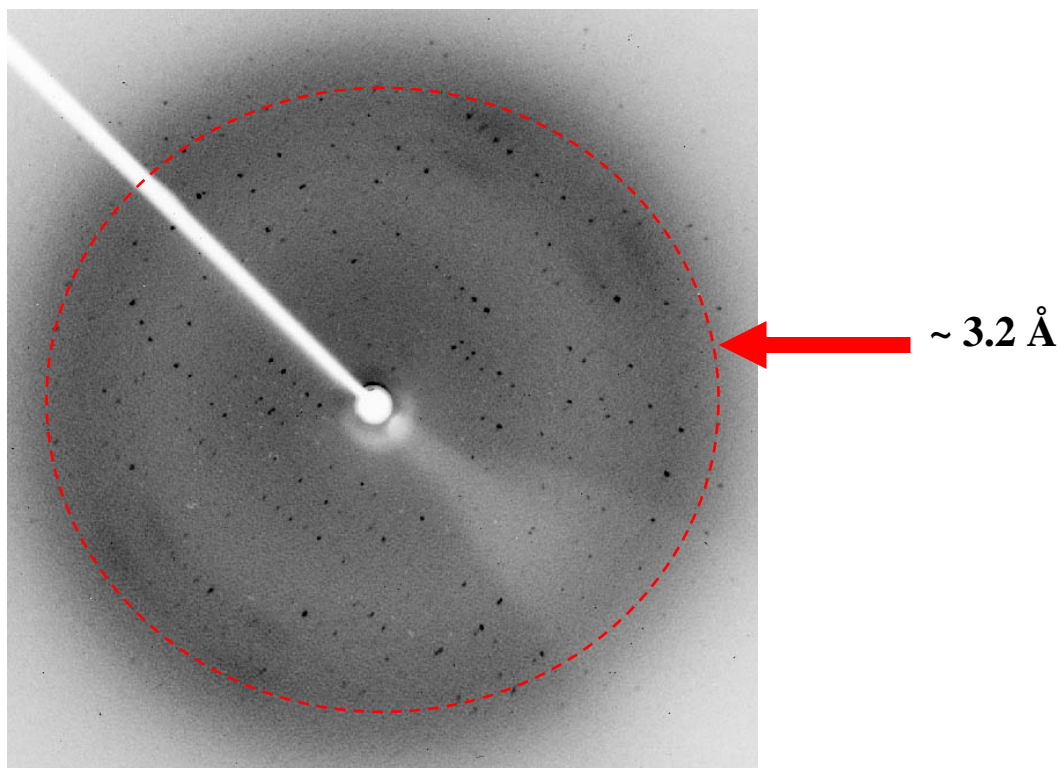


**Figure 3.22:** X-ray Diffraction Pattern of a Trx-2 crystal that cryoprotected by 10% PEG 400. The diffraction resolution is 3.2 Å.

There were another two Trx-2 protein crystals that were sent to synchrotron at Chicago for X- ray diffraction experiments in order to obtain better resolution data. The crystals that were sent for data collecting were under the crystallization conditions as shown below:

- 1) 7.6 mg/ml of Trx-2, 25% PEG 6,000, 10mM DTT, 100mM Citric Acid Buffer at pH 4.1, 20°C (Cryoprotectant: 10% glycerol)
- 2) 7.6 mg/ml of Trx-2, 25% PEG 6,000, 10mM DTT, 100mM Citric Acid Buffer at pH 4.0, 20°C (Cryoprotectant: 15% PEG 400)

The final result showed that these two crystals diffracted to 3.0 Å and 2.5 Å respectively. The outcomes were close to the in-house experimental data that had been

tested prior to sending to synchrotron. These two crystals were diffracted to 3.2 Å and 2.8 Å respectively using in-house X-ray diffractometer at the SSSC. However, the diffraction data showed that there was still some splitting on the high resolution data (Figure 3.23). Consequently, the previous published data (Filson *et al.*, 2003) was still considered as the best data set that was suitable for further protein structure refinement. Therefore, the structure refinement of Trx-2 shall be continued using the previous published data. Table 3.4 listed below is the summary for all crystals that have been cryoprotected by the cryosolution.

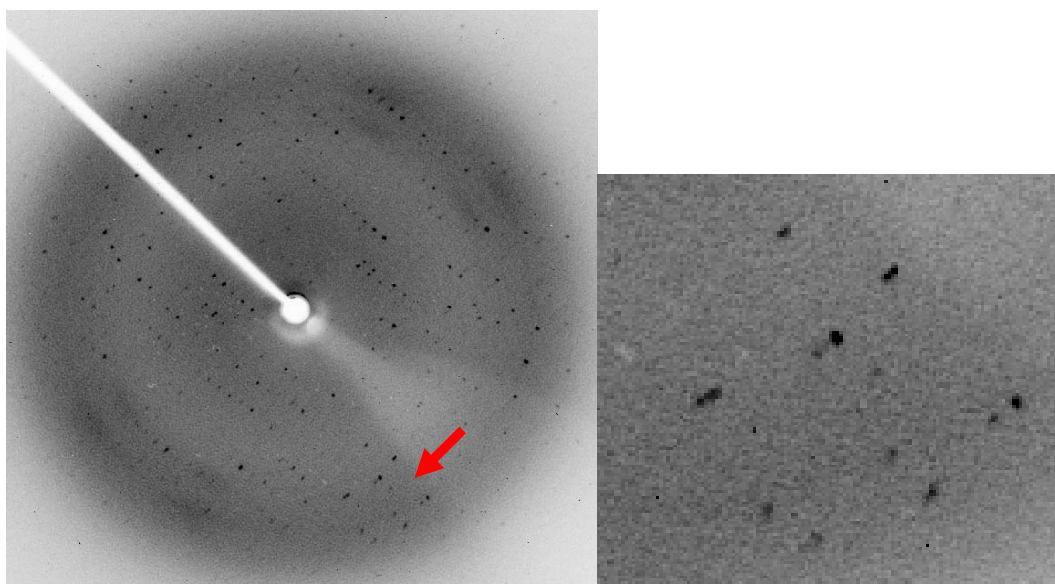


**Figure 3.23:** X-ray diffraction pattern of a Trx-2 crystal was collected at 3.2 Å resolution at the SSSC is shown on the left. The arrow indicates the splitting spots. The graph on the right is the enlarge portion of these split spots.

From Table 3.5, it clearly demonstrates that glucose is not an appropriate cryoprotectant. When the glucose was at 15%, ice rings were displayed in the diffraction pattern and the data showed high mosaicity. Once the concentration of glucose increased from 15% to 20%, the crystal only diffracted to a resolution of 4 Å. Thus, glucose was

not considered as an ideal cryoprotectant. On the other hand, 10% glycerol and 10 – 15% PEG 400 demonstrated that there were suitable cryoprotectants for Trx-2 crystals.

The crystals grown from the co-crystallization of PEG 6,000 with 10% glycerol was directly put under X-ray beam without transferring the crystal to a cryosolution prior to X-ray diffraction experiments. The 10% glycerol that was originally included in the crystallization condition can be used as a cryoprotectant to flash-cool the crystal. The resolution of those co-crystallized crystals was 2.8 Å which is similar to the ones grow in normal crystallization condition (without glycerol), and used glycerol as the cryoprotectant during cryocrystallography. The advantage of co-crystallization is when performing X-ray diffraction experiments, crystals can be directly mounted to goniometer position on the X-ray diffractometer without transferring to a cryosolution. The direct mounting of a crystal can save the operation time and reduce the crystal handling. Crystals are sensitive to physical environment. The longer a crystal is exposed to the air, the higher the chance that the crystal will deteriorate during the handling of the crystal.

| Cryoprotectant (Cy)              | [Cy] (%) | [Precipitant] | Buffer (pH) | Crystal (mm) | Resolution (Å) |
|----------------------------------|----------|---------------|-------------|--------------|----------------|
| Co-crystallization with glycerol | 10       | 25% PEG 6000  | CA/3.8      | 0.05 x 0.70  | ~3.3           |
|                                  | 10       | 26% PEG 6000  | CA/3.8      | 0.06 x 0.25  | ~2.8           |
|                                  | 10       | 27% PEG 6000  | CA/3.9      | 0.06 x 0.20  | ~3.1           |
| Glucose                          | 15       | 26% PEG 6000  | CA/4.1      | 0.08 x 1.0   | ND             |
|                                  | 20       | 26% PEG 6000  | CA/4.0      | 0.08 x 0.30  | ~4.0           |
| Glycerol                         | 10       | 24% PEG 6000  | CA/4.0      | 0.06 x 0.45  | ~3.8           |
|                                  | 10       | 25% PEG 6000  | CA/4.1      | 0.08 x 0.60  | ~3.2           |
|                                  | 10       | 25% PEG 6000  | CA/4.2      | 0.07 x 0.30  | ~3.2           |
|                                  | 10       | 25% PEG 6000  | CA/4.4      | 0.14 x 0.60  | ~3.8           |
|                                  | 10       | 26% PEG 6000  | CA/4.1      | 0.08 x 0.60  | ~3.1           |
|                                  | 10       | 26% PEG 6000  | CA/4.1      | 0.14 x 0.80  | ~3.6           |
|                                  | 10       | 27% PEG 6000  | CA/3.9      | 0.06 x 0.20  | ~3.1           |
|                                  | 10       | 27% PEG 6000  | CA/3.9      | 0.06 x 0.20  | ~3.1           |
| PEG 400                          | 10       | 22% PEG 6000  | CA/4.0      | 0.12 x 0.95  | ~3.3           |
|                                  | 10       | 25% PEG 6000  | CA/4.2      | 0.07 x 0.30  | ~ 3.2          |
|                                  | 10       | 25% PEG 6000  | CA/4.4      | 0.14 x 0.60  | ~4.1           |
|                                  | 10       | 27% PEG 6000  | CA/4.2      | 0.07 x 0.55  | ~3.5           |
|                                  | 15       | 25% PEG 6000  | CA/4.0      | 0.10 x 0.80  | ~2.8           |
|                                  | 15       | 26% PEG 6000  | CA/4.0      | 0.06 x 0.30  | ~3.9           |
|                                  | 15       | 27% PEG 6000  | CA/4.0      | 0.05 x 0.50  | ~4.8           |

**Table 3.5:** Summary results of various cryo-conditions of Trx-2 crystals that were prepared for X-ray diffraction experiments at the SSSC. The concentration of citric acid (CA) buffer and purified Trx-2 are 100 mM and 7.6 mg/ml respectively. The additives used are 10 mM DTT for all trials. The concentrations of PEG 6000 shown above are the crystallization conditions. ND: No diffraction.

## **Chapter 4: CONCLUSION AND FUTURE PERSPECTIVES**

### **4.1. SUMMARY OF BOVINE SERUM ALBUMIN**

Bovine Serum Albumin (BSA) is a soluble and large globular protein and has a molecular weight of approximately 66,400 Dalton. The primary structure of BSA has been determined for a number of years. However, the three-dimensional crystal structure of BSA has never been solved, probably because high quality protein crystals have not been crystallized.

The goal of determining the crystal structure of BSA is due to the interest in understanding how thiomolybdates bind to BSA and render copper unavailable for absorption by cattle. Copper deficiency is a nutritional issue that occurs among cattle in Saskatchewan. However, even though BSA crystals have been crystallized, due to the nature of the crystals themselves, the crystals only can be diffracted to a very low resolution of about 8 Å. Such resolution is not useful enough for solving the three-dimensional protein structure of BSA.

Initially, the crystallization conditions of BSA followed the previous results done by Dean Thome from Department of Chemistry at the University of Saskatchewan (Thome, 2001), which was originated from published work (Asanov *et al.*, 1997b). The first crystallization condition that I used to produce crystals was 2 µl droplets of 10 mg/ml unpurified BSA solution grown in 55% SAS/100 mM K-PO<sub>4</sub> buffer solution (pH 6.0) using hanging drop vapor diffusion technique . The time spent was about 2 – 3 months. However, this result was not reproducible. Therefore, characterization and

purification of BSA was carried out. At the same time, a number of salts and buffers as well as different precipitants were attempted. The screening strategy using sparse matrix approach (Jancarik and Kim, 1991) by Hampton Research was first initiated but the results were not satisfactory. Only PEG 6,000/LiCl/MES and PEG MME 2,000/NiCl<sub>2</sub>/Tris gave multi-crystals but these kinds of crystals could not be optimized to single crystals. So, SDS-PAGE and DLS techniques were applied to characterize the purity and homogeneity of BSA. Purity was initially suspected as the major issue to impede the crystal growth. However, once high concentrations of BSA were used to crystallize the protein, purification of BSA became unnecessary. The homogeneity of unpurified and purified BSA is not much different after performing the DLS measurements. Although extensive trial and error crystallization experiments have been conducted, the crystals do not diffract better than 3.5 Å. The optimization strategies that have been attempted to produce well-diffracted single crystals include changing the physical and chemical parameters of crystallization conditions such as pH and temperature, as well as adding different additives such as various kinds of salts, glycerol, sucrose and xylitol.

The crystallization of BSA was initiated by Thome previously at the University of Saskatchewan (Thome, 2001). Compared to our results, it showed that both crystals crystallized in different ways, in terms of protein concentration and buffer solution as well as different diffraction conditions. However, the unit cell information of both crystals demonstrated in a very similar result. Below is the comparison table for both data sets obtained from Dean and me (Table 4.1).

|                           | <b>Thome</b>   | <b>Tai</b>  |
|---------------------------|--|---|
| Crystallization Condition | 10 mg/ml purified BSA<br>50 – 65% SAS<br>50 mM K-PO <sub>4</sub> at pH 5.6 – 6.6<br>with 1 – 50 mM NaCl, KCl,<br>MgCl <sub>2</sub> NiCl <sub>2</sub> , and CoCl <sub>2</sub> | 50 – 60 mg/ml unpurified BSA<br>48 – 52 % SAS<br>25 mM NaAc at pH 5.2 – 5.6<br>with 10 mM CoCl <sub>2</sub> or 3% Xylitol<br>or 3 % sucrose |
| Diffraction Temperature   | Room temperature   | Cryo-temperature at 100 K   |
| Cryo-condition            | Not applicable   | 25 – 35 % Glycerol or<br>30 – 35% Glucose   |
| Cell Parameter            | 148.24 Å x 148.24 Å x 356.70 Å   | 147.62 Å x 147.62 Å x 351.12 Å  |
| Space Group               | P6   | P6  |
| Best Resolution           | 8 Å  | 8 Å   |

**Table 4.1:** The Comparison between BSA crystallographic data done by Thome and me.

## 4.2. SUMMARY OF THIOREDOXIN-2

*Helicobacter pylori* (*H. pylori*) was declared as a type I carcinogen by International Agency for Research on Cancer (IARC) (IARC, 1994). Two genes encoding thioredoxin which are Trx-1 and Trx-2 are found on the *H. pylori* genome (Tomb *et al.*, 1997). Thioredoxins are a class of small 12-kDa redox proteins known to be present in all eukaryotic and prokaryotic organisms. Both of them are capable of reducing protein disulfide bonds. However, the catalytic site of Trx-2 contains a unique non-conserved motif: Cys – Pro– Asp – Cys at the N-terminal domain of the molecule.

The crystal structure of Trx-2 has been solved. At high resolution of the data collected from X-ray diffraction experiments, there are some split spots, possibly owing to the tendency of the long thin (0.1 mm x 0.1 mm x 1 – 2 mm) crystals to bend with the contours of the frozen drops in the loop (Filson *et al.*, 2003). The crystallization condition of Trx-2 was optimized from its original published condition in an attempted to grow bigger crystals (in terms of shortening the length and widening the width of the crystal) in order to get higher resolution of diffraction data (e.g. above 2 Å) and avoid the spot splitting that occurred in the previous crystals. The crystallization condition was optimized from 30% PEG 6,000/0.1 M (NH<sub>4</sub>)<sub>2</sub>SO<sub>4</sub>/10 mM DTT to 24 – 26% PEG 6,000/100mM citric acid buffer (pH 4.0 – 4.2)/10 mM DTT. Both crystals were conducted in cryo-temperature for X-ray diffraction.

|                           | <b>Published Data</b>   | <b>Tai</b>  |
|---------------------------|---|---|
| Crystallization Condition | 10 mg/ml Trx-2<br>30% PEG 6,000/ 0.1 M<br>(NH <sub>4</sub> ) <sub>2</sub> SO <sub>4</sub> / 10 mM DTT | 7.6 mg/ml Trx-2<br>24 – 26 % PEG 6,000/<br>100mM citric acid/ 10 mM DTT |
| Crystal Dimension         | 0.1 mm x 0.1 mm x 1 – 2 mm  | 0.12 mm x 0.12 mm x 0.9 mm  |
| Cryo-condition            | 10 – 15% Glycerol   | 10% Glycerol or<br>10 – 15% PEG 400                                     |
| Cell Parameter            | 40.21 Å x 40.21 Å x 64.65 Å   | 42.65 Å x 42.65 Å x 64.64 Å   |
| Space Group               | P4 <sub>1</sub>   | P4  |
| Best Resolution           | 2.4 Å   | 2.8 Å (*2.5 Å )   |

**Table 4.2:** The Comparison between Trx-2 published crystallographic data and my results (\*Note: the crystal was diffracted to 2.8 Å at in-house X-ray diffractometer and the same crystal was diffracted to higher resolution, 2.5 Å, by synchrotron radiation).

### 4.3. CONCLUSIONS

The three-dimensional structure of BSA is not solved because well-diffracted crystals could not be crystallized even though extensive experiments have been conducted. For both protein crystallizations and X-ray diffraction experiments performed by Thome and me, either the less pure (directly purchased from supplier) or in-house purified protein, both gave the same resolution of crystallographic data after performing the diffractions experiments at room temperature or cryo-temperature. These unsatisfactory results might be attributed to the protein itself, although the reason remains unknown. I speculate that the flexible portions of BSA protein might be interfering with the formation of a well ordered crystal lattice. Other aspects that may be considered are the saturated ammonium sulfate was not a very ideal precipitant. When the crystals were exposed to the atmosphere during crystal handling, ammonium sulfate salt formed quickly in the protein droplet, and the crystals started to precipitate. Therefore, finding a replacement for saturated ammonium sulfate becomes important. Due to the lack of high resolution diffraction data of BSA crystals, the three-dimensional crystal structure of BSA still remains unknown. Therefore, the study of the binding site of copper on BSA and the mechanism of thiomolybdates that render the copper unavailable in cattle cannot be determined.

The crystallization conditions of Trx-2 were optimized using different crystallization strategies to grow crystals to much larger dimensions in order to improve the diffraction resolution limit, at least above 2.4 Å which would be higher than the published diffraction resolution limit and without any split spots. However, the improvement of crystal dimensions is slight, the diffraction resolution limits are similar

and the split spots at high resolution data are still observed. Compared to published data, only similar qualities (in terms of diffraction resolution limits and size of crystals) of Trx-2 crystals were grown. Therefore, the published X-ray diffraction data of Trx-2 is still considered as the best data that can begin to continue the protein structure refinement to determine the three-dimensional crystal structure of Trx-2.

#### **4.4. FUTURE WORK**

The crystallization conditions of BSA have been studied exhaustively; the buffer solutions such as sodium acetate and potassium phosphate have shown that crystals can grow under similar pH ranges in different buffers. Other buffer solutions which have parallel pH range are also worth trying in the future. I strongly suggest that the main focus should concentrate on changing the precipitant, saturated ammonium sulfate (SAS), using other replacements such as different kinds of salts or different types of PEGs to replace it.

Various cryoprotectants have been tried. Only glycerol and glucose have showed positive outcomes, so I propose to co-crystallize the BSA protein using the precipitating solution that gave crystals previously with glycerol or glucose in the crystallization trials in future (Sousa, 1995; Sousa, 1997). The concentrations of the co-solvent can use similar conditions that worked for the cryoprotection of BSA crystals. For example use 50 – 55% SAS/25% glycerol/25mM NaAc buffer/10mM CoCl<sub>2</sub> or 50 – 55% SAS/30% glucose/25mM NaAc buffer/10mM CoCl<sub>2</sub> to crystallize BSA proteins. Otherwise lower cryoprotectant concentration can be attempted as well if the crystallization doesn't work in the first place.

Limited proteolysis may offer another strategy to crystallize BSA protein, limited proteolytic digestion has been demonstrated as an alternative and valuable method for crystallizing hard-to-crystallize proteins (Danley *et al.*, 2000; Leppanen *et al.*, 1999) Evidence has shown that after BSA was cleaved by pepsin at pH 3.5, one of the fragments (COOH-terminal fragment) can be crystallized at 4% PEG 1,000/0.04 M cacodylate/pH 6.0. However, the dimensions of the BSA crystal grown in this method was not sufficient for conducting X-ray diffraction experiments and then no further results have been published (McPherson, 1976). But it might offer another clue for crystallizing BSA. Therefore, instead of purchasing the BSA from commercial sources, recombinant BSA may become necessary. In this case, the conditions of protein crystallization of mutated protein become broader, because one single protein can be mutated to various protein mutants and each mutant can have different crystallization conditions. The protein mutation includes N-terminal or C-terminal deletions, loop insertions, residues truncations and point mutations. These kinds of techniques may provide a number of choices for getting better quality crystals (Dale *et al.*, 2003).

Another alternative strategy is instead of growing of BSA crystals, crystallization of sheep serum albumin (OSA) or goat serum albumin (GSA) can be tried. These kinds of serum albums (BSA, GSA and OSA) from cattle, goat and sheep respectively all are ruminant species. All of them have faced the similar type of molybdenum-induced copper deficiency. Even a low intake of molybdenum can negatively affect copper intention in the sheep (Dick, 1954), and goat as well (Frank *et al.*, 2000).

On the other hand, in order to find out the solution to solve the protein structure of Trx-2, few strategies can be attempted. First, a much higher resolution data, beyond 2 Å,

might be useful for the structure solution to get a clearer electron density of polypeptide chains. Second, improving the freezing condition of the crystals, such as using bigger or longer loop to mount the crystals in order to not allow crystals to be bent, can be tried. Thus, the splitting of the spots in the X-ray diffraction data can be avoided. Third, changing the crystallization conditions of Trx-2 can be attempted in order to grow bigger crystals in terms of crystal dimensions, or growing crystals in a different space groups might produce higher resolution and more reliable diffraction data.

## REFERENCES

- Abola, E. E., Bernstein, F. C., and Koetzle, T. F. (1985). The Protein Data Bank. *Proceedings of The International CODATA Conference*. **1984**, 139-144.
- Arner, E. S. J. and Holmgren, A. (2000). Physiological Functions of Thioredoxin and Thioredoxin Reductase. *European Journal of Biochemistry*. **267**, 6102-6109.
- Asanov, A. N., DeLucas, L. J., Oldham, P. B., and Wilson, W. W. (1997a). Heteroenergetics of Bovine Serum Albumin Adsorption from Good Solvents Related to Crystallization Conditions. *Journal of Colloid and Interface Science*. **191**, 222-235.
- Asanov, A. N., DeLucas, L. J., Oldham, P. B., and Wilson, W. W. (1997b). Interfacial Aggregation of Bovine Serum Albumin Related to Crystallization Conditions Studied by Total Internal Reflection Fluorescence. *Journal of Colloid and Interface Science*. **196**, 62-73.
- Baker, L. M. S., Raudonikiene, A., Hoffman, P. S., and Poole, L. B. (2003). Essential Thioredoxin-Dependent Peroxiredoxin System from *Helicobacter Pylori*: Genetic and Kinetic Characterization. *Journal of Bacteriology*. **183**(6), 1961-1973.
- Behrens, P. Q., Spiekerman, A. M., and Brown, J. R. (1975). Structure of Human Serum Albumin. *Federation Proceedings*. **34**, 591.
- Bergfors, T. M. Protein Crystallography: Technique, Strategies and Tips- A Laboratory Manual. Bergfors, T. M. Ed.1. International University Line. 1999.
- Bergfors, T. M. (2003). Seeds to Crystals. *Journal of Structural Biology*. **142**, 66-76.
- Berman, H. M., Westbrook, J., Feng, Z., Gilliland, G., Bhat, T. N., Weissig, H., Shindyalov, I. N., and Bourne, P. E. (2000). The Protein Data Bank. *Nucleic Acids Research*. **28**, 235-242.
- Blow, D. Outline of Crystallography for Biologists. Ed.1. New York, Oxford University Press. 2002.
- Blundell, T. L. and Johnson, L. N. Protein Crystallography. (3), *Crystallization of Proteins*. Ed.1, 59-82. Academic Press. 1976.
- Bollag, D. M., Rozycki, M. D., and Edelstein, S. J. Protein Methods. Ed.2. Wiley-Liss. 1996.
- Bradford, M. M. (1976). A Rapid and Sensitive Method for the Quantitation of Microgram Quantities of Protein Utilizing the Principle of Protein-Dye Binding. *Analytical Biochemistry*. **72**, 248-254.

- Brown, J. R. (1975). Structure of Bovine Serum Albumin. *Federation Proceedings*. **34**, 591.
- Brown, J. R. (1976). Structural origins of mammalian albumin. *Federation Proceedings*. **35**, 2141-2144.
- Bunchanan, B. B. (1991). Regulation of CO<sub>2</sub> assimilation in oxygenic photosynthesis: the ferredoxin/thioredoxin system. Perspective on its discovery, present status, and future development. *Archives of biochemistry and biophysics*. **288**, 1-9.
- Capitani, G., Markovic-Housley, Z., DelVal, G., Morris, M., Jansonius, J. N., and Schurmann, P. (2000). Crystal Structures of Two Functionally Different Thioredoxins in Spinach Chloroplasts. *Journal of Molecular Biology*. **302**, 135-154.
- Carter, C. W. J. and Carter, C. W. (1979). Protein Crystallization Using Incomplete Factorial Experiments. *Journal of Biological Chemistry*. **254**, 12219-12223.
- Carter, D. C. and He, X. M. (1990). Structure of Human Serum Albumin. *Science*. **249**, 302-303.
- Carter, D. C., He, X. M., Munson, S. H., Twigg, P. D., Gernert, K. M., Broom, M. B., and Miller, T. Y. (1989). Three-Dimensional Structure of Human Serum Albumin. *Science*. **244**, 1195-1198.
- Carter, D. C. and Ho, J. X. (1994). Structure of Serum Albumin. *Advances in Protein Chemistry*. **45**, 153-203.
- Chayen, N. E. (1996). A Novel Technique for Containerless Protein Crystallization. *Protein Engineering*. **9**(10), 972-929.
- Chayen, N. E. (1997). A Novel Technique to control the Rate of Vapour Diffusion, Giving Larger Protein Crystals. *Journal of Applied Crystallography*. **30**, 198-202.
- Chayen, N. E. (1998). Comparison Studies of Protein Crystallization by Vapour-Diffusion and Microbatch Techniques. *Acta Crystallographica Section D*. **D54**, 8-15.
- Chayen, N. E. and Stewart, P. D. S. (1992). Microbatch Crystallization under Oil - A New Technique allowing Many Small-volume Crystallization Trials. *Journal of Crystal Growth*. **122**, 176-180.
- Christopher, G. K., Phipps, A. G., and Burley, S. K. (1998). Temperature-dependent Solubility of selected proteins. *Journal of Crystal Growth*. **191**, 820-826.
- Clark, N. J. and Laurie, S. H. (1980). The Copper-Molybdenum Antagonism in Ruminants. I. The Formation of Thiomolybdates in Animal Rumen. *Journal of Inorganic Biochemistry*, 37-43.

- Cudney, B., Patel, S., and McPherson, A. (1994). Crystallization of Macromolecules in Silica Gels. *Acta Crystallographica Section D*. **D50**, 479-483.
- Dale, G. E., Oefner, C., and D' Arcy, A. (2003). The Protein as a Variable in Protein Crystallization. *Journal of Structural Biology*. **142**, 88-97.
- Danley, D. E., Haggan, M. E., Cunningham, D., Fennell, K. F., Pauly, T. A., and LeMotte, P. K. (2000). A Crystallizable Form of RII $\beta$  Regulatory Domain Obtained by Limited Proteolysis. *Acta Crystallographica Section D*. **D56**, 1038-1041.
- Dauter, Z. (1997). Data Collection Strategy. *Methods in Enzymology*. **276**, 326-344.
- Dauter, Z. (1999). Data-collection Strategies. *Acta Crystallographica Section D*. **D55**, 1703-1717.
- Dick, A. T. (1954). The Assimilation and Storage of Copper in Crossbred Sheep. *Australian Journal of Agricultural Research*. **5**, 511-544.
- Ducruix, A. and Giege, R. Crystallization of Nuclei Acids and Proteins: A Practical Approach. *Ed.1*. IRL Press at Oxford University Press. 1992.
- Dunlop, K. V. and Hazes, B. (2003). When Less is More: A More Efficient Vapour Diffusion Protocol. *Acta Crystallographica Section D*. **D59**, 1797-1800.
- Feher, G. and Kam, Z. (1985). Nucleation and Growth of Protein Crystals: General Principles and Assays. *Methods in Enzymology*. **114**, 77-111.
- Ferre-D'Amare, A. R. and Burley, S. K. (1994). Use of Dynamic Light Scattering to assess Crystallizability of Macromolecules and Macromolecular Assemblies. *Structure*. **2**, 357-359.
- Ferre-D'Amare, A. R. and Burley, S. K. (1997). Dynamic Light Scattering in Evaluating Crystallizability of Macromolecules. *Methods in Enzymology*. **276**, 157-166.
- Filson, H., Fox, A., Kelleher, D., Windle, H. J., and Sanders, D. A. R. (2003). Purification, Crystallization and Preliminary X-ray Analysis of an Unusual Thioredoxin from the gastric pathogen *Helicobacter Pylori*. *Acta Crystallographica Section D*. **D59**, 1280-1282.
- Forsythe, E. L., Snell, E. H., and Pusey, M. L. (1997). Crystallization of Chicken Egg-white Lysozyme from Ammonium Sulfate. *Acta Crystallographica Section D*. **D53(6)**, 795-797.
- Foster, J F. The Plasma Protein. Putnam, F. W. (1), 179-233. New York, Academic Press. 1960.
- Frank, A., Danielsson, R., and Jones, B. (2000). The 'Mysterious' Disease in Swedish Moose. Concentrations of Trace Elements in Liver and Kidneys and Clinical Chemistry.

- Comparison with Experimental Molybdenosis and Copper Deficiency in the Goat. *The Science of Total Environment*. **249**, 107-122.
- Garfin, D. E. (1990). One-Dimensional Gel Electrophoresis. *Methods in Enzymology*. **182**, 425-441.
- Garman, E. F. (1999). Cool Data: Quantity and Quality. *Acta Crystallographica Section D*. **D55**, 1641-1653.
- Garman, E. F. (2003). 'Cool' crystals: Macromolecular Cryocrystallography and Radiation Damage. *Current Opinion in Structural Biology*. **13**, 545-551.
- Garman, E. F. and Mitchell, E. P. (1996). Glycerol Concentration required for Cryoprotection of 50 typical Protein Crystallization Solutions. *Journal of Applied Crystallography*. **29**, 584-587.
- Garman, E. F. and Schneider, T. R. (1997). Macromolecular Cryocrystallography. *Journal of Applied Crystallography*. **30**, 211-237.
- Gernert, K. M., Smith, R., and Carter, D. C. (1988). A Simple Apparatus for Controlling Nucleation and Size in Protein Crystal Growth. *Analytical Biochemistry*. **168**, 141-147.
- Gilliland, G. L. (1988). A Biological Macromolecule Crystallization Database: A Basis for a Crystallization Strategy. *Journal of Crystal Growth*. **90**, 51-59.
- Gilliland, G. L., Tung, M., Blakeslee, D. M., and Ladner, J. E. (1994). Biological Macromolecule Crystallization Database, Version 3.0: New Features, Data and the NASA Archive for Protein Crystal Growth Data. *Acta Crystallographica Section D*. **D50**, 408-413.
- Gilliland, G. L., Tung, M., and Ladner, J. E. (1996). Development of Crystallization Strategies Using the Biological Macromolecules Crystallization Database. *Journal of Research of the National Standards and Technology*. **D101**(3), 309-320.
- Glusker, J. P., Lewis, M., and Rossi, M. Crystal Structure Analysis for Chemist and Biologist. *Ed.1*. New York, VCH Publishers, Inc. 1994.
- Glusker, J. P. and Trueblood, K. N. Crystal Structure Analysis - A Primer. *Ed.2*. Oxford, Oxford University Press. 1985.
- Guan, R. J., Wang, M., Liu, X. Q., and Wang, D. C. (2001). Optimization of Soluble Protein Crystallization with Detergents. *Journal of Crystal Growth*, 273-279.
- Hahn, T. International Tables for Crystallography. *Ed.5*(Vol. A). 2002.
- Hampton Research. Crystallization Research Tools. (11). Hampton Research. 2001.

- Han, Q. and Lin, S. X. (1996). A Microcrystal Selection Technique in Protein Crystallization. *Journal of Crystal Growth*. **168**, 181-184.
- Harford, C. and Sarkar, B. (1997). Amino Terminal Cu(II)- and Ni(II) Binding (ATCUN) Motif of Proteins and Peptides: Metal Binding, DNA Cleavage, and Other Properties. *Accounts of Chemical Research*. **30**, 123-130.
- Harris, E. L. V. and Angal, S. Protein Purification Methods: A Practical Approach. *Ed.1*. Oxford, IRL Press. Rickwood, D. and Hames, B. D. 1989.
- He, X. M. and Carter, D. C. (1992). Atomic Structure and Chemistry of Human Serum Albumin. *Nature*. **358**, 209-215.
- Heidner, E. (1978). Protein Crystallizations- The Functional dependence of the nucleation rate on the protein concentration and the solubility. *Journal of Crystal Growth*. **44**, 139-144.
- Higgins, S. J. and Hames, B. D. Protein Expression: A Practical Approach. *Ed.1*. New York, Oxford University Press. 1999.
- Ho, J. X., Holowachuk, E. W., Norton, E. J., Twigg, P. D., and Carter, D. C. (1993). X-ray and Primary Structure of Horse Serum Albumin (*Equus Caballus*) at 0.27-nm Resolution. *European Journal of Biochemistry*. **215**, 205-212.
- Holmgren, A. (1981). Thioredoxin: Structure and Functions. *Trends in Biochemical Sciences*. **6**(1), 26-29.
- Holmgren, A. (1985). Thioredoxin. *Annual Review of Biochemistry*. **54**, 237-271.
- Holmgren, A. (1989). Thioredoxin and Glutaredoxin Systems. *The Journal of Biological Chemistry*. **264**(24), 13963-13966.
- Holmgren, A. and Bjornstedt, M. (1995). Thioredoxin and Thioredoxin Reductase. *Methods in Enzymology*. **252**, 199-208.
- Hope, H. (1988). Cryocrystallography of Biological Macromolecules: a Generally Applicable Method. *Acta Crystallographica Section B*. **B44**, 22-26.
- IARC. International Agency for Research on Cancer Working Group on the Evaluation of Carcinogenic Risks to Humans. (, *Schistosomes, Live Flukes and Helicobacter pylori: Views and Expert Opinions of an IARC Working Group on the Evaluation of Carcinogenic Risks to Humans*. 177-240. IARC Press. 1994.
- Israel, D. A. and Peek, R. M. (2001). Pathogenesis of *Helicobacter Pylori*-induced Gastric Inflammation. *Alimentary Pharamcology and Therapeutics*. **15**(9), 1271-1290.
- Jancarik, J. and Kim, S. H. (1991). Sparse Matrix Sampling: A Screening Method for Crystallization of Proteins. *Journal of Applied Crystallography*. **24**, 409-411.

Janson, J-C and Ryden, L. Protein Purification: Principles, High Resolution Methods and Applications. *Ed.2*. New York, John Wiley & Sons. 1998.

Juarez-Martinez, G., Garza, C., Castillo, R., and Moreno, A. (2001). A Dynamic Light Scattering Investigation of the Nucleation and Growth of Thaumatin Crystals. *Journal of Crystal Growth*. **232**, 119-131.

Kitano, K., Motohashi, K., Yoshida, M., and Miki, K. (1998). A Novel Approach to Crystallizing Proteins with Temperature-Induction Method: GrpE Protein from. *Journal of Crystal Growth*. **186**, 456-460.

Kragh-Hansen, U. (1981). Molecular Aspects of Ligand Binding to Serum Albumin. *Pharmacological Reviews*. **33**(1), 17-53.

Kwong, P. D. and Liu, Y. (1999). Use of Cryoprotectants in combination with Immersible Oils for Flash Cooling Macromolecular Crystals. *Journal of Applied Crystallography*. **32**, 102-105.

Lamarque, D. and Peek, R. M. J. (2003). Pathogenesis of Helicobacter Pylori Infection. *Helicobacter*. **8**(Suppl. 1), 21-30.

Leppanen, V. M., Parast, C. V., Wong, K. K., Kozarich, J. W., and Goldman, A. (1999). Purification and Crystallization of a Proteolytic Fragment of Escherichia Coli Pyruvate Formate-lyase. *Acta Crystallographica Section D*. **D55**, 531-533.

Littke, W. and John, C. (1984). Protein Single Crystal Growth under Microgravity. *Science*. **225**, 203-204.

Littlechild, J. A. (1991). Protein Crystallization: Magical or Logical: Can We Establish Some General Rules? *Journal of Physics D: Applied Physics*. **24**, 111-118.

Luft, J. R., Albright, D. T., Baird, J. K., and Detitta, G. T. (1996). The Rate of Water Equilibrium in Vapor-Diffusion Crystallizations: Dependence on the Distance from the Droplet to the Reservoir. *Acta Crystallographica Section D*. **D52**, 1098-1106.

Luft, J. R. and Detitta, G. T. (1997). Kinetic Aspects of Macromolecular Crystallization. *Methods in Enzymology*. **276**, 110-131.

Luft, J. R. and Detitta, G. T. (1999). A Method to Produce Microseed Stock for Use In The Crystallization of Biological Macromolecules. *Acta Crystallographica Section D*. **D55**, 988-993.

Masutani, H., Bai, J., Kim, Y.-C., and Yodoi, J. (2004). Thioredoxin as a neurotrophic cofactor and an important regulator of neuroprotection. *Molecular Neurobiology*. **29**(3), 229-242.

Matthews, B. W. (1968). Solvent Content of Protein Crystal. *Journal of Molecular Biology*. **33**, 491-497.

- Matthews, B. W. (1985). Determination of Protein Molecular Weight, Hydration, and Packing from Crystal Density. *Methods in Enzymology*. **114**, 176-187.
- McLachlan, A. D. and Walker, J. E. (1977). Evolution of Serum Albumin. *Journal of Molecular Biology*. **112**, 543-558.
- McPherson, A. (25-10-1976). Crystallization of Proteins from Polyethylene Glycol. *The Journal of Biological Chemistry*. **251**(20), 6300-6303.
- McPherson, A. Preparation and Analysis of Protein Crystals. *Ed.1*. John Wiley & Sons. 1982.
- McPherson, A. (1990). Current Approaches to Macromolecular Crystallization. *European Journal of Biochemistry*. **189**, 1-23.
- McPherson, A. (1991). A Brief History of Protein Crystal Growth. *Journal of Crystal Growth*. **110**, 1-10.
- McPherson, A. (1992). Two Approached to the Rapid Screening of Crystallization Conditions. *Journal of Crystal Growth*. **122**, 161-167.
- McPherson, A. (1995). Increasing the size of microcrystals by fine sampling of pH limits. *Journal of Applied Crystallography*. **28**, 362-365.
- McPherson, A. (1996). Incorporation of Impurities into Macromolecular Crystals. *Journal of Crystal Growth*. **168**, 74-92.
- McPherson, A. Crystallization of Biological Macromolecules. Cold Spring Harbor Laboratory Press. 1998.
- McPherson, A. (2001). A Comparison of Salts for the Crystallization of Macromolecules. *Protein Science*. **10**, 418-422.
- McPherson, A. Introduction to Macromolecular Crystallography. *Ed.1*. New Jersey, Wiley-Liss. 2003.
- McPherson, A., Koszelak, S., Axelrod, H., Day, J., Robinson, L., McGrath, M., Williams, R., and Cascio, D. (1986a). The Effects of Neutral Detergents on the Crystallization of Soluble Proteins. *Journal of Crystal Growth*. **76**, 547-553.
- McPherson, A., Koszelak, S., Axelrod, H., Day, J., Williams, R., Robinson, L., McGrath, M., and Cascio, D. (1986b). An Experiment Regarding Crystallization of Soluble Proteins in the Presence of  $\beta$ -Octyl Glucoside. *Journal of Biological Chemistry*. **261**(4), 1969-1975.
- McPhie, P. (1971). Dialysis. *Methods in Enzymology*. **22**, 23-32.
- McRee, D. E. Practical Protein Crystallography. *Ed.2*. Academic Press. 1999.

- Minarik, P. (1997). Thioredoxin: A Protein with a Thousand Faces. *Biologia (Bratislava)*. **52**(6), 691-696.
- Mustafa, A. O., Derrick, J. P., Tiddy, G. J. T., and Ford, R. C. (1998). A Novel Approach for the Crystallization of Soluble Proteins using Non-ionic Surfactants. *Acta Crystallographica Section D*. **D54**, 154-158.
- Oberg, K. A. and Uversky, V. N. (2001). Secondary Structure of the Homologous Proteins, alpha-Fetoprotein and Serum Albumin, from their Circular Dichroism and Infrared Spectra. *Protein and Peptide Letters*. **8**(4), 297-302.
- Oblong, J. E., Berggren, M., and Powis, G. (1994). Biochemical, Structural, and Biological Properties of Human Thioredoxin Active Site Peptides. *FEBS Letter*. **343**, 81-84.
- Parkin, S. and Hope, H. (1998). Macromolecular Cryocrystallography: Cooling, Mounting, Storage and Transportation of Crystals. *Journal of Applied Crystallography*. **31**, 945-953.
- Penkova, A., Chayen, N. E., Saridakis, E., and Nanev, C. N. (2002). Nucleation of Protein Crystals in a Wide Continuous Supersaturation Gradient. *Acta Crystallographica Section D*. **D58**, 1606-1610.
- Peters, T. Jr. *The Impact of Protein Chemistry on the Biomedical Science*. 39-55. New York, Academic Press. Schechter, A. N. and Goldberger, R. F. 1984.
- Peters, T. Jr. (1985). Serum Albumin. *Advances in Protein Chemistry*. **37**, 161-245.
- Petrucci, R. H., Harwood, W. S., and Herring, F. G. General Chemistry: Principles and Modern Applications. *Ed.8*. New Jersey, Prentice Hall. 2002.
- Petsko, G. (1975). Protein Crystallography at Sub-zero Temperatures: Cryo-protective Mother Liquors for Protein Crystals. *Journal of Molecular Biology*. **96**, 381-392.
- Powis, G. and Montfort, W. M. (2001). Properties and Biological Activities of Thioredoxins. *Annual Review of Pharmacology and Toxicology*. **41**, 261-295.
- Przybylska, M. (1989). A Double Cell for Controlling Nucleation and Growth of Protein Crystals. *Journal of Applied Crystallography*. **22**, 115-118.
- Quagraine, E. K. and Reid, R. S. (2001). UV/Visible Spectrophotometric Studies of The Investigation Thiomolybdates, Copper (II) and Other Ligands. *Journal of Inorganic Biochemistry*. **85**, 53-60.
- Ravelli, R. B. G. and McSweeney, S. M. (2000). The 'Fingerprint' that X-rays can leave on structures. *Structure*. **8**(3), 315-328.

- Reed, R. G., Putnam, F. W., and Peters, T. Jr. (1980). Sequence of Residues 400 - 403 of Bovine Serum Albumin. *Biochemical Journal*. **191**, 867-868.
- Rhode, G. Crystallography Made Crystal Clear. *Ed.2*. Academic Press. 2000.
- Ries-Kautt, M. and Ducruix, A. (1997). Interferences Drawn from Physiochemical Studies of Crystallogenesis and Precrystalline State. *Methods in Enzymology*. **276**, 23-59.
- Rodgers, D. W. (1994). Cryocrystallography. *Structure*. **2**, 1135-1140.
- Rodgers, D. W. (1997). Practical Cryocrystallography. *Methods in Enzymology*. **276**, 183-203.
- Rosenberg, I. M. Protein Analysis and Purification: Benchtop Techniques. *Ed.1*. Birkhauser. 1996.
- Rossomando, E. F. (1990). Ion-Exchange Chromatography. *Methods in Enzymology*. **182**, 309-317.
- Sambrook, J. and Russell, D. W. Molecular Cloning: A Laboratory Manual. *Ed.3* (Vol. 3). CSHL Press. 2001.
- Saridakis, E. and Chayen, N. E. (2000). Improving Protein Crystal Quality by Decoupling Nucleation and growth in Vapor Diffusion. *Protein Science*. **9**, 755-757.
- Sauter, C., Ng, J. D., Lorber, B., Keith, G., Brion, P., Hosseini, M. W., Lehn, J.-M., and Giege, R. (1999). Additives for the crystallization of proteins and nucleic acids. *Journal of Crystal Growth*. **196**, 365-376.
- Sharma, A., Hanai, R., and Mondragon, A. (1994). Crystal Structure of the Amino-terminal Fragment of Vaccinia Virus DNA Topoisomerase I at 1.6 Å Resolution. *Structure*. **2**(8), 767-777.
- Sheehan, D. Physical Biochemistry: Principles and Applications. John Wiley & Sons. 2000.
- Shirin, H., Pinto, J. T., Liu, L. U., Merzianu, M., Sordillo, E. M., and Moss, S. F. (2001). Helicobacter Pylori decrease Gastric Mucosal Glutathione. *Cancer Letters*. **164**, 127-133.
- Sousa, R. (1995). Use of Glycerol, Polyols and Other Protein Structure Stabilizing Agents in Protein Crystallization. *Acta Crystallographica Section D*. **D51**, 271-277.
- Sousa, R. (1997). Using Cosolvents to Stabilize Protein Conformation for Crystallization. *Methods in Enzymology*. **276**, 131-143.
- Stout, G. H. and Jensen, L. H. X-Ray Structure Determination: A Practical Guide. *Ed.2*. John Wiley & Sons. 1989.

Stura, E. A., Satterthwait, A. C., Calvo, J. C., Kaslow, D. C., and Wilson, I. A. (1994). Reverse Screening. *Acta Crystallographica Section D*. **D50**, 448-455.

Stura, E. A. and Wilson, I. A. (1990). Analytical and Production Seeding Techniques. *Methods: A Comparison to Methods in Enzymology*. **1**(1), 38-49.

Stura, E. A. and Wilson, I. A. (1991). Applications of Streak Seeding Technique in Protein Crystallography. *Journal of Crystal Growth*. **110**, 270-282.

Stura, E. A. and Wilson, I. A. Crystallization of Nuclei Acids and Proteins: A Practical Approach. "Chapter 5: Seeding Techniques". *Ed.1*, 99-126. IRL Press at Oxford University Press. 1992.

Suttle, N. F. (1991). The Interactions between Copper, Molybdenum, and Sulphur in Ruminant Nutrition. *Annual Reviews of Nutrition*. **11**, 121-140.

Tatusova, T. A. and Madden, T. L. (1999). Blast 2 sequences - a new tool for comparing protein and nucleotide sequences. *FEMS Microbiology Letters*. **174**, 247-250.

Teng, T. Y. (1990). Mounting of Crystals for Macromolecular Crystallography in a Free-Standing Thin Film. *Journal of Applied Crystallography*. **23**, 387-391.

Thome, D. M. X-Ray Crystallographic Studies of Thiomolybdates and Bovine Serum Albumin. 2001. University of Saskatchewan.

Tomb, J.-F., White, O., Kerlavage, A. R., Clayton, R. A., Sutton, G. G., Fleischmann, R. D., Ketchum, K. A., Klenk, H. P., Gill, S., Dougherty, B. A. N. K., Quackenbush, J., Zhou, L., Kirkness, E. F., Peterson, S., Loftus, B., Richardson, D., Dodson, R., Khalak, H. G., Glodek, A., Mckenney, K., Fitzgerald, L. M., Lee, N., Adams, M. D., Hickey, E. K., Berg, D. E., Gocayne, J. D., Utterback, T. R., Peterson, J. D., Kelley, J. M., Cotton, M. D., Weidman, J. M., Fujii, C., Bowman, C., Watthey, L., Wallin, E., Hayes, W. S., Borodovsky, M., Karp, P. D., Smith, H. O., Fraser, C. M., and Venter, J. C. (1997). The Complete Genome Sequence of the Gastric Pathogen *Helicobacter Pylori*. *Nature*. **388**(6642), 539-547.

Vekilov, P. G., Feeling-Taylor, A. R., Yau, S. T., and Petsev, D. (2004). Solvent Entropy Contribution to the Free Energy of Protein Crystallization. *Acta Crystallographica Section D*. **D58**, 1611-1616.

Walker, M. M. and Crabtree, J. E. (1998). *Helicobacter Pylori* Infection and the Pathogenesis of Duodenal Ulceration. *Annals of the New York Academy of Sciences*. **859**, 96-111.

Ward, J. D., Spears, J. W., and Kegley, E. B. (1996). Bioavailability of Copper Proteinate and Copper Carbonate Relative to Copper Sulfate in Cattle. *Journal of Dairy Science*. **79**(127), 132.

Watenpaugh, K. D. (1991). Macromolecular Crystallography at Cryogenic Temperatures. *Current Opinion in Structural Biology*. **1**, 1012-1015.

Weber, P. C. (1990). A Protein Crystallization Strategy Using Automated Grid Search on Successively Finer Grids. *Methods: A Comparison to Methods in Enzymology*. **1**(1), 31-37.

Williams, C. N. (1996). Helicobacter Pylori, Gastric Cancer and Gastric MALT Lymphoma. *Canadian Journal of Gastroenterology*. **10**(6), 359-360.

Woo, J. W., Kidd, R. D., Martin, J. L., and Kobe, B. (2003). Comparison of Three Commercial Sparse-matrix Crystallization Screens. *Acta Crystallographica Section D*. **D59**, 769-772.

Xie, X., Kokubo, T., Cohen, S. L., Mirza, U. J., Hoffmann, A., Chait, B. T., Roeder, R. G., Nakatani, Y., and Burley, S. K. (1996). Structural Similarity between TAFs and the Heterotetrameric Core of the Histone Octamer. *Nature*. **380**, 316-322.

Yonath, A., Mussig, J., and Wittmann, H. G. (1982). Parameters for Crystal Growth of Ribosomal Subunits. *Journal of Cellular Biochemistry*. **19**, 145-155.

Yoshida, T., Oka, S.-I., Masutani, H., Nakamura, H., and Yodoi, J. (2003). The Role of Thioredoxin in the Ageing Process: Involvement of Oxidative Stress. *Antioxidants & Redox Signaling*. **5**(5), 563-570.

Zeppezauer, M. (1971). Formation of Large Crystals. *Methods in Enzymology*. **22**, 253-266.

Zhang, Y., Akilesh, S., and Wilcox, D. E. (2000). Isothermal Titration Calorimetry Measurements of Ni(II) and Cu(II) Binding to His, GlyGlyHis, HisGlyHis, and Bovine Serum Albumin: A Critical Evaluation. *Inorganic Chemistry*. **39**, 3057-3064.

Zhang, Y. and Wilcox, D. E. (2002). Thermodynamic and Spectroscopic Study of Cu(II) and Ni(II) Binding to Bovine Serum Albumin. *Journal of Biological Inorganic Chemistry*(7), 327-337.

Zulauf, M. and D'Arcy, A. (1992). Light Scattering of Proteins as Criterion for Crystallization. *Journal of Crystal Growth*. **122**, 102-106.

# APPENDIX 1

Table A-1: Purified BSA Crystallization Trials

| Buffer      | pH                      | Precipitant | [Precipitant] (%)            | Additive  | [BSA]<br>(mg/ml) | Temp (°C) | Method       |
|-------------|-------------------------|-------------|------------------------------|---|------------------|-----------|--------------|
| 25 mM NaAc  | 5.1, 5.2, 5.3, 5.4      | SAS         | 47.5, 50, 52.5, 55, 57.5, 60 | N/A   | 50               | 20        | Hanging Drop |
| 25 mM NaAc  | 5.3, 5.4, 5.5, 5.6      | SAS         | 47, 48, 49, 50, 51, 52       | 20% Glycerol  | 40               | 20        | Hanging Drop |
| 25 mM NaAc  | 5.3, 5.4, 5.5, 5.6      | SAS         | 48, 49, 50, 51, 52, 53       | N/A   | 40               | 20        | Hanging Drop |
| 100 mM NaAc | 4.0, 4.5, 5.0, 5.5, 6.0 | IPA         | 10, 15, 20, 25, 30           | 0.2 M CaCl <sub>2</sub>   | 10               | 20        | Microbatch   |
| 100 mM NaAc | 4.0, 4.5, 5.0, 5.5, 6.0 | IPA         | 10, 15, 20, 25, 30           | 0.2 M CaCl <sub>2</sub>   | 10               | 20        | Sitting Drop |
| 50 mM K-PO4 | 5.5, 5.6, 5.7, 5.8      | SAS         | 52, 53, 54, 55, 56, 57       | N/A   | 10               | 20        | Hanging Drop |
| 50 mM K-PO4 | 5.5, 5.6, 5.7, 5.8      | SAS         | 52, 53, 54, 55, 56, 57       | 10 mM NaCl  | 10               | 20        | Hanging Drop |
| 50 mM K-PO4 | 5.5, 5.6, 5.7, 5.8      | SAS         | 52, 53, 54, 55, 56, 57       | 50 mM NaCl  | 10               | 20        | Hanging Drop |
| 50 mM K-PO4 | 5.5, 5.6, 5.7, 5.8      | SAS         | 52, 53, 54, 55, 56, 57       | 10 mM KCl + 10 mM MgCl <sub>2</sub>   | 10               | 20        | Hanging Drop |
| 50 mM K-PO4 | 5.5, 5.6, 5.7, 5.8      | SAS         | 52, 53, 54, 55, 56, 57       | 50 mM KCl + 50 mM MgCl <sub>2</sub>   | 10               | 20        | Hanging Drop |
| 50 mM K-PO4 | 5.9, 6.0, 6.1, 6.2      | SAS         | 52, 53, 54, 55, 56, 57       | N/A   | 10               | 20        | Hanging Drop |
| 50 mM K-PO4 | 5.9, 6.0, 6.1, 6.2      | SAS         | 52, 53, 54, 55, 56, 57       | 10 mM NaCl  | 10               | 20        | Hanging Drop |
| 50 mM K-PO4 | 5.9, 6.0, 6.1, 6.2      | SAS         | 52, 53, 54, 55, 56, 57       | 50 mM NaCl  | 10               | 20        | Hanging Drop |
| 50 mM K-PO4 | 5.9, 6.0, 6.1, 6.2      | SAS         | 52, 53, 54, 55, 56, 57       | 10 mM KCl + 10 mM MgCl <sub>2</sub>   | 10               | 20        | Hanging Drop |
| 50 mM K-PO4 | 5.9, 6.0, 6.1, 6.2      | SAS         | 52, 53, 54, 55, 56, 57       | 50 mM KCl + 50 mM MgCl <sub>2</sub>   | 10               | 20        | Hanging Drop |
| 50 mM K-PO4 | 5.7,5.8,5.9,6.0         | SAS         | 55, 56, 57, 58, 59, 60       | 1, 5, 10, 20 mM CoCl <sub>2</sub>   | 10               | 20        | Hanging Drop |
| 50 mM K-PO4 | 5.7, 5.8                | SAS         | 57, 58, 59                   | 10, 25 mM CoCl <sub>2</sub>   | 10               | 20        | Hanging Drop |
| 50 mM K-PO4 | 5.6, 5.7,5.8,5.9        | SAS         | 55, 56, 57, 58, 59, 60       | 10 mM CoCl <sub>2</sub> / NiCl <sub>2</sub> /ZnCl <sub>2</sub> /CdCl <sub>2</sub> | 10               | 20        | Hanging Drop |
| 50 mM K-PO4 | 5.6, 5.7,5.8,5.9        | SAS         | 55, 56, 57, 58, 59, 60       | 50 mM NaCl/KCl/MgCl <sub>2</sub> /LiCl  | 10               | 20        | Hanging Drop |
| 50 mM K-PO4 | 5.6, 5.8                | SAS         | 56, 58, 60                   | 100, 250, 500, 1000 mM LiCl   | 10               | 20        | Hanging Drop |

Table A-1 (continued)

|             |                         |                 |                              |   |     |    |              |
|-------------|-------------------------|-----------------|------------------------------|---|-----|----|--------------|
| 50 mM K-PO4 | 5.8                     | SAS             | 55, 56, 57, 58, 59, 60       | 0, 1, 5, 10 mM CoCl <sub>2</sub>              | 12  | 20 | Hanging Drop |
| 50 mM K-PO4 | 5.6, 5.7, 5.8, 5.9      | SAS             | 55, 56, 57, 58, 59, 60       | 10 mM CoCl <sub>2</sub>                       | 10  | 20 | Hanging Drop |
| 50 mM K-PO4 | 5.7, 5.8, 5.9, 6.0      | SAS             | 55, 56, 57, 58, 59, 60       | 10 mM CoCl <sub>2</sub>                       | 10  | 20 | Hanging Drop |
| 50 mM K-PO4 | 5.6, 5.7, 5.8, 5.9      | SAS             | 48, 49, 50, 51, 52, 53       | N/A   | 47  | 20 | Hanging Drop |
| 100 mM MES  | 5.6, 5.8, 6.0, 6.2, 6.4 | PEG 6000        | 28                           | 1 M LiCl                                      | 10  | 4  | Hanging Drop |
| 100 mM MES  | 5.6, 5.8, 6.0, 6.2, 6.4 | PEG 6000        | 26, 28                       | 1 M LiCl                                      | 10  | 4  | Sitting Drop |
| 100 mM MES  | 5.8, 6.0, 6.2, 6.4      | PEG 6000        | 20, 22, 24, 26, 28, 30       | 1 M LiCl                                      | 5   | 20 | Hanging Drop |
| 100 mM MES  | 5.8, 6.0, 6.2           | PEG 6000        | 28                           | 25, 50, 100, 200 mM (KCl/ CoCl <sub>2</sub> ) | 10  | 20 | Hanging Drop |
| 100 mM MES  | 5.5, 6.0, 6.5, 7.0      | PEG 6000        | 28                           | 0.011, 0.11, 0.55, 1.1, 2.2, 3.3 M LiCl       | 10  | 20 | Hanging Drop |
| 100 mM MES  | 5.0, 5.5, 6.0, 6.5, 7.0 | PEG 6000        | 2.5, 5.0, 7.5, 10, 12.5      | N/A   | 10  | 20 | Sitting Drop |
| 100 mM MES  | 5.0, 5.5, 6.0, 6.5, 7.0 | PEG 6000        | 2.5, 5.0, 7.5, 10, 12.5      | N/A   | 10  | 20 | Hanging Drop |
| 100 mM MES  | 5.0, 5.5, 6.0, 6.5, 7.0 | PEG 6000        | 2.5, 5.0, 7.5, 10, 12.5      | N/A   | 10  | 20 | Microbatch   |
| 100 mM MES  | 5.6, 5.8, 6.0, 6.2      | PEG 6000        | 26, 28, 30, 32, 34, 36       | 1 M LiCl                                      | 10  | 20 | Hanging Drop |
| 100 mM MES  | 5.6, 5.8, 6.0, 6.2      | PEG 6000        | 28                           | 25, 50, 100, 200, 1000 mM LiCl                | 10  | 20 | Hanging Drop |
| 100 mM MES  | 5.6, 5.8, 6.0, 6.2      | PEG 6000        | 22.5, 25, 27.5, 30, 32.5, 35 | 0.1 M LiCl                                    | 10  | 20 | Hanging Drop |
| 100 mM MES  | 5.6, 5.8, 6.0, 6.2      | PEG 6000        | 20, 22, 24, 26, 28, 30       | 1 M LiCl                                      | 10  | 20 | Hanging Drop |
| 100 mM MES  | 6.0                     | PEG 6000        | 24, 26, 28, 30, 32, 34       | 1 M LiCl                                      | 5   | 20 | Hanging Drop |
| 100 mM MES  | 6.0                     | PEG 6000        | 24, 26, 28, 30, 32, 34       | 1 M LiCl                                      | 10  | 20 | Hanging Drop |
| 100 mM MES  | 5.8, 6.0, 6.2, 6.4      | PEG 6000        | 20, 22, 24, 26, 28, 30       | 1 M LiCl                                      | 5   | 20 | Hanging Drop |
| 100 mM MES  | 5.8, 6.0, 6.2, 6.4      | PEG 400         | 10, 15, 20, 25, 30, 35       | 1 M LiCl                                      | 8.5 | 20 | Hanging Drop |
| 100 mM MES  | 5.8, 6.0, 6.2           | PEG 400         | 28                           | 1 M LiCl                                      | 10  | 20 | Hanging Drop |
| 100 mM MES  | 5.8, 6.0, 6.2           | PEG MME<br>2000 | 28                           | 1 M LiCl                                      | 10  | 20 | Hanging Drop |

Table A-1 (continued)

|                |                              |                 |                        |  |     |    |              |
|----------------|------------------------------|-----------------|------------------------|--|-----|----|--------------|
| 100 mM MES     | 5.6, 5.8, 6.0, 6.2           | PEG 4000        | 24, 26, 28, 30, 32, 34 | 1 M LiCl                                     | 10  | 20 | Hanging Drop |
| 100 mM MES     | 5.8, 6.0, 6.2                | PEG 4000        | 28                     | 1 M LiCl                                     | 10  | 20 | Hanging Drop |
| 100 mM MES     | 5.8, 6.0, 6.2                | PEG 8000        | 28                     | 1 M LiCl                                     | 10  | 20 | Hanging Drop |
| 100 mM Tris    | 7.0, 7.5, 8.0, 8.5, 9.0      | PEG 6000        | 20, 25, 30, 35, 40     | N/A  | 10  | 20 | Microbatch   |
| 100 mM Tris    | 7.0, 7.5, 8.0, 8.5, 9.0      | PEG MME<br>2000 | 20, 25, 30, 35, 40     | 10 mM NiCl <sub>2</sub>                      | 10  | 20 | Microbatch   |
| 100 mM Tris    | 8.3, 8.6, 8.9, 9.2, 9.5      | PEG MME<br>2000 | 21, 23, 25, 27, 29     | 10 mM NiCl <sub>2</sub>                      | 10  | 20 | Sitting Drop |
| 100 mM Tris    | 9.0, 9.1, 9.2, 9.3, 9.4, 9.5 | PEG MME<br>2000 | 21, 23, 25, 27, 29     | 10 mM NiCl <sub>2</sub>                      | 10  | 20 | Sitting Drop |
| 100 mM Tris    | 7.0, 7.5, 8.0, 8.5, 9.0      | PEG MME<br>2000 | 20, 25, 30, 35, 40     | 10 mM NiCl <sub>2</sub>                      | 4.5 | 20 | Sitting Drop |
| 100 mM HEPES   | 6.0, 6.5, 7.0, 7.5, 8.0      | PEG 6000        | 20, 25, 30, 35, 40     | N/A  | 10  | 20 | Microbatch   |
| 100 mM Na-CACO | 5.5, 6.0, 6.5, 7.0           | PEG 8000        | 5, 10, 15, 20, 25, 30  | 200 mM (CH <sub>3</sub> COO) <sub>2</sub> Zn | 10  | 20 | Hanging Drop |

Table A-2: Unpurified BSA Crystallization Trials

| Buffer     | pH                 | Precipitant | [Precipitant] (%)                  | Additive                | [BSA] (mg/ml) | Temp ( °C) | Method       |
|------------|--------------------|-------------|------------------------------------|-------------------------|---------------|------------|--------------|
| 25 mM NaAc | 4.7, 4.8, 4.9, 5.0 | SAS         | 37.5, 40, 42.5, 45, 47.5, 50       | N.A                     | 60, 120       | 20         | Hanging Drop |
| 25 mM NaAc | 4.5, 5.0, 5.5      | SAS         | 37.5, 40, 42.5, 45, 47.5, 50       | N.A                     | 60            | 20         | Hanging Drop |
| 25 mM NaAc | 4.7, 4.9, 5.1, 5.3 | SAS         | 37.5, 40, 42.5, 45, 47.5, 50       | N/A                     | 50, 60        | 20         | Hanging Drop |
| 25 mM NaAc | 5.1, 5.2, 5.3, 5.4 | SAS         | 47.5, 50, 52.5, 55, 57.5, 60       | N/A                     | 50, 60        | 20         | Hanging Drop |
| 25 mM NaAc | 5.2, 5.3           | SAS         | 53, 54, 55, 56, 57, 58             | N/A                     | 50            | 20         | Hanging Drop |
| 25 mM NaAc | 5.2, 5.3           | SAS         | 53, 54, 55, 56, 57, 58             | 10 mM CoCl <sub>2</sub> | 50            | 20         | Hanging Drop |
| 25 mM NaAc | 5.1, 5.2, 5.3, 5.4 | SAS         | 45, 47, 49, 51, 53 - 58            | N/A                     | 50, 60        | 20         | Sitting Drop |
| 25 mM NaAc | 5.1, 5.2, 5.3, 5.4 | SAS         | 45, 47, 49, 51, 53, 55             | N/A                     | 50, 60        | 20         | Hanging Drop |
| 25 mM NaAc | 5.1, 5.2, 5.3, 5.4 | SAS         | 54, 55, 56, 57, 58, 59             | N/A                     | 50, 60        | 20         | Hanging Drop |
| 25 mM NaAc | 5.1, 5.2, 5.3, 5.4 | SAS         | 54, 55, 56, 57, 58, 59             | N/A                     | 50, 60        | 20         | Sitting Drop |
| 25 mM NaAc | 5.1, 5.2, 5.3, 5.4 | SAS         | 45, 47, 49, 51, 53 - 58            | N/A                     | 50, 60        | 20         | Sitting Drop |
| 25 mM NaAc | 5.3, 5.4, 5.5, 5.6 | SAS         | 47, 48, 49, 50, 51, 52             | 20% Glycerol            | 30            | 20         | Hanging Drop |
| 25 mM NaAc | 5.1, 5.2, 5.3, 5.4 | SAS         | 48, 50, 52, 54, 56, 58             | 25% Glycerol            | 50, 60        | 20         | Sitting Drop |
| 25 mM NaAc | 5.2, 5.3           | SAS         | 48, 50, 52, 54, 56, 58             | N/A                     | 50, 60        | 20         | Hanging Drop |
| 25 mM NaAc | 5.0 - 5.5          | SAS         | 48, 50, 52, 54, 56, 58             | 10 mM CoCl <sub>2</sub> | 50, 60        | 20         | Hanging Drop |
| 25 mM NaAc | 5.0, 5.2, 5.4, 5.6 | SAS         | 50, 52, 54, 56, 58, 60             | 10 mM ZnSO <sub>4</sub> | 50, 60        | 20         | Hanging Drop |
| 25 mM NaAc | 4.9 - 5.6          | SAS         | 48, 50, 52, 54, 56, 58             | N/A                     | 50, 60        | 20         | Hanging Drop |
| 25 mM NaAc | 5.2, 5.3, 5.4, 5.5 | SAS         | 48, 50, 52, 54, 56, 58             | N/A                     | 50, 60        | 20         | Hanging Drop |
| 25 mM NaAc | 5.3, 5.4, 5.5, 5.6 | SAS         | 47, 48, 49, 50, 51, 52             | 10 mM CoCl <sub>2</sub> | 50, 60        | 20         | Hanging Drop |
| 25 mM NaAc | 5.0, 5.1, 5.2, 5.3 | SAS         | 38, 40, 42, 44, 46, 48, 50, 52, 54 | 1% Sucrose              | 30, 40        | 20         | Sitting Drop |

Table A-2 (continued)

|            |                    |     |                                |                                       |                |    |              |
|------------|--------------------|-----|--------------------------------|---------------------------------------|----------------|----|--------------|
| 25 mM NaAc | 5.0, 5.1, 5.2, 5.3 | SAS | 36, 38, 40, 42, 44, 46, 48, 50 | 1% Sucrose                            | 50, 60         | 20 | Sitting Drop |
| 25 mM NaAc | 5.2, 5.3, 5.4, 5.5 | SAS | 54                             | 1, 3, 5, 10, 15, 20% Sucrose          | 60             | 20 | Hanging Drop |
| 25 mM NaAc | 5.2, 5.3, 5.4, 5.5 | SAS | 54                             | 1, 3, 5, 10, 15, 20% Xylitol          | 60             | 20 | Hanging Drop |
| 25 mM NaAc | 4.9 - 5.6          | SAS | 44, 46, 48, 50, 52, 54, 56, 58 | 3% Xylitol                            | 30, 40, 50, 60 | 20 | Sitting Drop |
| 25 mM NaAc | 5.1, 5.2, 5.3, 5.4 | SAS | 40, 45, 50, 55, 60, 65         | N/A                                   | 70, 80         | 20 | Hanging Drop |
| 25 mM NaAc | 5.1, 5.2, 5.3, 5.4 | SAS | 27.5, 32.5, 37.5               | N/A                                   | 70, 80         | 20 | Hanging Drop |
| 25 mM NaAc | 5.0, 5.1, 5.2, 5.3 | SAS | 40, 41, 42, 43, 44, 45         | N/A                                   | 70, 80         | 20 | Hanging Drop |
| 25 mM NaAc | 5.3, 5.4, 5.5, 5.6 | SAS | 40, 42, 44, 46, 48, 50         | 10 mM CoCl <sub>2</sub>               | 70, 80         | 20 | Hanging Drop |
| 25 mM NaAc | 5.3, 5.4, 5.5, 5.6 | SAS | 43, 44, 45, 46, 47, 48         | N/A                                   | 70, 80         | 20 | Hanging Drop |
| 25 mM NaAc | 4.9 - 5.6          | SAS | 44, 46, 48, 50, 52, 54, 56, 58 | 3% Sucrose                            | 10, 20, 30, 40 | 20 | Sitting Drop |
| 25 mM NaAc | 4.9 - 5.6          | SAS | 44, 46, 48, 50, 52, 54, 56, 58 | 3% Sucrose                            | 50, 60, 70, 80 | 20 | Sitting Drop |
| 25 mM NaAc | 5.3, 5.4, 5.5, 5.6 | SAS | 49                             | 0.5, 1.0, 1.5, 2.0, 2.5, 3.0% Sucrose | 30             | 20 | Sitting Drop |
| 25 mM NaAc | 5.2, 5.3, 5.4, 5.5 | SAS | 52, 53, 54, 55, 56, 57         | 20, 25, 30% Glycerol                  | 50, 60         | 20 | Hanging Drop |
| 25 mM NaAc | 5.1, 5.2, 5.3, 5.4 | SAS | 40, 45, 50, 55, 60, 65         | N/A                                   | 30, 40         | 20 | Hanging Drop |
| 25 mM NaAc | 5.3, 5.4, 5.5, 5.6 | SAS | 46, 48, 50, 52, 54, 56         | N/A                                   | 30, 40         | 20 | Hanging Drop |
| 25 mM NaAc | 5.1, 5.2, 5.3, 5.4 | SAS | 45, 47, 49, 51, 53 - 58        | N/A                                   | 30, 40         | 20 | Sitting Drop |
| 25 mM NaAc | 5.3, 5.4, 5.5, 5.6 | SAS | 47, 48, 49, 50, 51, 52         | N/A                                   | 30, 40         | 20 | Hanging Drop |
| 25 mM NaAc | 5.3, 5.4, 5.5, 5.6 | SAS | 47, 48, 49, 50, 51, 52         | 10 mM CoCl <sub>2</sub>               | 30, 40         | 20 | Hanging Drop |
| 25 mM NaAc | 5.1, 5.2, 5.3, 5.4 | SAS | 50, 52.5, 55, 57.5, 60, 62.5   | 10 mM Na-Citrate                      | 50, 60         | 20 | Hanging Drop |
| 25 mM NaAc | 5.1, 5.2, 5.3, 5.4 | SAS | 49, 51, 53, 55, 57, 59         | 3% Sucrose                            | 60, 70         | 20 | Hanging Drop |
| 25 mM NaAc | 5.1, 5.2, 5.3, 5.4 | SAS | 49, 51, 53, 55, 57, 59         | 3% Xylitol                            | 50, 60         | 20 | Hanging Drop |
| 25 mM NaAc | 5.1, 5.2, 5.3, 5.4 | SAS | 45, 47, 49, 51, 53, 55         | 3% Xylitol                            | 50             | 20 | Hanging Drop |

Table A-2 (continued)

|                          |                         |             |                                |                                      |        |    |              |
|--------------------------|-------------------------|-------------|--------------------------------|--------------------------------------|--------|----|--------------|
| 25 mM NaAc               | 5.0, 5.1, 5.2, 5.3      | SAS         | 52, 53, 54, 55, 56, 57         | 3% Sucrose                           | 60     | 20 | Hanging Drop |
| 25 mM NaAc               | 5.0, 5.1, 5.2, 5.3      | SAS         | 52, 53, 54, 55, 56, 57         | 3% Xylitol                           | 50     | 20 | Hanging Drop |
| 25 mM NaAc               | 5.2, 5.3, 5.4, 5.5      | SAS         | 48, 49, 50                     | N/A                                  | 60     | 20 | Hanging Drop |
| 25 mM NaAc               | 5.2, 5.3, 5.4, 5.5      | SAS         | 48, 49, 50                     | 10 mM CoCl <sub>2</sub>              | 60     | 20 | Hanging Drop |
| 25 mM NaAc               | 5.2, 7.2                | Na-Malonate | 50 - 60                        | N/A                                  | 50, 60 | 20 | Hanging Drop |
| 25 mM NaAc               | 5.2, 5.3, 5.4, 5.5      | Na-Malonate | 2.7, 2.8, 2.9, 3.0, 3.1, 3.2 M | 10 mM CoCl <sub>2</sub>              | 60     | 20 | Hanging Drop |
| 50 mM NaAc               | 5.0, 5.2, 5.4, 5.6      | SAS         | 40, 42, 44, 46, 48, 50         | 0.2 M K/Na Tartrate                  | 60     | 20 | Hanging Drop |
| 100 mM NaAc              | 4.0, 4.5, 5.0, 5.5, 6.0 | MPD         | 20, 25, 30, 35, 40             | 0.02 M CaCl <sub>2</sub>             | 5, 10  | 20 | Sitting Drop |
| 100 mM NaAc              | 4.0, 4.5, 5.0, 5.5, 6.0 | MPD         | 10, 15, 20, 25, 30             | 0.2 M CaCl <sub>2</sub>              | 10     | 20 | Sitting Drop |
| 100 mM K-PO <sub>4</sub> | 5.5 - 6.2               | SAS         | 52, 53, 54, 55, 56, 57         | N/A                                  | 10     | 4  | Hanging Drop |
| 100 mM K-PO <sub>4</sub> | 5.5 - 6.2               | SAS         | 52, 53, 54, 55, 56, 57         | N/A                                  | 10     | 15 | Hanging Drop |
| 100 mM K-PO <sub>4</sub> | 5.5 - 6.2               | SAS         | 52, 53, 54, 55, 56, 57         | 50 mM NaCl                           | 10     | 4  | Hanging Drop |
| 100 mM K-PO <sub>4</sub> | 5.5 - 6.2               | SAS         | 52, 53, 54, 55, 56, 57         | 50 mM NaCl                           | 10     | 15 | Hanging Drop |
| 100 mM K-PO <sub>4</sub> | 5.5 - 6.2               | SAS         | 52, 53, 54, 55, 56, 57         | 50 mM MgCl <sub>2</sub>              | 10     | 4  | Hanging Drop |
| 100 mM K-PO <sub>4</sub> | 5.5 - 6.2               | SAS         | 52, 53, 54, 55, 56, 57         | 50 mM MgCl <sub>2</sub>              | 10     | 15 | Hanging Drop |
| 100 mM K-PO <sub>4</sub> | 5.5 - 6.2               | SAS         | 52, 53, 54, 55, 56, 57         | N/A                                  | 10     | 4  | Sitting Drop |
| 100 mM K-PO <sub>4</sub> | 5.5 - 6.2               | SAS         | 52, 53, 54, 55, 56, 57         | N/A                                  | 10     | 15 | Sitting Drop |
| 100 mM K-PO <sub>4</sub> | 5.0, 5.5, 6.0, 6.5      | SAS         | 40, 45, 50, 55, 60, 65         | N/A                                  | 10     | 4  | Sitting Drop |
| 100 mM K-PO <sub>4</sub> | 5.0, 5.5, 6.0, 6.5      | SAS         | 40, 45, 50, 55, 60, 65         | 50mM (NaCl, KCl, MgCl <sub>2</sub> ) | 10     | 4  | Sitting Drop |
| 100 mM K-PO <sub>4</sub> | 5.0, 5.5, 6.0, 6.5      | SAS         | 40, 45, 50, 55, 60, 65         | N/A                                  | 10     | 15 | Sitting Drop |
| 100 mM K-PO <sub>4</sub> | 5.0, 5.5, 6.0, 6.5      | SAS         | 40, 45, 50, 55, 60, 65         | 50mM (NaCl, KCl, MgCl <sub>2</sub> ) | 10     | 15 | Sitting Drop |
| 100 mM K-PO <sub>4</sub> | 5.5, 6.0                | SAS         | 50, 52.5, 55, 57.5, 60, 62.5   | N/A                                  | 5      | 20 | Hanging Drop |

Table A-2 (continued)

|                 |                    |     |                              |  |               |    |              |
|-----------------|--------------------|-----|------------------------------|--|---------------|----|--------------|
| 100 mM K-PO4    | 5.5, 6.0           | SAS | 50, 52.5, 55, 57.5, 60, 62.5 | 50 mM MgCl <sub>2</sub>  | 5             | 20 | Hanging Drop |
| 100 mM K-PO4    | 5.6, 5.8           | SAS | 54, 55, 56, 57, 58, 59       | N/A  | 5             | 20 | Hanging Drop |
| 100 mM K-PO4    | 5.6, 5.8           | SAS | 54, 55, 56, 57, 58, 59       | 50 mM NaCl   | 5             | 20 | Hanging Drop |
| 100 mM K-PO4    | 5.4, 5.6, 5.8, 6.0 | SAS | 40, 45, 50, 55, 60, 65       | 50 mM NaCl   | 3.0, 5.0, 7.5 | 20 | Hanging Drop |
| 100 mM K-PO4    | 5.6, 5.8, 6.0, 6.2 | SAS | 50 - 61                      | N/A  | 20            | 20 | Sitting Drop |
| 100 mM K-PO4    | 5.6, 5.8, 6.0, 6.2 | SAS | 50 - 61                      | 50 mM NaCl   | 20            | 20 | Sitting Drop |
| 100 mM K-PO4    | 5.9, 6.0, 6.1, 6.2 | SAS | 52, 53, 54, 55, 56, 57       | N.A  | 10            | 20 | Hanging Drop |
| 100 mM K-PO4    | 5.9, 6.0, 6.1, 6.2 | SAS | 52, 53, 54, 55, 56, 57       | 50 mM NaCl/ KCl/ MgCl <sub>2</sub>   | 10            | 20 | Hanging Drop |
| 100 mM K-PO4    | 5.0, 5.5, 6.0, 6.5 | SAS | 40, 45, 50, 55, 60, 65       | 1 mM CdCl <sub>2</sub> /CoCl <sub>2</sub> /NiCl <sub>2</sub> /ZnCl <sub>2</sub>  | 10            | 20 | Hanging Drop |
| 100 mM K-PO4    | 5.0, 5.5, 6.0, 6.5 | SAS | 40, 45, 50, 55, 60, 65       | 50 mM CdCl <sub>2</sub> /CoCl <sub>2</sub> /NiCl <sub>2</sub> /ZnCl <sub>2</sub> | 10            | 20 | Hanging Drop |
| 100 mM K-PO4    | 5.0, 5.5, 6.0, 6.5 | SAS | 40, 45, 50, 55, 60, 65       | N/A, 50 mM NaCl/KCl/MgCl <sub>2</sub>  | 5, 10         | 20 | Sitting Drop |
| 100 mM K-PO4    | 5.5 - 6.2          | SAS | 52, 53, 54, 55, 56, 57       | N/A  | 5, 10         | 20 | Sitting Drop |
| 50 mM K-PO4     | 5.4 - 6.1          | SAS | 45, 47.5, 50, 52.5, 55, 57.5 | 10 mM CoCl <sub>2</sub>  | 10            | 20 | Hanging Drop |
| 50 mM K-PO4     | 5.4 - 6.1          | SAS | 45, 47.5, 50, 52.5, 55, 57.5 | 10 mM NiCl <sub>2</sub>  | 10            | 20 | Hanging Drop |
| 50 mM K-PO4     | 5.6, 5.7, 5.8, 5.9 | SAS | 55, 57, 59, 61, 63, 65       | N/A  | 10, 20        | 20 | Hanging Drop |
| 50 mM K-PO4     | 5.7, 5.8, 5.9, 6.0 | SAS | 55, 57, 59, 61, 63, 65       | 10 mM CoCl <sub>2</sub>  | 10, 20        | 20 | Hanging Drop |
| 50 mM K-PO4     | 5.4, 5.6, 5.8, 6.0 | SAS | 40, 45, 50, 55, 60, 65       | N/A  | 30, 40        | 20 | Hanging Drop |
| 50 mM K-PO4     | 5.7, 5.8, 5.9, 6.0 | SAS | 45, 47, 49, 51, 53, 55       | 10 mM CoCl <sub>2</sub>  | 20, 30        | 20 | Hanging Drop |
| 50 mM K-PO4     | 5.4, 5.6, 5.8, 6.0 | SAS | 47.5, 50, 52.5, 55, 57.5, 60 | N.A  | 30, 40        | 20 | Hanging Drop |
| 50 mM K-PO4     | 5.4, 5.6, 5.8, 6.0 | SAS | 47.5, 50, 52.5, 55, 57.5, 60 | 10 mM CoCl <sub>2</sub>  | 30, 40        | 20 | Hanging Drop |
| 50 mM K-PO4     | 5.7, 5.8, 5.9, 6.0 | SAS | 51, 52, 53                   | 5, 10 mM CoCl <sub>2</sub>   | 50            | 20 | Hanging Drop |
| 50/100 mM K-PO4 | 5.7, 5.8, 5.9, 6.0 | SAS | 51, 52, 53                   | 10 mM CoCl <sub>2</sub>  | 50            | 20 | Hanging Drop |

Table A-2 (continued)

|             |                         |          |                              |  |           |    |              |
|-------------|-------------------------|----------|------------------------------|--|-----------|----|--------------|
| 50 mM K-PO4 | 5.7, 5.8, 5.9, 6.0      | SAS      | 48, 49, 50, 51, 52, 53       | N/A  | 50, 60    | 20 | Hanging Drop |
| 50 mM K-PO4 | 5.4, 5.6, 5.8, 6.0      | SAS      | 47.5, 50, 52.5, 55, 57.5, 60 | N.A  | 60        | 20 | Hanging Drop |
| 50 mM K-PO4 | 5.6, 5.7, 5.8, 5.9,     | SAS      | 51, 52, 53                   | N.A  | 60        | 20 | Hanging Drop |
| 50 mM K-PO4 | 5.6, 5.7, 5.8, 5.9      | SAS      | 51, 52, 53, 54, 55, 56       | N.A  | 50, 60    | 20 | Hanging Drop |
| 50 mM K-PO4 | 5.6, 5.7, 5.8, 5.9      | SAS      | 45, 46, 47, 48, 49, 50       | N.A  | 50, 60    | 20 | Hanging Drop |
| 50 mM K-PO4 | 5.5-6.0                 | SAS      | 51, 52, 53                   | N.A  | 50, 60    | 20 | Hanging Drop |
| 50 mM K-PO4 | 5.6, 5.8, 6.0, 6.2      | SAS      | 40, 45, 50, 55, 60, 65       | N.A  | 70, 80    | 20 | Hanging Drop |
| 50 mM K-PO4 | 5.4 - 6.5               | SAS      | 42, 44, 46, 48, 50, 52       | N.A  | 70, 80    | 20 | Hanging Drop |
| 50 mM K-PO4 | 5.5, 6.0, 6.5, 7.0      | PEG 400  | 10, 20, 30, 40, 50, 60       | N/A  | 60, 120   | 20 | Hanging Drop |
| 50 mM K-PO4 | 5.5, 5.7, 5.9, 6.1      | PEG 400  | 46, 48, 50, 52, 54, 56       | N/A  | 120, 180  | 20 | Hanging Drop |
| 100 mM MES  | 5.0, 5.5, 6.0, 6.5, 7.0 | PEG 6000 | 10, 15, 20, 25, 30           | 1 M LiCl   | 10, 20    | 20 | Hanging Drop |
| 100 mM MES  | 5.0, 5.5, 6.0, 6.5, 7.0 | PEG 6000 | 20, 25, 30, 35, 40           | N/A  | 10, 20    | 20 | Sitting Drop |
| 100 mM MES  | 5.0, 5.5, 6.0, 6.5, 7.0 | PEG 6000 | 10, 15, 20, 25, 30           | 1 M LiCl   | 5, 10, 20 | 20 | Sitting Drop |
| 100 mM MES  | 5.5, 6.0, 6.5, 7.0      | PEG 6000 | 10, 15, 20, 25, 30           | 1 M LiCl   | 10        | 20 | Hanging Drop |
| 100 mM MES  | 5.8, 6.0, 6.2           | PEG 6000 | 28%                          | 5, 10, 25, 50 mM CoCl <sub>2</sub>   | 10        | 20 | Hanging Drop |
| 100 mM MES  | 6.0                     | PEG 6000 | 28                           | 0.01, 0.05, 0.2, 0.5, 1.0, 1.5 M NaCl  | 10        | 20 | Hanging Drop |
| 100 mM MES  | 6.0                     | PEG 6000 | 28                           | 0.01, 0.05, 0.2, 0.5, 1.0, 1.5 M KCl   | 10        | 20 | Hanging Drop |
| 100 mM MES  | 6.0                     | PEG 6000 | 28                           | 0.01, 0.05, 0.2, 0.5, 1.0, 1.5 M NH <sub>4</sub> (SO <sub>4</sub> ) <sub>2</sub> | 10        | 20 | Hanging Drop |
| 100 mM MES  | 6.0                     | PEG 6000 | 28                           | 0.01, 0.05, 0.2, 0.5, 1.0, 1.5 M MgCl <sub>2</sub>                               | 10        | 20 | Hanging Drop |
| 100 mM MES  | 6.0                     | PEG 6000 | 24, 26, 28, 30, 32, 34       | 1 M LiCl   | 5, 10     | 20 | Hanging Drop |
| 100 mM MES  | 5.6, 5.8, 6.0, 6.2      | PEG 6000 | 28                           | 1 M LiCl   | 30, 60    | 20 | Hanging Drop |
| 100 mM MES  | 5.6, 5.8, 6.0, 6.2      | PEG 6000 | 10, 15, 20, 25, 30, 35       | 1 M LiCl   | 30        | 20 | Hanging Drop |

Table A-2 (continued)

|             |                         |                |                           |                         |               |    |              |
|-------------|-------------------------|----------------|---------------------------|-------------------------|---------------|----|--------------|
| 100 mM MES  | 5.5, 5.8, 6.2, 6.5      | PEG 6000       | 5, 10, 15, 20, 25, 30     | 1 M LiCl                | 30            | 20 | Hanging Drop |
| 100 mM MES  | 5.0, 5.5, 6.0, 6.5      | PEG 6000       | 5, 10, 15, 20, 25, 30     | 1 M LiCl                | 20, 30        | 20 | Hanging Drop |
| 100 mM MES  | 5.7, 5.8, 5.9, 6.0      | PEG 6000       | 10, 15, 20, 25, 30, 35    | 1 M LiCl                | 30, 60        | 20 | Hanging Drop |
| 100 mM MES  | 5.5, 5.7, 5.9, 6.1      | PEG 6000       | 46, 46, 50, 52, 54, 56    | 1 M LiCl                | 60            | 20 | Hanging Drop |
| 100 mM MES  | 5.8, 6.0, 6.2, 6.4      | PEG 6000       | 5, 10, 15, 20, 25, 30     | 1 M LiCl                | 60            | 20 | Hanging Drop |
| 100 mM MES  | 5.8, 6.0, 6.2, 6.4      | PEG 400        | 10, 15, 20, 25, 30, 35    | 1 M LiCl                | 30            | 20 | Hanging Drop |
| 100 mM MES  | 5.5, 5.7, 5.9, 6.1      | PEG 400        | 30, 35, 40, 45, 50, 55    | 1 M LiCl                | 30            | 20 | Hanging Drop |
| 100 mM MES  | 5.5, 6.0, 6.5, 7.0      | PEG 400        | 40, 45, 50, 55, 60, 65    | N/A                     | 30            | 20 | Hanging Drop |
| 100 mM MES  | 6.0                     | PEG 400        | 28                        | 1 M LiCl                | 10-60         | 20 | Hanging Drop |
| 100 mM MES  | 6.0                     | PEG 600        | 28                        | 1 M LiCl                | 10-60         | 20 | Hanging Drop |
| 100 mM MES  | 6.0                     | PEG 1000       | 28                        | 1 M LiCl                | 10-60         | 20 | Hanging Drop |
| 100 mM MES  | 6.0                     | PEG MME 2000   | 28                        | 1 M LiCl                | 10-60         | 20 | Hanging Drop |
| 100 mM Tris | 7.5, 8.0, 8.5, 9.0, 9.5 | PEG MME 2000   | 10, 15, 20, 25, 30        | 10 mM NiCl <sub>2</sub> | 10            | 20 | Microbatch   |
| 100 mM Tris | 8.3, 8.6, 8.9, 9.2, 9.5 | PEG MME 2000   | 21, 23, 25, 27, 29        | 10 mM NiCl <sub>2</sub> | 5, 10, 20     | 20 | Sitting Drop |
| 100 mM Tris | 7.0, 7.5, 8.0, 8.5, 9.0 | PEG MME 2000   | 20, 25, 30, 35, 40        | 10 mM NiCl <sub>2</sub> | 5, 7.5        | 20 | Sitting Drop |
| 100 mM Tris | 7.0, 7.5, 8.0, 8.5, 9.0 | PEG MME 2000   | 20, 25, 30, 35, 40        | 10 mM NiCl <sub>2</sub> | 5, 10, 20, 30 | 20 | Sitting Drop |
| 100 mM Tris | 7.0, 7.5, 8.0, 8.5      | PEG MME 2000   | 5, 10, 15, 20, 25, 30     | 10 mM NiCl <sub>2</sub> | 10, 30        | 20 | Hanging Drop |
| 100 mM Tris | 7.5, 8.0, 8.5, 9.0, 9.5 | 1,6 Hexanediol | 1.8, 2.6, 3.4, 4.2, 5.0 M | 0.2 M MgCl <sub>2</sub> | 10            | 20 | Microbatch   |
| 100 mM Tris | 7.5, 8.0, 8.5, 9.0, 9.5 | 1,6 Hexanediol | 1.8, 2.6, 3.4, 4.2, 5.0 M | 0.2 M MgCl <sub>2</sub> | 10            | 20 | Sitting Drop |
| 100 mM Tris | 7.0, 7.5, 8.0, 8.5, 9.0 | PEG 6000       | 20, 25, 30, 35, 40        | N/A                     | 10            | 20 | Microbatch   |
| 100 mM CA   | 5.0, 5.3, 5.6, 5.9      | SAS            | 46, 48, 50, 52, 54, 56    | N/A                     | 60            | 20 | Hanging Drop |

Table A-2 (continued)

|                 |                         |   |                                |   |         |    |               |
|-----------------|-------------------------|---|--------------------------------|---|---------|----|---------------|
| 100 mM HEPES    | 7.0, 7.5, 8.0, 8.5, 9.0 | PEG 6000  | 20, 25, 30, 35, 40             | N/A   | 10      | 20 | Microbatch    |
| 100 mM HEPES    | 6.0, 6.5, 7.0, 7.5, 8.0 | PEG 6000  | 2.5, 5.0, 7.5, 10, 12.5        | N/A   | 10      | 20 | HD/Microbatch |
| 100 mM HEPES-Na | 6.5, 7.0, 7.5, 8.0, 8.5 | IPA   | 20, 25, 30, 35, 40             | 0.2 M MgCl <sub>2</sub>                         | 10      | 20 | Microbatch    |
| 100 mM Na-CACO  | 5.0, 5.5, 6.0, 6.5      | SAS   | 10, 15, 20, 25, 30, 35         | 200 mM<br>(CH <sub>3</sub> COO) <sub>2</sub> Zn | 25, 50  | 20 | Hanging Drop  |
| 100 mM Na-CACO  | 5.0, 5.3, 5.5, 5.8      | SAS   | 46, 48, 50, 52, 54, 56         | N/A   | 60      | 20 | Hanging Drop  |
| 100 mM NaCit    | 5.6, 5.8, 6.0, 6.2      | SAS   | 1.6, 2.0, 2.4 M / 55, 57.5, 60 | 0.2 M K/Na Tartrate                             | 10      | 20 | Hanging Drop  |
| 100 mM NaCit    | 5.0, 5.3, 5.6, 5.9      | SAS   | 10, 20, 30, 40, 50, 60         | 0.2 M K/Na Tartrate                             | 25, 50  | 20 | Hanging Drop  |
| 100 mM NaCit    | 5.2, 5.4, 5.6, 5.8      | SAS   | 46, 48, 50, 52, 54, 56         | 0.2 M K/Na Tartrate                             | 60      | 20 | Hanging Drop  |
| 100 mM NaCit    | 5.6, 5.8, 6.0, 6.2      | SAS   | 55, 57.5, 60                   | 0.2 M K/Na Tartrate                             | 10      | 20 | Hanging Drop  |
| 100 mM NaCit    | 5.2, 5.4, 5.6, 5.8      | SAS   | 44, 46, 48, 50, 52, 54         | 0.2 M K/Na Tartrate                             | 80, 160 | 20 | Hanging Drop  |
| 100 mM NaCit    | 5.6, 5.8, 6.0, 6.2      | NH <sub>4</sub> (SO <sub>4</sub> ) <sub>2</sub> | 1.6, 2.0, 2.4 M                | 0.2 M K/Na Tartrate                             | 10      | 20 | Hanging Drop  |

Table A-3: Purified Trx-2 Crystallization Trials at 20° C

| Buffer    | pH                      | Precipitant | [Precipitant] (%)          | Additive               | [Trx-2] (mg/ml) | Method       |
|-----------|-------------------------|-------------|----------------------------|------------------------|-----------------|--------------|
| 100 mM CA | 4.1, 4.3, 4.5, 4.7, 4.9 | PEG 6000    | 24, 27, 30, 33, 36         | 0.025% Dichloromethane | 7.5             | Sitting Drop |
| 100 mM CA | 4.1, 4.3, 4.5, 4.7, 4.9 | PEG 6000    | 24, 27, 30, 33, 36         | 4% Acetonitrile        | 7.5             | Sitting Drop |
| 100 mM CA | 3.7, 3.9, 4.1, 4.3, 4.5 | PEG 6000    | 24, 26, 28, 30, 32         | 0.7% N-Butanol         | 5.0             | Sitting Drop |
| 100 mM CA | 4.1, 4.3, 4.5, 4.7, 4.9 | PEG 6000    | 24, 27, 30, 33, 36         | 0.7% N-Butanol         | 7.5             | Sitting Drop |
| 100 mM CA | 3.6 - 4.3               | PEG 6000    | 20, 22, 24, 26, 28, 30     | 10 mM DTT              | 7.5             | Hanging Drop |
| 100 mM CA | 4.1, 4.3, 4.5, 4.7, 4.9 | PEG 6000    | 24, 27, 30, 33, 36         | 10 mM DTT              | 7.5             | Sitting Drop |
| 100 mM CA | 3.7, 3.9, 4.1, 4.3, 4.5 | PEG 6000    | 25, 27, 29, 31, 33         | 10 mM DTT              | 5.0             | Sitting Drop |
| 100 mM CA | 3.7, 3.9, 4.1, 4.3, 4.5 | PEG 6000    | 25, 27, 29, 31, 33         | 10 mM DTT              | 7.5             | Hanging Drop |
| 100 mM CA | 3.7, 3.9, 4.1, 4.3, 4.5 | PEG 6000    | 25, 27, 29, 31, 33         | 10 mM DTT              | 7.5             | Sitting Drop |
| 100 mM CA | 3.7, 3.9, 4.1, 4.3, 4.5 | PEG 6000    | 25, 27, 29, 31, 33         | 10 mM DTT              | 7.5             | MicroBatch   |
| 100 mM CA | 3.6 - 4.5               | PEG 6000    | 25, 26, 27, 28, 29         | 10 mM DTT              | 7.5             | Sitting Drop |
| 100 mM CA | 4.0 - 4.5               | PEG 6000    | 25, 26, 27, 28             | 10 mM DTT              | 7.5             | Hanging Drop |
| 100 mM CA | 3.7, 3.9, 4.1, 4.3      | PEG 6000    | 20, 22, 24, 26, 28, 30     | N/A                    | 7.5             | Hanging Drop |
| 100 mM CA | 3.6 - 4.3               | PEG 6000    | 24, 26, 28, 30, 32, 34     | 10 mM DTT              | 7.5             | Hanging Drop |
| 100 mM CA | 3.6 - 4.3               | PEG 6000    | 14, 16, 18, 20, 22, 24     | 10 mM DTT              | 7.5             | Hanging Drop |
| 100 mM CA | 3.7, 3.8, 3.9, 4.0      | PEG 6000    | 24, 25, 26, 27, 28, 29     | 10 mM DTT              | 7.5             | Hanging Drop |
| 100 mM CA | 4.1, 4.2, 4.3, 4.4      | PEG 6000    | 23, 24, 25, 26, 27, 28     | 10 mM DTT              | 7.5             | Hanging Drop |
| 100 mM CA | 3.7, 3.8, 4.0, 4.2, 4.3 | PEG 6000    | 21, 22, 23, 24, 25, 26     | 10 mM DTT              | 7.5             | Hanging Drop |
| 100 mM CA | 3.7, 3.8, 4.0, 4.2, 4.3 | PEG 6000    | 21, 22, 23, 24, 25, 26, 27 | 10 mM DTT              | 7.5             | Sitting Drop |
| 100 mM CA | 3.7, 3.8, 3.9, 4.0      | PEG 6000    | 21, 23, 25, 26, 27, 28     | 10 mM DTT              | 7.5             | Hanging Drop |
| 100 mM CA | 3.7 - 4.4               | PEG 6000    | 21, 22, 23, 24, 25, 26     | 10 mM DTT              | 7.5             | Hanging Drop |
| 100 mM CA | 3.7 - 4.4               | PEG 6000    | 21, 22, 23, 24, 25, 26     | 10 mM DTT              | 7.5             | Sitting Drop |

Table A-3: (continued)

|           |                         |          |                        |                        |     |              |
|-----------|-------------------------|----------|------------------------|------------------------|-----|--------------|
| 100 mM CA | 3.7, 3.8, 3.9, 4.0      | PEG 6000 | 20, 22, 24, 26, 28     | 10 mM DTT              | 7.5 | Sitting Drop |
| 100 mM CA | 3.8, 4.0, 4.2, 4.4      | PEG 6000 | 20, 22, 24, 26, 28, 30 | 10 mM DTT              | 7.5 | Sitting Drop |
| 100 mM CA | 3.8, 4.0, 4.2, 4.4      | PEG 6000 | 24, 25, 26, 27, 28, 29 | 10 mM DTT              | 7.5 | Hanging Drop |
| 100 mM CA | 3.8, 4.0, 4.2, 4.4      | PEG 6000 | 24, 25, 26, 27, 28, 29 | 10 mM DTT              | 7.5 | Sitting Drop |
| 100 mM CA | 3.6, 3.8, 4.0, 4.2, 4.4 | PEG 6000 | 22, 24, 26, 28, 30, 32 | 10 mM DTT              | 7.6 | Sitting Drop |
| 100 mM CA | 4.0, 4.2                | PEG 6000 | 25, 26, 27             | 10 mM DTT              | 7.5 | Hanging Drop |
| 100 mM CA | 3.9, 4.0, 4.1, 4.2      | PEG 6000 | 22, 23, 24, 25, 26, 27 | 10 mM DTT              | 7.5 | Hanging Drop |
| 100 mM CA | 3.8                     | PEG 6000 | 21, 22, 23, 24, 25, 26 | 10 mM DTT              | 7.5 | Hanging Drop |
| 100 mM CA | 3.8, 4.2                | PEG 6000 | 21, 23, 25             | 10 mM DTT              | 7.5 | Hanging Drop |
| 100 mM CA | 3.8, 4.0, 4.2, 4.4      | PEG 6000 | 24, 25, 26             | 10 mM DTT              | 7.5 | Hanging Drop |
| 100 mM CA | 4.0                     | PEG 6000 | 24, 25, 26             | 10 mM DTT              | 7.5 | Hanging Drop |
| 100 mM CA | 4.0, 4.1                | PEG 6000 | 22, 23, 24, 25, 26, 27 | N/A                    | 7.5 | Hanging Drop |
| 100 mM CA | 4.0, 4.1                | PEG 6000 | 22, 23, 24, 25, 26, 27 | 10 mM DTT              | 7.5 | Hanging Drop |
| 100 mM CA | 4.1, 4.2, 4.3, 4.4      | PEG 6000 | 26, 27, 28             | 10 mM DTT              | 6.3 | Hanging Drop |
| 100 mM CA | 3.8, 4.2                | PEG 6000 | 21, 22, 23, 24, 25, 26 | 10 mM DTT/5% Glycerol  | 7.5 | Hanging Drop |
| 100 mM CA | 3.8, 4.2                | PEG 6000 | 21, 22, 23, 24, 25, 26 | 10 mM DTT/10% Glycerol | 7.5 | Hanging Drop |
| 100 mM CA | 3.8, 4.2                | PEG 6000 | 16, 18, 20, 22, 24, 26 | 10 mM DTT/5% Glycerol  | 7.5 | Hanging Drop |
| 100 mM CA | 3.8, 4.2                | PEG 6000 | 5, 10, 15              | 10 mM DTT/5% Glycerol  | 7.5 | Hanging Drop |
| 100 mM CA | 3.8, 4.2                | PEG 6000 | 19, 20, 21, 22, 23     | 10 mM DTT/5% Glycerol  | 7.5 | Hanging Drop |
| 100 mM CA | 4.0, 4.1                | PEG 6000 | 24, 25, 26             | 10 mM DTT/10% Glycerol | 7.5 | Hanging Drop |
| 100 mM CA | 4.0, 4.1                | PEG 6000 | 24, 25, 26             | 10 mM DTT/15% Glycerol | 7.5 | Hanging Drop |

Table A-3 (continued)

|                            |                    |                    |                        |                        |     |              |
|----------------------------|--------------------|--------------------|------------------------|------------------------|-----|--------------|
| 100 mM CA                  | 4.0, 4.2           | PEG 6000           | 20, 22, 24, 26, 28, 30 | 10 mM DTT/10% Glycerol | 6.3 | Hanging Drop |
| 100 mM CA                  | 4.0, 4.2           | PEG 6000           | 20, 22, 24, 26, 28, 30 | 20 mM DTT/10% Glycerol | 6.3 | Hanging Drop |
| 100 mM CA                  | 4.0, 4.1           | PEG 6000           | 24, 25, 26, 27, 28, 29 | N/A                    | 6.3 | Hanging Drop |
| 100 mM CA                  | 4.0, 4.1           | PEG 6000           | 24, 25, 26, 27, 28, 29 | 10 mM DTT              | 6.3 | Hanging Drop |
| 100 mM CA                  | 4.0, 4.2           | PEG 6000           | 20, 22, 24, 26, 28, 30 | 10 mM DTT/10% PEG 400  | 6.3 | Hanging Drop |
| 100 mM CA                  | 4.0, 4.2           | PEG 6000           | 20, 22, 24, 26, 28, 30 | 20 mM DTT/10% PEG 400  | 6.3 | Hanging Drop |
| 50 mM CA                   | 3.9, 4.0, 4.1, 4.2 | PEG 6000           | 22, 23, 24, 25, 26, 27 | 10 mM DTT              | 7.5 | Hanging Drop |
| 20/50/150/200 mM CA        | 4.0                | PEG 6000           | 25                     | 10 mM DTT              | 7.5 | Hanging Drop |
| 10/25/50/100/200/300 mM CA | 4.5                | PEG 6000           | 33                     | 5/10/25/50 mM DTT      | 7.5 | Hanging Drop |
| 25/50/75 mM CA             | 4.1                | PEG 6000           | 25, 27, 29             | 10 mM DTT              | 7.5 | Sitting Drop |
| 20/50/150/200 mM CA        | 3.8                | PEG 4000/6000/8000 | 23, 28                 | 10 mM DTT              | 7.5 | Hanging Drop |
| 100 mM NaAc                | 3.9, 4.0, 4.1, 4.2 | PEG 6000           | 24, 25, 26             | 10 mM DTT              | 7.5 | Hanging Drop |
| 100 mM NaCit               | 3.9, 4.0, 4.1, 4.2 | PEG 6000           | 24, 25, 26             | 10 mM DTT              | 7.5 | Hanging Drop |

153

**Note:**

N/A: no additive is applied

Na-CACO: Sodium-Cacodylate

NaAc: Sodium Acetate

NaCit: tri-Sodium Citrate

CA: Citric Acid

## APPENDIX 2

### SDS-PAGE Recipes for Preparing 2 Gels in 15 ml Separating Gel Solution

APS: 50 mg in 500  $\mu$ L prepared freshly every time

| Component              | 6% Gel<br>(50 – 200) | 8% Gel<br>(35 – 90) | 10% Gel<br>(20 – 80) | 12% Gel<br>(12 – 60) | 15% Gel<br>(10 – 43) |
|------------------------|----------------------|---------------------|----------------------|----------------------|----------------------|
| H <sub>2</sub> O       | 8.7 ml               | 7.9 ml              | 7.1 ml               | 6.4 ml               | 5.3 ml               |
| 1.5 M Tris (pH 8.8)    | 3.8 ml               | 3.8 ml              | 3.8 ml               | 3.8 ml               | 3.8 ml               |
| 40% Acrylamide Mixture | 2.3 ml               | 3.0 ml              | 3.8 ml               | 4.5 ml               | 5.6 ml               |
| 10% SDS                | 150 $\mu$ l          | 150 $\mu$ l         | 150 $\mu$ l          | 150 $\mu$ l          | 150 $\mu$ l          |
| 10% APS                | 150 $\mu$ l          | 150 $\mu$ l         | 150 $\mu$ l          | 150 $\mu$ l          | 150 $\mu$ l          |
| TEMED                  | 15 $\mu$ l           | 15 $\mu$ l          | 15 $\mu$ l           | 15 $\mu$ l           | 15 $\mu$ l           |

### SDS-PAGE Recipe for Preparing 2 Gels in 5 ml Stacking Gel Solution

| Component              | 5% Staking Gel |
|------------------------|----------------|
| H <sub>2</sub> O       | 3.6 ml         |
| 1.0 M Tris (pH 6.8)    | 630 $\mu$ l    |
| 40% Acrylamide Mixture | 630 $\mu$ l    |
| 10% SDS                | 50 $\mu$ l     |
| 10% APS                | 50 $\mu$ l     |
| TEMED                  | 5 $\mu$ l      |